Development of Chondroinductive Hydrogel Pastes from Naturally Derived Cartilage Matrix

By

Emily Claire Beck

B.S., Biological and Agricultural Engineering, Kansas State University, 2008

Submitted to the Bioengineering program
and the Graduate Faculty of the University of Kansas
in partial fulfillment of the degree requirements for the degree of
Doctor of Philosophy

Committee Members:

Dr. Michael Detamore, Committee Chair

Dr. Cory Berkland

Dr. Stevin Gehrke

Dr. Sarah Kieweg

Dr. Brian Andrews

October 6, 2015
Date Defended

The Dissertation Committee for Emily Claire Beck certifies that this is the approved version of the following dissertation:

Development of Chondroinductive Hydrogel Pastes from Naturally Derived Cartilage Matrix

Committee Chair

Dr. Michael Detamore, Committee Chair

October 6, 2015

Date Approved

ABSTRACT

The main focus of hydrogel technology is on hydrogels in their crosslinked form. Although hydrogels are promising materials for cartilage tissue engineering, the clinical translation of these materials are hindered because they lack the ability to be molded into a defect site by a surgeon due to hydrogel precursors being liquid solutions that are prone to leaking from the implantation site during placement. Therefore, the current thesis work focuses on the hydrogels in their precursor form prior to crosslinking and describes the development of creating hydrogel pastes that have the potential to be clinically translatable. The current thesis first developed a platform hydrogel paste composed of methacrylated hyaluronic acid (MeHA), which is a more traditional hydrogel material, and hyaluronic acid nanoparticles. The hyaluronic acid nanoparticles were shown to impart a yield stress on the hydrogel precursors, allowing the precursors to be molded and shaped prior to crosslinking. Furthermore, the mixtures containing hyaluronic acid nanoparticles were able to be crosslinked and further characterized as solids and they could encapsulate bone marrow-derived stem cells that remained viable. The next major focus of the thesis was tailoring the platform system for cartilage tissue specifically, by gradually replacing each of the two components of the platform system with naturally derived cartilage extracellular matrix, to create a chondroinductive material. Devitalized (DVC) and decellularized cartilage (DCC) particles were found to impart paste-like behavior in MeHA gels, where DVC significantly upregulated chondrogenic gene expression. DCC that was solubilized and methacrylated (MeSDCC) was created and crosslinked, which formed hydrogels with a compressive modulus in the range of native cartilage tissue. Finally, DVC particles mixed

in with solubilized and methacrylated DVC created pastes that significantly upregulated chondrogenic gene expression compared to gels without DVC particles. The important next steps will be to further evaluate these MeSDVC and DVC particle pastes in an *in vivo* model, and further explore whether decellularization of the tissue is necessary. Ultimately, this thesis successfully developed a hydrogel paste that is inherently chondroinductive and promising for future cartilage tissue engineering applications.

ACKNOWLEDGMENTS

I began pursuing this Ph.D. because I understood it was the path that would allow me to follow my passion. It was a path that would let me conduct research, it was a path that would lead to the excitement of discovery and learning, and it was a path that would allow me to continue mentoring others and maybe even ever so slightly change the world for the better. I knew this path would not be easy, but I had absolutely no idea how incredibly difficult, treacherous, and emotionally tasking the journey would be. Throughout this journey, I had many academic achievements and yet many, many academic failures. I lived a lot of beautiful life and yet experienced some major personal hardships. I had many academic and personal struggles and at one point I even lost myself in the thick of it all and thought I was not going to make it to the end of this journey. So in these next pages, I would not only like to thank those who helped, funded, and guided my research throughout this journey, but I would additionally like to thank those who helped me find myself, for those who helped me pick up the pieces, and for those whose constant encouragement and support kept me on this path as hard as it was at first. For it is all of these people who have kept me on the path of pursuing my dreams and it is to all them, that I am forever indebted:

I would first like to thank my advisor, Dr. Michael Detamore. Through his unconditional support and guidance in my academic and personal life, through his patience and constant encouragement to never give up and continue to strive for what seems impossible, and through his willingness to let me pursue my own research interests, I have learned and achieved more than I ever could have imagined. I am eternally grateful for him

going above and beyond the call of duty of an advisor to ensure that regardless of personal and academic hardships, I would persevere and continue my Ph.D. I am thankful for his impeccable intuition, for his ability to see potential in me that I could not even see, and for encouraging me to pursue the path in life that would make me the most fulfilled and happy. His mentorship, without a doubt, has changed my life for the better and I can only hope that through his example, I might be able to do the same for others one day.

I would like to thank my committee members, Dr. Cory Berkland, Dr. Stevin Gehrke, and Dr. Sarah Kieweg for their guidance, for the many meetings to brainstorm and troubleshoot, and for taking the time to enrich my project with their expertise. In addition, I would like to thank my committee member, Dr. Brian Andrews, for inviting me to witness how my research could impact the surgical world, which was an amazing learning experience and it has helped me tailor my research to ensure it has the potential to become translational.

I have worked with many wonderful undergraduate researchers who have been a tremendous help in completing this project. I would like to thank Marina Rasuck and Bharath Krishnamoorthi for helping me get started in the lab and for their aid in troubleshooting my project when it seemed like we would never get something to work, and I would like to thank Daniel Tabakh for helping me with the first successful version of my product. I would like to thank Brooke Lohman and Tony Libeer for their many hours of help to tailor my product for cartilage tissue applications. Additionally, I would like to give a tremendous thank you to Marilyn Barragan and Madeleine Tadros for their many hours of help as I completed the last portions of my research. Last, I would like to thank

Harley Astorga for making videos to promote my materials. To all of these undergraduates and former undergraduates, I would like to thank not just for their hard work and help in my research, but additionally for their questions that helped me continue to learn and for their own research accomplishments and awards, which has made me incredibly proud and humbled.

In addition, there are many individuals that took the time to train me and help me learn new techniques, and among them I would like to thank Amir Fakhari, Qun Wang, Justin Douglas of the KU NMR lab, Prem Thapa and Heather Shinogle of the MAI lab, Dr. Karen Peltier of the TORP lab, and Dr. Joshua Sestak. Furthermore, I would like to thank the many individuals who helped guide my research and my career paths, including Dr. Jennifer Laurence, Dr. Laird Forrest, Dr. Bruce Toby, and especially Dr. Udayan Apte for all of his help and guidance as I began my research path. I am thankful for my undergraduate advisor, Stacy Hutchinson, for her research guidance and mentorship that helped me realize I wanted to pursue a career in research and in addition, I am thankful for my high school science teacher, Patrick Lamb, for instilling in me a spark of passion for medicine and medical technology. An internship through the Bioengineering Summer Internship Program at the National Institutes of Health sparked my interest in tissue engineering and additionally, I was able to learn an immense amount about the industry side of my field with an internship experience from AlloSource, of which both internship experiences I am exceptionally grateful.

I could not have been blessed with better current and former labmates throughout this journey. I would like to thank my former and senior labmates, Dr. Nathan Dormer, Dr.

A.J. Mellott, Dr. Lindsey Ott, and Dr. Neethu Mohan, for training me on all of the techniques, imparting their wisdom, and teaching me the ropes of being a graduate student, which included how to stay sane, laugh, and persist, even when nothing ever seemed like it would work. Additionally, I would like to thank other former graduate students, Amanda Sutherland and Dr. Connor Dennis for all of their help and teamwork on a collaborative project, I would like to thank Emi Kiyotake and Francisca Acosta for their help with IHC, and I would like to thank all of the past, present, and associated members of the KU Biomaterials and Tissue Engineering Lab that have helped me with cartilage harvests over the years. I am so grateful for the support, friendship, and encouragement from fellow labmates, Vineet Gupta and Dr. BanuPriya Sridharan as we all raced to the finish lines of our degrees. Furthermore, I am thankful for the friendship, memories, and the laughs I have shared with all current and former labmates of Dr. Detamore's lab, especially with Lindsey, Banu, Deena Rennerfeldt, Cate Wisdom, and Jakob Townsend.

I would like to give a huge thank you to our lab manager, Peggy Keefe, for all of her training, support, encouragement, for the talks about our dogs, and for all of her help throughout the years, especially dealing with my many last minute orders. I could not have completed this journey without her. In addition, I would like to thank Denise Bridwell, the Bioengineering Program Assistant, for all of her help, encouragement, and mountains of banana-flavored taffy. Likewise, I would like to thank the Bioengineering Program director, Dr. Sara Wilson, for her support and nomination for the KU Summer Research Fellowship and the KU Women of Distinction Calendar, both of which were an incredible honor to receive.

Furthermore, I could not have completed this journey without the help from some major funding sources, including a National Science Foundation Graduate Research Fellowship, a KU Summer Graduate Research Fellowship, and a National Science Foundation GK-12 Fellowship. These funding sources allowed me the freedom to pursue my own unique interests and provided me with several tools that I undoubtedly will treasure throughout my lifetime. The NSF GK-12 fellowship allowed me to mentor K-12 students as well as undergraduates, and not only did the fellowship help me communicate science to a variety of ages and academic backgrounds, it additionally helped me understand how people learn, and I have used this knowledge to help improve my teaching. I would like to thank the Duke Talent Identification Program for giving me the opportunity to teach numerous times throughout the last 5 years to gifted 6^{th}-12^{th} graders. This program has certainly improved my teaching because it led me to discover some major misconceptions of my field, and I was able to study and research different teaching methods to determine new approaches and techniques to correct these misconceptions for students.

In addition to academic and financial support, I am thankful to many individuals for the personal support throughout my time at KU. There was a time in the middle of my graduate career when I contemplated quitting the program, and although there are definitely many individuals in my academic endeavors who helped me persevere and overcome my struggles, there are many individuals outside of my academic life that I would like to thank and played a crucial role in helping me through both the difficult times and through rest of my graduate career.

I would first like to thank Sharadvi Thati, another graduate student at KU. Our friendship started when she was tasked with teaching me how to use the peptide synthesizer and it blossomed into one of the most important and valuable friendships I have obtained at KU. Not only am I thankful for learning how to use and know all the ways to troubleshoot the peptide synthesizer and learning about the amazing and time-saving wonders of the program GraphPad, I am additionally incredibly thankful for the encouragement, support, long talks, dog walks, and adventures we have had throughout our graduate careers.

Another close friend I would like to thank is Blair Schneider, who I met through the GK-12 program. Her support, encouragement, and advice certainly helped me through tough times. I will cherish the many memories of our adventures, from Washington D.C., to Denver, and even in Lawrence.

I am indeed tremendously thankful for members of the community who helped me get started in playing soccer, piano, and doing CrossFit in Lawrence, three hobbies that have undoubtedly provided much needed joy and stress relief during hard times. I would specifically like to thank the Lawrence Adult Soccer League community, St. John's Celebration Singers, CrossFit AlterEgo, the KU Intramural Program, and all of the members of my KU intramural soccer team, IM Legend. Obtaining four back-to-back intramural soccer championships at KU is a memory I will truly treasure forever.

I am thankful for other members and organizations of the community who helped me during the rough times of my graduate career, including the Emily Taylor Women's center, CAPS, GaDuGi, and St. John's Catholic Church. I am so incredibly indebted to the members of these organizations for helping me continue on a path that seemed blocked and

impassable. The help, support, and guidance I received from these individuals without a doubt is one of the main reasons I was able to continue on during rough times. So to these individuals I am forever truly grateful.

I am thankful for my long time best friend, Michelle Nelsen. From grade school science fairs through college, Michelle has been my science buddy. Her passion for research and science is infectious and I know some of that passion was passed on to me. I am so tremendously thankful for all of her encouragement, science talks, and all of the non-academic related adventures we have had over the years and I look forward to having many more of all of the above.

I am thankful for my boyfriend, Rob Timberlake, for all of his love, support, and encouragement as I raced to the graduation finish line. From the long days and seemingly endless writing spells, and through listening as I exclaimed my non-existent love for pipetting, he provided me with the necessary encouragement to keep me on the path toward the finish line and helped me look forward to even the most tasking of days.

I am thankful for my sister, Connie Beck, for the much needed comic relief and encouragement through the tough days and for her advice, help, and abiding support as I went through the rough days of my Ph.D. The hilarious quotes, the long talks, the many adventures we have had over the years are memories that I will always cherish.

I am thankful for my parents, my first teachers, who without a doubt I am indebted for being on the path I am today. I would like to thank my Mom for her constant encouragement as I embarked on a career that was more male-associated. I was forever reminded that I could achieve whatever I put my mind to, that it was ok that I enjoyed

math, and that I could certainly “beat the boys” in anything I set out to achieve. I would like to thank my Dad for being one of the best teachers, mentors, and role-models in my life. I would have never known about bioengineering had he not introduced me to it in high school. Growing up, he taught me not only how to learn, but how to teach, and he instilled me with a passion for the pursuit of learning. Overall, I am so incredibly thankful for my family’s love, support, wisdom, and encouragement growing up and throughout my graduate career.

Finally, I want to thank my loving and loyal dog, Pepper, for making the bad days seem not so bad, and for making the good days even better.

TABLE OF CONTENTS

LIST OF FIGURES

CHAPTER 6

CHAPTER 7

LIST OF TABLES

CHAPTER 1
No Tables

CHAPTER 2

CHAPTER 3
No Tables

CHAPTER 4
No Tables

CHAPTER 5
No Tables

CHAPTER 6
No Tables

CHAPTER 7
No Tables

CHAPTER 1: INTRODUCTION TO THESIS

The overall objective of thesis was to develop a mechanically dynamic, "paste-like" hydrogel material that could retain its molded or extruded shape, would "set" after placement and withstand mechanical loading, and would be inherently chondroinductive. The overall progression was to first develop a platform hydrogel paste system and then tailor it specifically for cartilage tissue engineering. This platform system entailed a two component system that was mixed together (Figure 1.1): one component was comprised of particles that provided the paste-like rheological properties, and the other component was a photocrosslinkable linear polymer that, after crosslinking, provided the mechanical integrity needed to withstand mechanical loading. The two components were then replaced one by one to create a chondroinductive paste. Therefore, characterization and progression of this hydrogel paste design incorporated the following three specific aims (Figure 1.2): (1) characterize methacrylated hyaluronic acid (MeHA) and hyaluronic acid nanoparticle pastes with modulated rheological properties, (2) engineer and refine MeHA pastes incorporating decellularized (DCC) and devitalized cartilage (DVC) and evaluate chondroinductivity *in vitro*, and (3) Characterize solubilized and methacrylated DCC (MeSDCC) and solubilized and methacrylated DVC (MeSDVC) and evaluate chondroinductivity of DVC pastes *in vitro*.

The first aim was to develop a platform technology to create hydrogel pastes that were capable of encapsulating rat bone marrow-derived stem cells that remained viable. The second aim was to replace the hyaluronic acid nanoparticles with chondroinductive materials, DCC and DVC, and compare and evaluate these materials *in vitro*. The third aim

first characterized hydrogels composed only of MeSDCC and evaluated them for their biomechanics and for their chondroinductive potential, comparing them to methacrylated gelatin. The final part of the third aim was to evaluate MeSDVC and DVC particle pastes for their chondroinductive potential *in vitro*. The chapters that follow reflect the chronological progression of these aims, and the organization of these chapters is as follows:

Chapter 2 provides a background of the structural and functional characteristics of hard-soft tissue interfaces and then contains a thorough literature review on the two main types of nanomaterials emerging in interfacial tissue engineering strategies: nanoparticles and nanofibers. Additionally, the chapter provides approaches used to employ these nanomaterials in interfacial constructs. Although the current thesis work did not evaluate the hydrogel pastes as interfacial constructs, Chapter 2 addresses the entire thesis as it provided valuable insight on the development of materials that would be successful in cartilage tissue engineering strategies and it addresses the first aim by providing reasoning for using nanomaterials for cartilage tissue engineering.

Chapter 3 addresses the first aim of developing a platform hydrogel paste system. MeHA was mixed with hyaluronic acid nanoparticles and linear hyaluronic acid in various formulations, where the solutions were evaluated for their yield stress prior to crosslinking. Additionally, the solutions were crosslinked and characterized as solids for swelling, mechanical compression, and cell viability after encapsulation. This chapter therefore provided the foundation for the rest of the current thesis, as it validated the two-component hydrogel system as effectively producing hydrogel pastes.

Chapter 4 addresses the second aim, by introducing DCC and DVC particles as a means to achieve yield stress in hydrogel precursors. DCC and DVC particles were mixed with MeHA in various formulations, evaluated for their yield stress, and were then crosslinked, where the compressive modulus, swelling, gene expression, and histology were compared and evaluated for chondroinductive potential *in vitro*. Therefore, the results of this chapter were crucial in designing the final portion of the third aim, where it was decided to focus on the use of DVC rather than DCC.

Chapter 5 addresses the first part of the third aim, i.e., characterizing MeSDCC hydrogels, and provides insight on the use of this newly developed material for future work. MeSDCC gels were fabricated and encapsulated with cells and were then evaluated for their compressive modulus, swelling, and chondroinductivity *in vitro*, where the MeSDCC gels were compared alongside methacrylated gelatin (GelMA) gels. The results of this chapter affirmed that MeSDCC is a potential promising material for cartilage tissue engineering and therefore, methacrylated extracellular matrix was chosen to be further evaluated in Chapter 6.

Chapter 6 further addresses aim 3 by evaluating chondroinductive pastes composed of MeSDVC and DVC. DVC was chosen from the results based on aim 2, and various formulations of DVC particles mixed with MeSDVC were evaluated for a yield stress prior to crosslinking, and after crosslinking, the compressive modulus, swelling, and chondroinductivity of these formulations were analyzed *in vitro*. The findings of this chapter further validated the use of the two-component hydrogel paste system and provided

evidence that hydrogel pastes composed entirely of cartilage ECM have potential for cartilage tissue engineering.

Chapter 7 addresses the concluding remarks of this current thesis. It summarizes the key findings and then describes and presents comparisons made among and between all three aims. Finally, recommendations are made regarding future work with these materials.

Overall, the work conducted in this current thesis proposed a potential solution to overcome the major drawback of traditional hydrogels, which is leaking from the defect site after implantation. Hydrogels are promising materials for treating arthritis. Current clinical treatments for arthritis include autologous chondrocyte implantation, mosiacplasty, and microfracture. Other treatments available are products such as Zimmer's DeNovo® product, which is composed of living, human juvenile cartilage. However, not only do these treatments involve high risk of donor site morbidity and/or the need for multiple surgeries, or require living donated cartilage, of which availability of donors is a concern, but they all still lack the ability to regenerate fully functional cartilage tissue. Although many promising improvements are being made in hydrogel technology for cartilage regeneration, without the potential for clinical translation, it will be difficult for these advancements to reach commercialization. Therefore, although the work in this current thesis did not encompass regenerating the entire osteochondral interface, it did provide the mindset of clinical translation for hydrogel advancements, and it provided for the first time a foundation for a potential hydrogel solution that is paste-like and chondroinductive to regenerate damaged cartilage tissue.

CHAPTER 2: NANOMATERIALS FOR HARD-SOFT TISSUE INTERFACES*

ABSTRACT

The field of interfacial tissue engineering is striving to restore the structural and functional characteristics of hard-soft tissue interfaces, which include osteochondral and bone-tendon/ligament interfaces. This chapter first discusses the structural and functional characteristics of these interfaces and then describes the two main types of nanomaterials emerging in interfacial tissue engineering strategies: nanoparticles and nanofibers. Additionally, the chapter discusses approaches used to employ these nanomaterials in interfacial constructs.

INTRODUCTION

Engineering of interfacial tissues is emerging as one of the grandest challenges of tissue engineering. This emergence is in part because of the complexity of the interface itself, but additionally because interfacial tissues are in high clinical demand. Hard-soft tissue interfaces (e.g., bone-cartilage, bone-tendon, bone-ligament), which are the focus of this chapter, are especially prone to injury. Considering the bone-tendon/ligament interface alone, repair methods using grafts are not necessarily focused on regenerating the tissue interface, which can lead to compromised graft function and poor long-term clinical outcome.[82, 89] Therefore, the field of interfacial tissue engineering is striving to restore the

---

*Published as **Beck E.C.** and Detamore M.S., "Nanomaterials for hard-soft tissue interfaces," Chapter 13 in: Nanomaterials in Tissue Engineering: Characterization, Fabrication and Applications, eds. Gaharwar AK, Sant S, Hancock MJ, Hacking SA. Woodhead Publishing, Philadelphia, PA, pages 363 – 386, 2013.

structural and functional characteristics of the interface itself to form a seamless transition from hard-soft tissues.

The structural and functional characteristics of the interfaces of bone-cartilage, and bone-tendon/ligament will be described here. These characteristics are highly complex because the interface is responsible for the transfer of mechanical loads between two dissimilar and heterogeneous tissues.[89, 149] Therefore, the physiology and function of each interface must be understood prior to designing interfacial constructs. The bone-cartilage interface, known as the osteochondral interface, unites hyaline cartilage with subchondral bone and is the most extensively studied interface in tissue engineering. Cartilage can be further divided into three zones (Figure 2.1). The superficial zone at the articular surface is characterized by flattened chondrocytes and thin collagen II fibrils that run parallel to the joint surface.[138] The middle zone contains more rounded chondrocytes and slightly larger and less parallel collagen II fibers.[99] The deep zone contains chondrocytes and collagen II fibrils that run perpendicular to the articular surface.[138] Underlying the three cartilage zones is a wavy tidemark that marks the beginning of the calcified cartilage zone, which extends the collagen fibrils from the deep zone to the subchondral bone. Finally, the subchondral bone is composed of primarily collagen I and hydroxyapatite crystals.[154] The subchondral bone is secured to the calcified cartilage by interdigitation at the interface of these two zones. In addition to providing a secure attachment, this interdigitation reduces stress concentrations at the bone-cartilage interface to allow for efficient transfer of mechanical loading.[82]

Although osteochondral constructs are more widely explored in interfacial tissue engineering, the bone-tendon/ligament interfaces are gaining attention as well. Tendons transfer loads from muscle to bone, while ligaments link bone to bone and help ensure joint stability.[86] The insertions of tendons and ligaments to bones can vary drastically, but they can generally be classified as direct or indirect.[86] Direct insertions are characterized by four transition zones (Figure 2.1). The first zone is fibrous connective tissue that contains fibroblasts with aligned collagen fibrils. These collagen fibrils extend to the next zone, the uncalcified fibrocartilage zone, which contains larger collagen fibrils that are less parallel than the previous region. A wavy tidemark separates the uncalcified fibrocartilage zone from the calcified cartilage zone. Finally, interdigitation secures the calcified cartilage zone to the fourth zone, which is the underlying bone.[7] Indirect insertions do not contain the fibrocartilage zones, but instead the tendon is directly secured to the bone through Sharpey's fibers, which are collagen fibers that extend directly into the underlying bone.[86]

Primarily, tissue engineering strategies to regenerate osteochondral and bone-tendon/ligament interfacial tissues are stratified in nature. These stratified designs are considered "graded" designs, as they combine two or more distinct layers that aim to hone in on the characteristics of the various interfacial zones. More recently, continuously graded approaches have been considered, where instead of containing discrete layers, the constructs provide a more gradual tissue interface transition, similar to the native interface itself.[27] These interfacial tissue engineering approaches and strategies have been thoroughly reviewed in the literature,[24, 27, 45, 75, 82-84, 89, 90, 98, 112, 117, 118, 124, 154, 160] however the quest for the best approach continues.

An emerging trend in interfacial tissue engineering is the incorporation of nanomaterials in the interfacial design. Prior to 2009, few publications existed that incorporated nanomaterials for interfacial constructs. However, the number of publications in this area continues to increase steadily each year, with just over five publications in 2009 alone and doubling to more than ten publications in 2011 alone. Additionally, the number of publications in this area so far for 2012 are on a similar pace to that of 2011, emphasizing that nanomaterials are rapidly gaining attention and generating interest in the field of interfacial tissue engineering. Nanomaterials are typically classified as materials that are 1-100 nm in size, although many groups consider materials smaller than 1 μm to be nanoscale. Nanomaterials can take many forms, including nanoparticles, nanofibers, nanocrystals, nanorods, nanotubes, etc. In a relatively short period, nanomaterials have exhibited extraordinary potential to advance medical therapies. In the field of tissue engineering, nanomaterials have become of growing interest recently because the extracellular matrices of tissues are composed of hierarchically nanostructured materials that can regulate cellular functions such as differentiation, morphogenesis, adhesion, proliferation, and migration.[137] Thus, nanomaterials have the potential to advance current strategies for interfacial tissue engineering.

The following sections review the two nanomaterial components currently being used in hard-soft tissue engineering: nanoparticles and nanofibers. In addition, a section is included that discusses strategies incorporating nanomaterials in hard-soft tissue interfaces. Although this text is organized by nanomaterial component, because of overlap in nanomaterial use in some strategies, the tables are arranged by interface type. Table 2.1

provides the nanomaterials employed in osteochondral strategies and Table 2.2 provides the nanomaterials used in bone-tendon/ligament strategies.

NANOPARTICLES

Recent interfacial tissue engineering constructs have incorporated nanoparticles of various types of materials. Because all hard-soft tissues include bone, it is not surprising that the majority of nanoparticles used in interfacial tissue engineering constructs are ceramic. Not only are ceramics part of the native extracellular matrix (ECM) of bone, they can additionally increase the mechanical strength, biocompatibility, and osteoconductivity of tissue engineered scaffolds.[21, 31] In the following sections, we will discuss interfacial constructs that incorporate ceramic nanoparticles of hydroxyapatite (HAp), the most commonly incorporated ceramic nanoparticle, β-tricalcium phosphate (β-TCP), and other mineral-based materials. Although most of the nanoparticle materials in the following sections are mineral-based, newly emerging nanoparticle materials, including magnetic and fluorescent nanoparticles, will be discussed in the following sections.

Hydroxyapatite (HAp) Nanoparticles

It is well known that the nanostructure of bone, including HAp, plays an important role in the overall mechanical properties of bone.[106] HAp nanocrystals constitute approximately 70% of native bone matrix.[58] These HAp nanocrystals are roughly 50 nm long, 25 nm wide, and 2-5 nm thick.[56, 107] One method used in interfacial tissue engineering is to directly incorporate synthetic HAp in the constructs.[18, 19, 62, 91, 102, 113, 152] Samavedi *et*

al.[113] fabricated a continuously graded mesh by co-electrospinning nano-HAp/polycaprolactone (PCL) with poly(ester urethane). This approach for the bone-ligament/tendon interface resulted in a continuous mineral gradient as well as a gradient in tensile moduli throughout the scaffold.[113] Mohan *et al.*[91] additionally constructed a continuous mineral gradient for the osteochondral interface by incorporating nano-HAp into poly(D,L-lactic-co-glycolic acid) (PLGA) microspheres. The gradient was formed by filling a mold with opposing types of microspheres, PLGA with or without nano-HAp, and microspheres loaded with transforming growth factor-β1 for chondrogenesis. Scaffolds containing both mineral and signal gradients were found to promote the greatest extent of regeneration.[91] Another group used a bi-layered approach, composed of a poly vinyl alcohol (PVA)/gelatin/nano-HAp layer and a polyamide6 layer.[102] Osteogenically induced bone marrow stem cells (BMSCs) were seeded onto the HAp layer and chondrogenically induced BMSCs were seeded onto the polyamide6 layer, and the constructs were implanted intramuscularly. After 12 weeks, the layers retained the corresponding osteogenic and chondrogenic gene expression.[102] Other groups have used non-stratified nanocomposites that have shown promise for osteochondral tissue engineering. These nanocomposites incorporated HAp and synthetic polymers, including PLGA[152] and poly(1,8-octanediol-co-citrate) (POC).[18, 19] Xue *et al.*[152] implanted PLGA constructs containing HAp into rat osteochondral defects and observed superior osteochondral regeneration in the scaffolds incorporating HAp compared to PLGA control scaffolds.

In addition to solely incorporating nano-HAp, some groups compared both HAp microparticle and nanoparticle incorporation.[19, 62] For bone tissue engineering, a debate

currently exists on the use of HAp microparticles versus nanoparticles.[143] In comparison to microparticles, nanoparticles are hypothesized to better mimic the native bone environment and enhance osteogenic differentiation.[96] However, drawbacks of nanoparticles include reduced scaffold porosity and particle aggregation.[143] In interfacial tissue engineering, this microscale versus nanoscale debate exists as well. Chung *et al*.[19] directly compared HAp microcomposites versus nanocomposites and found that nanocomposites displayed the highest strength and stiffness and allowed for more trabecular bone formation at the implant-tissue interface. However, Khanarian *et al*.[62] compared HAp microparticle and nanoparticle incorporation in agarose gels and found superior mechanical properties and matrix production with HAp microparticles relative to HAp nanoparticles. These studies suggest the need for further research and characterization of microscale and nanoscale interfacial constructs.

Not all studies that incorporate HAp used synthetic HAp. An newer alternative technique to incorporate HAp is by inducing the nucleation and growth of HAp crystals.[159] This approach mimics native HAp deposition by the use of simulated body fluid (SBF), which is a solution that contains the approximate concentrations of ions found *in vivo*. Scaffolds can be soaked in this solution and HAp crystals are directly nucleated on the surface, where the size of HAp crystals can be regulated by the amount of soak time.[123] In native bone, HAp is deposited on collagen I fibers, and the size and orientation of the deposited HAp crystals are regulated by the collagen fibers.[106] Although this nucleation technique may be used for bone tissue engineering,[158] several interfacial tissue engineering studies tried to directly mimic this native mineralization by allowing collagen I nanofibers

to soak in SBF.[39, 65-69, 77, 130, 131] Tampieri *et al*.[131] developed a tri-layered osteochondral scaffold, which consisted of a biomineralized collagen layer to mimic native subchondral bone, an intermediate layer composed of collagen and less mineral, and an upper layer composed of hyaluronic acid and collagen to mimic the articular cartilage. These constructs were implanted subcutaneously in mice for 8 weeks and the layers of the construct were found to selectively support osteogenesis or chondrogenesis.[131] From the same group, Kon *et al*.[67] studied a similar tri-layered scaffold in sheep, except the cartilaginous layer lacked hyaluronic acid. Blank scaffolds and scaffolds seeded with autologous chondrocytes were implanted in sheep osteochondral defects. The extent of regeneration in the seeded constructs was similar to that of the blank scaffolds, suggesting the scaffold induced local cellular infiltration *in vivo*.[67] This scaffold has even been further tested in horses and in human clinical trials.[66, 68, 69] In another study, Liu *et al*.[77] created a continuous gradient of HAp on a collagen construct by a controlled diffusion-precipitate method that allowed calcium and phosphate solutions to diffuse into the construct via opposing gradients. This resulted in a calcium rich and a calcium depleted side, where nano-HAp precipitation was the most prominent in the interior of the scaffold.[77]

HAp nucleation has additionally been performed on PCL[74, 97, 113] and poly(D,L-lactide) (PDLLA).[157, 162] Li *et al*.[74] created a continuously graded HAp scaffold by locally varying the immersion time of PCL nanofibers in SBF. The PCL scaffold was placed in a tilted position in a glass beaker and a mineral solution was fed into the beaker at a constant rate. Thus, because the scaffold region at the bottom of the beaker was exposed to SBF for a longer period, there was more HAp deposition at the bottom than in the scaffold region

at the top of the beaker. After seeding with mouse preosteoblasts for 3 days *in vitro*, the cell density within the scaffold was found to increase with increasing mineral content along the mineral gradient.[74] HAp has additionally been nucleated onto scaffoldless osteochondral constructs, which were composed of ECM directly secreted by mesenchymal stem cells (MSCs).[87] HAp was deposited onto the constructs with an alternate soaking process with calcium and phosphate solutions. Scaffolds containing HAp exhibited accelerated osteoinduction *in vivo* as compared to scaffolds without HAp.[87]

β-Tricalcium Phosphate (TCP) Nanoparticles

In addition to being osteoconductive and biocompatible, β-TCP has received great attention from the interfacial and bone tissue engineering communities due to its tunable bioresorption rates.[100] Erisken *et al.*[34] recently created a functionally graded β-TCP scaffold via a hybrid twin-screw extrusion/electrospinning (TSEE) process for osteochondral interfaces. This process allowed the time-dependent feeding of β-TCP nanoparticles and PCL solution resulting in a continuous gradation of β-TCP in an electrospun nanofibrous mesh. The same group further tested the scaffold for its linear viscoelastic and compressive properties by testing scaffolds seeded with mouse preosteoblasts and unseeded scaffolds.[35] They found that the viscoelastic and biomechanical properties increased (i.e., became closer to the native osteochondral interface) by increasing the culture period. Another group fabricated a multilayer scaffold that employed β-TCP, in which the scaffold contained a bone phase, a cartilage phase, and a transition phase in between. The bone phase was created by ceramic stereolithography

and the cartilage phase, consisting of collagen I, was added to the bone phase by gel casting. In addition, the gel casting method was proposed to aid in the reduction of delamination between bone and cartilage layers.[8]

Other Mineral Nanoparticles

Although the primary mineral components used in tissue engineering are hydroxyapatite and β-TCP, other mineral nanomaterial components such as amorphous calcium phosphate and β-glycerophosphate (β-GP) have been incorporated into interfacial constructs.[36, 47, 48, 103] Harley *et al.*[47] developed a layered scaffold with a continuous interface via a liquid-phase cosynthesis technique. The bone phase was composed of a mineralized type I collagen/chondroitin sulfate and the cartilage phase was composed of unmineralized collagen II/chondroitin sulfate. The layers were then allowed to diffuse, creating a graded interface.[47] Erisken *et al.*[36] used the previously described TSEE process to create scaffolds with opposing gradients of insulin and β-GP. The scaffolds were seeded with human adipose-derived stromal cells and it was found that the cells differentiated selectively towards chondrogenic or osteogenic lineages depending upon the location in the scaffold.[36] As an alternative electrospinning technique, Ramalingham *et al.*[103] used a two-spinnerette approach to create a scaffold of continuously graded amorphous calcium phosphate nanoparticles. The spinnerettes were set 2.5 cm apart oriented vertically above a spinning mandrel, where each spinnerette was connected to a syringe loaded with either PCL or PCL with calcium phosphate nanoparticles. Preosteoblast cells were seeded onto

the constructs for 7 days and it was observed that cell adhesion and proliferation increased as the calcium phosphate concentration increased along length of scaffold.[103]

Emerging Nanoparticle Materials

Although most nanoparticle materials used in interfacial tissue engineering are mineral-based, it is important to consider the potential benefits of other nanoparticle materials as well. Some emerging nanoparticle materials in interfacial tissue engineering are magnetic,[46, 130] fluorescent,[72] or silver.[97] Grogan *et al.*[46] fabricated a graded scaffold by mixing alginate hydrogels with cells labeled with magnetic iron-oxide nanoparticles and exposing the cells to varying external magnetic fields. The resulting scaffold produced a scaffold with varying cellular orientations that closely mimicked that of the osteochondral interface.[46] Lee *et al.*[72] developed another interesting use for fluorescent nanoparticles in interfacial tissue engineering. They created an *in vivo* cell tracking system to monitor the migration of mesenchymal stem cells in osteochondral defects.[72] Nirmala *et al.*[97] introduced the use of silver nanoparticles for osteochondral constructs. They incorporated hydroxyapatite and silver nanoparticles in PCL electrospun nanofibers and then submerged the constructs in SBF to allow for further mineralization. Incorporating the silver nanoparticles resulted in superior mechanical properties and apatite deposition.[97] Additionally, silver nanoparticles are known for their antimicrobial properties, providing a further advantage of silver nanoparticle incorporation.[125]

Summary of Nanoparticles

Overall, nanoparticle use in interfacial tissue engineering is primarily focused on the incorporation of natural materials like hydroxyapatite and β-TCP. The most common methods utilize the nucleation of hydroxyapatite onto collagen scaffolds, which closely mimics the natural mineral deposition *in vivo*. In general, scaffolds incorporating nano-HAp and other mineral gradients appear to result in superior interface mechanical properties as well as enhance the selective cellular response within the constructs. Although there is some debate on whether nanoscale or microscale minerals are superior for interfacial constructs, nanomaterials certainly show promise for the field. Additionally, further developments in the newly emerging nanoparticle materials have the potential to advance the interfacial tissue engineering field. These emerging nanomaterials provide new methods to produce gradient scaffolds (e.g., using magnetic fields) and fluorescent nanoparticles additionally provide a new method to evaluate the constructs *in vivo.*

NANOFIBERS

Nanofibers are another promising nanomaterial used in interfacial tissue engineering due to their high surface-to-volume ratio and their ability to mimic the fibrous organization of the ECM.[118] Nanofibers possess unique mechanical properties whereby the tensile modulus, shear modulus, and tensile strength have shown the capacity to increase as the diameter of the nanofiber decreases.[16, 153] These properties are especially useful to the bone-tendon/ligament interface, where the native mechanical loading transitions from primarily compressive in bone to tensile loading. Three common methods to produce

nanofibers are self-assembly, electrospinning, and phase separation. Additionally, the materials that constitute these nanofibers in interfacial tissue engineering are primarily collagen and synthetic polymers. Thus, the following sections will discuss the collagen and synthetic nanofibers for interfacial tissue applications and each section will discuss how the materials are incorporated.

Collagen Nanofibers

As the most common bodily protein, accounting for 30% of all proteins in the body, and giving rise to the structural support and tensile strength of the native ECM,[61] collagen is the most commonly employed nanofibrous material in interfacial tissue engineering. Collagen I is the most prevalent type of collagen in bone, while collagen II is more prevalent in hyaline cartilage. However, collagen I is primarily the only type of collagen currently being incorporated into interfacial constructs. Additionally, all publications currently employing collagen I nanofibers into their interfacial constructs use collagen self-assembly to create the nanofibers.[12, 39, 65-69, 130, 131] Cheng *et al.*[12] encapsulated rabbit MSCs into collagen microspheres that were fabricated out of self-assembled collagen I nanofibers. The encapsulated microspheres were then either chondrogenically or osteogenically induced and the microspheres were brought together to form three layers, a chondrogenic and osteogenic layer, and an intermediate layer in between containing undifferentiated MSCs in collagen microspheres. Compared to biphasic control scaffolds that did not contain an intermediate layer, the triphasic scaffolds successfully formed a calcified cartilage layer.[12] As previously mentioned in the HAp nanoparticle section, the

other group incorporating collagen nanofibers via self-assembly developed a tri-layered osteochondral scaffold, which consisted of a biomineralized collagen layer to mimic native subchondral bone, an intermediate layer composed of collagen and less mineral, and an upper layer composed of hyaluronic acid and collagen to mimic the articular cartilage.[131] This group went on to study a similar tri-layered scaffold in sheep, horses, and even in human clinical trials.[66-69]

Synthetic Nanofibers

Although natural material incorporation more closely mimics the native ECM of tissues, due to the ability to control degradation and tune mechanical properties,[139] synthetic nanofibers have additionally received a lot of attention in interfacial tissue engineering. Primarily synthetic nanofibers are made via electrospinning, however one interfacial tissue engineering strategy used phase separation to make nanofibers.[132] Through this phase separation technique, Tan *et al.*[132] created nanofibrous scaffolds out of poly(l-lactic acid) (PLLA). The PLLA scaffolds supported the differentiation of human bone marrow stem cells along osteogenic or chondrogenic lineages when exposed to the respective growth signals.[132]

As previously described, several studies have incorporated synthetic nanofibers with mineral-based nanoparticles, where the fibers were electrospun PCL, PLGA, or PDLLA.[34-36, 74, 97, 103, 113, 157] Other electrospun interfacial constructs incorporate only the synthetic nanofiber itself.[78, 126, 151] Xie *et al*.[151] fabricated a unique "aligned-to-random" oriented nanofibrous scaffold by specifically designing a collector with varying electric fields. These scaffolds were created to mimic the change in collagen fiber orientation in

the bone-tendon insertion site. Tendon fibroblasts cultured on these scaffolds were observed to be aligned in the aligned fiber portion and were oriented more randomly in the random fiber portion. Although collagen II was not observed on any portion of the scaffolds after 7 days of culture, collagen I deposition was oriented in the direction of the nanofibers in the aligned portion of the scaffold and was randomly distributed in the random portion.[151] Aside from electrospinning and phase separation, Liu *et al*.[78] fabricated nanofibrous hollow microspheres via self-assembled star-shaped PLLA. These microspheres were designed to be injectable for cartilage and osteochondral defects, mimic the nanoscale topography of native ECM, and they were designed to be highly porous. In comparison to solid microspheres composed of the same material, the nanofibrous microspheres supported a significantly larger amount of cartilage regeneration in an ectopic model.[78]

Alternative synthetic materials that have emerged are carbon nanofibers and nanorods.[108] Rodrigues *et al*.[136] tested both pure polyvinyl alcohol (PVA) hydrogels and carbon-reinforced hydrogels in osteochondral defects. The reinforced gels contained either carbon nanofibers or carbon nanorods. These carbon nanomaterials are desirable because they are light weight and possess high stiffness and axial strength.[136] After 12 weeks of implantation, the carbon nanofiber-reinforced PVA accumulated the most calcium and phosphorus suggesting carbon nanofibers may have potential for treating osteochondral defects.[108]

Summary of Nanofibers

Although self-assembled collagen fibers are the most commonly employed nanofiber for interfacial tissue engineering applications, other promising synthetic nanofiber materials are being explored, including carbon nanofibers. The unique mechanical properties as well as the ability to mimic the native ECM of interfacial tissues make these materials highly desirable for interfacial constructs. Specifically, electrospinning has been successfully used to spatially control the alignment of nanofibers, which resulted in a gradation in cellular alignment and ECM secretion. Overall, it appears nanofibers are used primarily in conjunction with nanoparticles and are used as a tool to create gradients in mineral content. Thus, nanofiber use may create gradients in mechanical properties and cellular responses that mimic native tissue interfaces.

STRATEGIES INCORPORATING NANOMATERIALS IN HARD-SOFT TISSUE INTERFACES

Though it is certainly important to consider types of nanomaterials to be used in interfacial tissue engineering, it is essential to consider the overall interfacial strategy used that employs these materials. As stated in the introduction, interfacial tissue engineering strategies as a whole are primarily stratified in nature. This trend certainly remains evident (Tables 2.1 and 2.2) in strategies that employ nanomaterials, where the majority of the strategies are stratified (i.e. biphasic or triphasic) or homogeneous (i.e. nanocomposite). The stratified approaches more closely mimic the native tissue components and/or structure, however, they may risk delamination between phases. The use of homogeneous constructs reduces the risk of delamination,[47, 152] although homogeneous approaches lack

to regenerate the structural/functional anisotropy that exists in tissue interfaces. Consequently, continuous interfaces have received recent attention in the literature as they provide a more seamless transition between tissues.[27] Continuous interfaces that employ nanomaterials are certainly a minority (Tables 2.1 and 2.2) as compared to the stratified and homogeneous approaches, although continuous approaches are more common in bone-tendon/ligament interfaces. Interestingly, the main continuous approaches involve electrospinning techniques. However, Detamore and Berkland *et al*.[28-30, 91, 122] have created continuous interfaces by loading a mold with opposing gradients of osteogenic and chondrogenic microspheres. Additionally, strategies that incorporate a continuous or stratified design primarily create a gradient of ceramic components. However, other gradient approaches exist, including gradients in fiber[151] and cellular[46] alignment.

CONCLUSION AND FUTURE DIRECTIONS

As the field of interfacial tissue engineering progresses, the underlying goal remains, which is to regenerate a structural and functional interface that transitions between two dissimilar tissues. This chapter has provided an overview of the structural and functional characteristics of the most widely explored tissue interfaces, specifically the osteochondral and bone-tendon/ligament interfaces. However, tissue engineering studies of other tissue interfaces (e.g., muscle-tendon interface) are beginning to emerge as well.[71]

Highlighted in this chapter is the burgeoning integration of nanomaterial use in interfacial tissue engineering strategies. The nanomaterials currently being used in interfacial applications are nanoparticles and nanofibers. Interestingly, the most common

nanomaterials used in interfacial strategies are mineral-based nanoparticles and collagen nanofibers, which are components found in the native interfaces. This use of raw materials further emphasizes the potential of using raw materials in tissue engineering strategies.[26] However, nanomaterial use in general provides many benefits to interfacial strategies, including superior mechanical properties of the interface, and providing a more biomimetic environment.

In addition to the type of nanomaterial employed, the overall strategy to regenerate the interface is crucial as well. As previously mentioned, interfacial strategies that employ nanomaterials are primarily stratified or homogeneous, although continuous gradient approaches are gaining attention in the field. Furthermore, it is important to note that although these strategies are defined as osteochondral or bone-tendon/ligament strategies, approaches from either interface can be tailored for the design of a desired interface. Because interface structure and function are both crucial entities for successful regeneration of interfaces, future successful interfacial designs will likely incorporate a strategy that mimics the gradient of natural interface as well as incorporate the nanoscale components of the interface. Thus, continuous gradients that incorporate gradients of minerals, collagen, and/or other nanoscale elements may become the next generation of interfacial designs.

CHAPTER 3: ENABLING SURGICAL PLACEMENT OF HYDROGELS THROUGH ACHIEVING PASTE-LIKE RHEOLOGICAL BEHAVIOR IN HYDROGEL PRECURSOR SOLUTIONS[†]

ABSTRACT

Hydrogels are a promising class of materials for tissue regeneration, but they lack the ability to be molded into a defect site by a surgeon because hydrogel precursors are liquid solutions that are prone to leaking during placement. Therefore, although the main focus of hydrogel technology and developments are on hydrogels in their crosslinked form, our primary focus is on improving the fluid behavior of hydrogel precursor solutions. In this work, we introduce a method to achieve paste-like hydrogel precursor solutions by combining hyaluronic acid nanoparticles with traditional crosslinked hyaluronic acid hydrogels. Prior to crosslinking, the samples underwent rheological testing to assess yield stress and recovery using linear hyaluronic acid as a control. The experimental groups containing nanoparticles were the only solutions that exhibited a yield stress, demonstrating that the nanoparticulate rather than the linear form of hyaluronic acid was necessary to achieve paste-like behavior. Furthermore, the gels were photocrosslinked and further characterized as solids, where it was demonstrated that the inclusion of nanoparticles did not adversely affect the compressive modulus and that encapsulated bone marrow-derived mesenchymal stem cells remained viable. Overall, this nanoparticle-based approach provides a platform hydrogel system that exhibits a yield stress prior to

---

[†]Published as **Beck E.C.**, Lohman B.L., Tabakh D.B., Kieweg S.L., Gehrke S.H., Berkland C.J., and Detamore M.S., Enabling Surgical Placement of Hydrogels Through Achieving Paste-Like Rheological Behavior in Hydrogel Precursor Solutions, *Annals of Biomedical Engineering*, 1-8, 2015 (PMC4540702).

crosslinking, and can then be crosslinked into a hydrogel that is capable of encapsulating cells that remain viable. This behavior may hold significant impact for hydrogel applications where a paste-like behavior is desired in the hydrogel precursor solution.

INTRODUCTION

Hydrogels are a promising class of tissue regenerative materials because of their high water content, 3D structure, tunable mechanical properties, and their ability to be delivered in a minimally invasive manner.[9, 23, 33] However, hydrogels lack the ability to be molded into a defect site by a surgeon because hydrogel precursors are liquid solutions that are prone to leaking after placement,[110, 135] which confounds their ability to be used by surgeons in the clinic. Therefore, although the main focus of hydrogel technology and developments are on hydrogels in their crosslinked form, our primary focus is on the fluid behavior of hydrogel precursor solutions (i.e., the fluid behavior of the hydrogel prior to crosslinking). As an alternative to traditional hydrogels, colloidal gels are mechanically dynamic paste-like materials that can be easily molded into place and will 'set' after placement.[147] Colloidal gels attain their cohesiveness through disruptable particle interactions and our research group has shown that these gels can successfully fill tissue defects, deliver bioactive signals, and promote new tissue formation in non-load bearing cranial defect applications.[25, 144-146] Our recent work has shown that colloidal gels with shear-thinning rheological behavior can be made out of solutions of hyaluronic acid (HA) nanoparticles.[37] These HA-based colloidal gels have the ability to fully recover after compression to high strains and after physically destroying and reassembling the gel, which

may be attractive for applications such as for cartilage regeneration.[37] However, preliminary work demonstrated that these colloidal gels do not retain their integrity over time in culture. Therefore, we have created a platform system that combines the HA colloidal gels systems with traditional crosslinked HA hydrogels to form a hydrogel suitable for load-bearing applications that is paste-like prior to crosslinking for effective delivery *in situ*. Although other systems, including dermal fillers, employ HA particles with traditional crosslinked HA hydrogels,[51-55, 111, 134] or use alternate means to induce a set strength in injectable materials,[32, 81] our HA nanoparticles (HAnp) are fabricated with a specific molecular weight (MW) designed to achieve paste-like rheological behavior and a yield stress and they have never before been encapsulated within crosslinked HA hydrogels.[37] This yield stress is especially desirable to enable a surgeon to mold the material into the defect site without the concern that the material will flow or leak from the defect, which is the main concern for traditional hydrogel precursor solutions. The HAnp will additionally allow the surgeon to mold the hydrogel precursor solution to obtain appropriate contouring of the defect site, which in some cases may not be possible with traditional hydrogel precursor solutions. Therefore, combining these HAnp with traditional crosslinked HA hydrogels may allow the material to be implanted *in situ* with appropriate placement and contouring, and the precursor solution can then be crosslinked to form a more rigid structure. Thus, the primary objective of this work was to characterize the rheological behavior of HAnp-incorporated hydrogel precursor solutions. An additional objective was to ensure that HAnp did not negatively influence the mechanics or cytocompatibility of the hydrogel after crosslinking.

MATERIALS AND METHODS

Materials

Unless otherwise stated, all materials were purchased from Sigma-Aldrich (St. Louis, MO). EDC (1-Ethyl-3-[3-dimethylaminopropyl]carbodiimide hydrochloride) was purchased from Thermo Scientific (Rockford, IL). HA (16 kDa and 1 MDa) was purchased from Lifecore Biomedical (Chaska, MN). All cell culture materials were purchased from Invitrogen (Grand Island, NY).

Synthesis and Characterization of Methacrylated HA (MeHA) and HAnp

MeHA was prepared by reacting HA (MW 1 MDa) with 20-fold molar excess glycidyl methacrylate (e.g., 20 mol glycidyl methacrylate per 1 mol HA monomer) in the presence of 20-fold molar excess triethylamine and tetrabutyl ammonium bromide for 12 days stirring in a 50:50 water:acetone solution at 200 rpm. MeHA was then dialyzed against deionized (DI) water for 2 days and was then frozen and lyophilized. The degree of methacrylation was analyzed with ^{1}H NMR (Avance AV-III 500, Bruker) by calculating the ratio of the relative peak area of methacrylate protons to methyl protons.[63] HAnp were prepared using carbodiimide crosslinking chemistry using EDC with adipic acid dihydrazide (AAD) as the crosslinker.[37] Briefly, 300 mg HA (16 kDa) was dissolved in 120 mL DI water in a 500 mL round flask stirring at 300 rpm. Then, 200 mL acetone was added to the flask and stirred for 15 min. AAD (60 mg) was dissolved in 1 mL DI water and added to the flask for 10 min. Similarly, 140 mg EDC was dissolved in 1 mL DI water and added to the flask for 20 min. Another 200mL acetone was then added to the flask and

the reaction was allowed to stir for 3 hours. The solution was then dialyzed against DI water for 2 days and the particles were frozen and lyophilized. Repeated batches of HAnp were fabricated in this manner and combined for later testing. Particle size was measured using a ZetaPALS dynamic light scattering instrument (Brookhaven, USA). Particle morphology was examined with Scanning Transmission Electron Microscopy (STEM) images using a FEI Technai G_2 transmission electron microscope at 200 kV.

Preparation of Colloidal Gels

Gels were made by mixing varying weight percents of HA (i.e., MeHA and HAnp) in 0.01M phosphate buffered saline (PBS) containing 0.05% (w/v) Irgacure (I-2959) photoinitiator (e.g., 15% HAnp = 15 mg HAnp in 100 µL PBS). Additionally, linear HA (HAlin) at 16 kDa (i.e., the same MW used to make the HAnp) was mixed with MeHA as a control to discern whether yield stress differences were due to the HA being in the nanoparticulate form or due to the mere addition of extra HA.

Rheological Testing

Prior to crosslinking the hydrogels, the shear stress of the precursor solutions (n=5) were measured over a shear rate sweep of 1-100 s^{-1} using an AR-2000 rheometer (TA Instruments, New Castle, DE) equipped with a 20 mm diameter plate at 37 °C at a gap of 500 µm. Preliminary work suggested that a 15% HAnp solution was sufficient to obtain a yield stress, and 4% MeHA was chosen because it was at the reconstitution limit of MeHA. Formulations tested were 4% MeHA, 15% HAlin, 4% MeHA + 15% HAlin, 30% HAlin,

4% MeHA + 30% HAlin, 15% HAnp, 4% MeHA + 15% HAnp, 30% HAnp, and 4% MeHA + 30% HAnp. The yield stresses of solutions were calculated using a three parameter fitting technique in MATLAB (MathWorks, Natick, MA) to fit the data to the Herschel-Bulkley equation (Equation 3.1), where τ is the shear stress, τ_0 is the yield stress, κ is the consistency index, γ is the shear rate, and n is the flow behavior index.

$$\tau = \tau_0 + \kappa(\gamma)^n \qquad \text{(Equation 3.1)}$$

Oscillatory tests were performed first by doing a stress sweep at 1 Hz to determine the linear viscoelastic region of the solutions. Solutions (n=5) were then exposed to three phases of oscillatory shearing at 1 Hz: 5 minutes at a constant shear stress of 10 Pa (i.e., within the linear viscoelastic region of the pseudoplastic solutions), a disruption phase lasting 30 seconds at a constant shear stress of 1000 Pa (i.e., sheared above the yield stress), and another 5 minutes at a constant shear stress of 10 Pa.

Characterization of Crosslinked Hydrogels

Gel solutions of experimental groups containing 4% MeHA were placed in a 2 mm thick mold between glass slides and exposed to 312 nm UV light at 3.0 mW/cm^2 (Spectrolinker XL-100; Spectronics Corp.) for 15 min on each side. Gels were cut using a 3 mm biopsy punch. To calculate the swelling degree, gels were swollen in PBS for 24 hours and then weighed and lyophilized (n=6). The dry weight was recorded after lyophilization and the swelling ratio (Q) was calculated as the ratio of total wet mass to dry mass. To obtain the compressive modulus, gels were swollen in PBS for 24 hours or two weeks (n=6) and were compressed using a RSA-III dynamic mechanical analyzer (TA

Instruments) at a rate of 0.005 mm/s until mechanical failure and the elastic modulus was calculated as the slope under the linear portion of the stress-strain curve.

Cell Viability

Rat Bone Marrow-Derived Mesenchymal Stem Cells (rBMSCs) were harvested from the femurs of male Sprague-Dawley rats (200-250g) following an approved University of Kansas IACUC protocol. The rBMSCs were cultured in monolayer until passage 4 for cell seeding. Media consisted of low glucose Dulbecco's Modified Eagle's Medium, 10% Qualified Fetal Bovine Serum, 1% Antibiotic-Antimycotic and was replaced every other day throughout culture. For encapsulation, cells were suspended in the photoinitiator solution at a cell density of 10 million cells mL^{-1} and then mixed with either 4% MeHA or 4% MeHA + 15% HAnp. Hydrogels were then fabricated using the same previously described technique to make acellular gels. After 4 weeks of culture, the gels were stained with live/dead reagent (2 mM calcein AM, 4 mM ethidium homo-dimer-1; Molecular Probes), incubated for 20 min, and then analyzed using fluorescence microscopy on a Zeiss Axio Observer A1 (Carl Zeiss, Oberkochen, Germany).

Statistics

SPSS statistical software was used to compare experimental groups using a single-factor ANOVA followed by a Tukey's *post hoc* test, where $p \leq 0.05$ was considered significant. In addition, SPSS was used to construct standard box plots to eliminate outliers for compression testing. After outlier removal, n=5-6 samples for statistical analysis.

RESULTS

Macroscopic Observation of Hydrogel Formulations

When HAnp (average diameter = 246 nm) were mixed with MeHA (degree of methacrylation = 21%), non-Newtonian paste-like behavior with shape-retention were observed (Figure 3.1A-C). In contrast, solutions composed of pure MeHA or MeHA solutions containing HAlin did not exhibit this behavior, and instead exhibited Newtonian or zero yield stress pseudoplastic behavior. STEM images of HAnp confirmed the formation of nanoparticles (Figure 3.1D).

Yield Stress Evaluation of Hydrogel Formulations Prior to Crosslinking

The experimental groups containing HAnp were the only solutions that exhibited a yield stress (Figure 3.2A-C). Although the yield stress of the 15% HAnp gels was 177 ± 31 Pa (average ± standard deviation), this yield stress was not found to be significantly different from the linear HA groups. However, solutions that contained unreacted HAlin polymer instead of HAnp did not exhibit a yield stress even though they were fit to Equation 3.1. The combination of 4% MeHA with 15% HAnp produced a synergistic effect, increasing the yield stress of the HAnp by a factor of 3.4 with the addition of the MeHA ($p < 0.001$).

Rheological Recovery of Hydrogel Formulations Prior to Crosslinking

The storage modulus of solutions lacking HAnp was negligible (i.e., all storage moduli were less than 20 Pa), but the storage modulus increased with increasing HAnp

concentration (Figure 3.2D). Specifically, compared to the storage modulus of 4% MeHA, the storage moduli of 4% MeHA increased 380- and 770- fold with the addition of either 15% HAnp or 30% HAnp, respectively ($p<0.001$). Recovery was assessed by the restoring of the original storage modulus after the disruption phase. All samples containing HAnp recovered their original storage moduli within 5 min of disruption.

Mechanical Analysis of Gels After Crosslinking

After characterizing the rheological behavior of the gels prior to crosslinking in their precursor solution form, the gels were crosslinked with ultraviolet (UV) light and further characterized as solids. Preliminary tests revealed that crosslinked MeHA was necessary to obtain gels with stable integrity over time in a 37^{o}C saline environment, therefore only gels containing MeHA were characterized after crosslinking. It should first be noted that gels containing 4% MeHA and either 15% HAlin or 30% HAlin were tested to compare with the associated HAnp gels, however, the mixtures containing 30% HAlin remained as solutions after crosslinking, rendering it impossible to cut gels for further testing, so the 30% HAlin mixtures were therefore discarded from further analysis. Although the addition of HAnp concentration resulted in at least a 5-fold increase in the compressive modulus compared to 4% MeHA gels, the increase was not significant. However, the addition of HAnp did significantly decrease the swelling degree after one day of swelling from 57 for 4% MeHA gels to 25 and 19 with the addition of 15% HAnp and 30% HAnp, respectively ($p<0.001$) (Figure 3.3A-B). After 14 days of swelling, the

compressive moduli of the MeHA + HAnp gels decreased to a range where they were not significantly different from that of 4% MeHA gels after one day of swelling.

Cell Viability of Cells Encapsulated within Crosslinked Gel Networks

Due to autofluorescence of the HAnp gels, live/dead quantification could not be performed. However, after 4 weeks, rBMSCs encapsulated in the MeHA and HAnp networks were viable as indicated by green fluorescence and minimal cell death (i.e., red fluorescence) was observed (Figure 3.3C-D).

DISCUSSION

In this work, we have introduced a method to overcome one of the major drawbacks of using hydrogels in the clinic (i.e., leaking from the defect site) by modifying traditional crosslinked hydrogels with the inclusion of HAnp. The combination of MeHA mixed with HAnp resulted in a hydrogel that exhibited 'paste-like' rheological behavior in its precursor solution. Although the underlying mechanism for the resulting paste-like behavior associated with the inclusion of HAnp is currently unknown, it has been hypothesized to be a result of dangling HA chains on the surface of the HAnp.[38] These dangling chains are hypothesized to cause physical entanglements between individual HAnp and entanglements between HAnp and MeHA. The goal of this current experimental work was to first characterize the rheological effect of adding our unique HAnp to MeHA and therefore, further research is necessary to understand the mechanism for the induced paste-like behavior of incorporating HAnp into hydrogel precursor solutions.

This desired paste-like behavior is attributed to the yield stress. The yield stress denotes the threshold where the solution transitions between an elastic solid and a pseudoplastic liquid, and it is desirable because it will prevent the hydrogel from flowing away from the site of interest. In a surgical context, this translates to allowing appropriate shaping and contouring to the defect site of interest. Yield stresses of up to 62 Pa have been previously reported for HA-based solutions,[101] but this yield stress may not be sufficient for topical application. In the current study, we demonstrated the ability to obtain solutions with yield stresses over 700 Pa. For context, the yield stresses for common paste-like materials, such as toothpaste, are approximately 200 Pa. Because the only solutions exhibiting a yield stress were solutions that incorporated HAnp, the yield stress was attributed to the HA being in the nanoparticulate form, as the addition of HA that was the same MW but was linear instead of in nanoparticle form was insufficient for achieving a yield stress. Furthermore, the combination of 4% MeHA with 15% HAnp produced a synergistic effect upon the yield stress. It should be noted that the 4% MeHA with 15% HAnp solution is a 19% overall concentration compared to the 15% HAnp solution, but this small increase in concentration is not assumed to account for the 3.4-fold increase in yield stress when 4% MeHA and 15% HAnp were combined. Additionally, preliminary work using a lower MW MeHA (16 kDa) did not result in this synergistic effect seen with the 1 MDa MeHA,[4] suggesting the synergistic effect is MW dependent. Results suggest a desirable yield stress can be obtained for various applications by modulating the concentration of HAnp and the concentration and MW of MeHA, and future work will focus on creating a model to predict the yield stress based on these components.

In addition to exhibiting a yield stress, it is desirable for injectable materials to be able to recover rapidly after shearing.[93] All samples containing HAnp recovered their original storage moduli within 5 min of disruption. Additionally, in contrast to the yield stress, which was dependent upon the presence of MeHA and concentration of HAnp, the storage modulus was dependent only on the concentration of HAnp, regardless of the presence of MeHA. Overall, because HAnp gels exhibit a yield stress and recover rapidly, including HAnp in a gel network may allow for precise molding without the risk of material leaking from an implantation site (Figure 3.4), making these gels suitable for a variety of topical and minimally invasive applications.

After appropriate shaping and contouring of these hydrogel pastes, it is important for the pastes to set up to form a rigid hydrogel network, thus emphasizing the importance of incorporating MeHA in the gel precursor solutions. Although the HAnp-incorporated solutions exhibited the desirable yield stress and recovery after shearing, HAnp networks alone disintegrated rapidly in solution without the addition of MeHA. Therefore, we further characterized our MeHA-containing experimental groups as solids after photocrosslinking. The standard deviations of the compressive moduli for gels containing 15% HAlin were much larger than that of the other gels, including gels containing 15% or higher HAnp, which suggests that the mechanical properties of MeHA gels are better controlled with HA when it is in the nanoparticle form rather than in the linear form. Although the incorporation of HAnp did not have a significant effect on the compressive modulus after 1 day of swelling, after 14 days of swelling, the compressive moduli of the HAnp gels decreased to a range where they were not significant from that of 4% MeHA gels after one day of

swelling. This decrease in the mean values of moduli for the HAnp groups may alert us to the possibility that the HAnp network may be short-lived, although it should be noted that the 4% MeHA gels were disintegrated at two weeks, while the presence of HAnp kept the gels intact. In these particular gels, the HAnp are only physically entrapped in the system, so it is possible that chemically crosslinking the HAnp into the system may preserve and increase the mechanical properties if desirable. Furthermore, although the HAnp network may be short lived, the entire purpose of adding these HAnp into traditional hydrogel precursor solutions is to allow for the precursor solution to achieve paste-like rheological behavior, which is only necessary up until the point of crosslinking the solution. After crosslinking, the paste-like rheology is irrelevant to the network, given that we have shown we do not significantly alter the mechanical properties of the HAnp-incorporated hydrogels in their final crosslinked form.

Finally, rBMSCs encapsulated in these HAnp networks were viable at 4 weeks, which suggests that minimal cytotoxicity is feasible for HAnp-incorporated networks. Furthermore, the 4% MeHA gels with cells remained integrated at 4 weeks, suggesting that the inclusion of cells may be beneficial to the network given the disintegration of acellular 4% MeHA gels within 2 weeks, although it is unknown at this time whether cells were maintaining this network through attachments to the material or through ECM secretion. Although it does appear that there was some cell death in the HAnp networks, due to autofluorescence, the extent of cellular death could not be quantified. However, the goal of cell encapsulation for this study was to show that cells could remain viable in these networks, and future work will in addition consider biochemical content and gene

expression of encapsulated cells to further characterize cellular viability and performance. Additionally, because it is likely that these materials will be crosslinked *in situ,* future *in vivo* work with these materials will evaluate the toxicity of UV light to surrounding tissues. However, UV photocrosslinking has already been successfully performed *in situ* without toxicity concerns associated with UV light.[95]

CONCLUSION

Overall, the present work provides a platform hydrogel system that exhibits a yield stress prior to crosslinking, can recover its network rapidly, and can then be crosslinked into a more rigid hydrogel that is capable of encapsulating cells that remain viable. This behavior holds significant impact for any application of a hydrogel where a paste-like behavior is desired for its precursor solution, including but not limited to healthcare applications. As an example, for applications that cannot tolerate a liquid draining away from an irregularly shaped defect, or spilling from any kind of container at an angle to the direction of gravity, a Herschel-Bulkley or 'paste-like' rheology enables placement of the material prior to crosslinking. The yield stress in this platform system can be tailored by modulating the HAnp and MeHA MW and concentration. Furthermore, the MW of MeHA can be adjusted to result in crosslinked hydrogels of desirable mechanical properties, or alternately the HAnp can be crosslinked into the system. Additionally, the current study employed this system comprised of HA, however this platform hydrogel technology may perhaps be fabricated from other various polymers or biopolymers to suit a variety of

applications where a paste-like material is desirable over a low-viscosity hydrogel precursor solution.

CHAPTER 4: CHONDROINDUCTION FROM NATURALLY-DERIVED CARTILAGE MATRIX: A COMPARISON BETWEEN DEVITALIZED AND DECELLULARIZED CARTILAGE ENCAPSULATED IN HYDROGEL PASTES[‡]

ABSTRACT

Hydrogel precursors are liquid solutions that are prone to leaking after surgical placement. This problem was overcome by incorporating either decellularized cartilage (DCC) or devitalized cartilage (DVC) microparticles into traditional photocrosslinkable hydrogel precursors in an effort to achieve a paste-like hydrogel precursor. DCC and DVC were selected specifically for their potential to induce chondrogenesis of stem cells, given that materials that are chondroinductive on their own without growth factors are a revolutionary goal in orthopedic medicine. We hypothesized that DVC, lacking the additional chemical processing steps in DCC to remove cell content, would lead to a more chondroinductive hydrogel with rat bone marrow-derived mesenchymal stem cells. Hydrogels composed of methacrylated hyaluronic acid and either DCC or DVC microparticles were tested with and without exposure to transforming growth factor (TGF)-β_3 over a 6 week culture period, where swelling, mechanical analysis, and gene expression were observed. For collagen II, Sox-9, and aggrecan expression, MeHA precursors containing DVC consistently outperformed the DCC-containing groups, even when the DCC groups were exposed to TGF-β_3. DVC consistently outperformed all TGF-β_3-exposed

---

[‡]To be submitted as **Beck E.C.**, Barragan M., Libeer T.B., Kieweg S.L., Converse, G.L., Hopkins, R.A., Berkland C.J., and Detamore M.S., Chondroinduction from Naturally-Derived Cartilage Matrix: A Comparison Between Devitalized and Decellularized Cartilage Encapsulated in Hydrogel Pastes, *Biomaterials*, 2015.

groups in aggrecan and collagen II gene expression as well. Additionally, when the same concentrations of MeHA with DCC or DVC microparticles were evaluated for yield stress, the yield stress with the DVC microparticles was 2.7 times greater. Furthermore, the only MeHA-containing group that exhibited shape retention was the group containing DVC microparticles. DVC appeared to be superior to DCC in both chondroinductivity and rheological performance of hydrogel precursors, and therefore DVC microparticles may hold translational potential for cartilage regeneration.

INTRODUCTION

Traditional hydrogels are a promising class of regenerative materials for cartilage regeneration, but they lack the ability to be molded into a defect site by a surgeon because hydrogel precursors are liquid solutions that are prone to leaking after placement.[110, 135] To overcome this drawback, we recently introduced a method to achieve paste-like hydrogel precursor solutions by combining hyaluronic acid nanoparticles with traditional crosslinked hyaluronic acid hydrogels, where the paste-like behavior was induced by the presence of the hyaluronic acid nanoparticles.[5] These hyaluronic acid formulations were then crosslinked to form a rigid traditional hydrogel structure. In an effort to introduce bioactivity to the material, in the current study we substituted the hyaluronic acid nanoparticles for particles made from naturally derived cartilage extracellular matrix (ECM).

ECM-based materials are attractive for regenerative medicine because of their ability to potentially aid in stem cell recruitment, infiltration, and differentiation without

supplementing with additional biological factors.[6, 10, 104] These ECM materials can be obtained from cell-derived matrices secreted during *in vitro* culture or from native tissue,[6, 11, 13, 22, 116, 156] and they have either been decellularized to remove cellular components and nucleic acids or they have been devitalized to kill but not necessarily remove cells within the matrix.[129] We and other groups have already established that cartilage matrix has chondroinductive potential,[11, 15, 41, 73, 115, 128] and we recently were the first to compare the chondroinductive potential of devitalized cartilage (DVC) with decellularized cartilage (DCC) in pellet culture,[128] where we observed that rat bone marrow stem cells (rBMSCs) exposed to DCC outperformed those cells exposed to DVC or TGF-β_3 in chondroinductivity.[128] However, gene expression was only observed over a period of 7 days and was only monitored for cells in pellet culture and not within a 3D scaffold.

Although it is widely emphasized that for ECM-based tissues in general, improper decellularization can result in detrimental inflammatory responses and hinder tissue regeneration,[59] cartilage matrix is uniquely immunoprivileged in part because cartilage matrix is so dense that it protects chondrocytes from T and natural killer cells that are released in graft rejection.[105] Regarding immune response of allogeneic cartilage matrix, the success of Zimmer's DeNovo® product supports the potential for DVC, as DeNovo® relies on juvenile human cartilage donation with living chondrocytes. Therefore, for some cartilage tissue applications, this success with a technology that includes cells brings up the question of whether or not decellularization is even necessary. Although the goal of decellularization is to remove all of the cells without destroying the structure and composition of the ECM, all decellularization processes inevitably cause some disruption

to the matrix architecture, orientation, and surface landscape,[60] which may ultimately limit or hinder the chondroinductive potential of the matrix, especially if the decellularization removes or alters the bioactive molecules that are responsible inducing chondrogenesis.

Therefore, because the long-term chondroinductive potential of DCC and DVC has yet to be explored, the objective of this current work was to compare the chondroinductivity of DVC versus DCC in MeHA hydrogel pastes for 6 weeks *in vitro*. Additionally, another objective was to observe how DVC and DCC affected the rheology of the hydrogel precursors. We hypothesized that a paste-like material composed of DVC would induce superior chondrogenesis compared to DCC and compared to hydrogels exposed to TGF-β_3 or the combination of DCC and TGF-β_3 over the 6 week period.

MATERIALS AND METHODS

Synthesis and Characterization of Methacrylated Hyaluronic Acid (MeHA)

MeHA was prepared by reacting hyaluronic acid (MW 1 MDa, Lifecore Biomedical, Chaska, MN) with 20 fold molar excess glycidyl methacrylate (Sigma-Aldrich, St. Louis, MO) in the presence of triethylamine and tetrabutyl ammonium bromide (Sigma-Aldrich) in a 50:50 water:acetone mixture stirring at 200 rpm for 12 days. MeHA was then dialyzed against deionized (DI) water for two days and then frozen at -80 °C and lyophilized. The degree of methacrylation was determined using ^{1}H NMR (Avance AV-III 500, Bruker) by calculating the ratio of the relative peak area of methacrylate protons to methyl protons.[63]

Tissue Retrieval, Devitalization, and Decellularization

Ten porcine knees obtained from Berkshire hogs (castrated males that were approximately 7-8 months old and 120 kg) were purchased from a local abattoir (Bichelmeyer Meats, Kansas City, KS). Articular cartilage from both the knee and hip joints was carefully removed and collected with a scalpel. The cartilage was rinsed twice in DI water and stored at -20 ºC. After freezing overnight, the cartilage was thawed and then coarsely cryoground with dry ice pellets using a cryogenic tissue grinder (BioSpec Products, Bartlesville, OK). The dry ice was allowed to sublime overnight in the freezer and at this point all of the cartilage was devitalized due to undergoing the freeze/thaw processes. Some of the DVC was saved for the study and the rest was processed to make DCC. To decellularize the cartilage, the coarse ground cartilage was packed into dialysis tubing (3500 MWCO) and decellularized using an adapted version of our previously established method using osmotic shock, detergent, and enzymatic washes.[20] The packets were placed in a hypertonic salt solution (HSS) overnight at room temperature under gentle agitation (70 rpm). The packets were then subjected to 220 rpm agitation with two reciprocating washes, encompassing triton X-100 (0.01% v/v) followed with HSS, to permeabilize intact cellular membranes. The tissue was then treated overnight with benzonase (0.0625 KU ml^{-1}) at 37 ºC and then the tissue was treated with sodium-lauroylsarcosine (NLS, 1% v/v) overnight to further lyse cells and denature cellular proteins. After NLS exposure, the tissue was washed with ethanol (40% v/v) at 50 rpm and then was subjected to organic exchange resins to extract the organic solvents at 65 rpm. The tissue was then washed in saline-mannitol solution at 50 rpm followed by two hours

of rinsing with DI water at 220 rpm. The tissue was then removed from the packets and was then frozen and lyophilized. Both the DVC and DCC were then further cryoground into a fine powder with a freezer-mill (SPEX SamplePrep, Metuchen, NJ) and then lyophilized. The DCC and DVC powders were filtered using a 45 µm mesh (ThermoFisher Scientific, Waltham, MA) to remove large particles and then frozen until use.

Scanning Electron Microscopy

DCC and DVC microparticles were sputter coated with gold and imaged with a Versa 3D Dual Beam (FEI, Hillsboro, OR) to observe their surface morphology and size.

Rat Bone Marrow Stem Cell Harvest and Culture

Rat bone marrow stem cells (rBMSCs) were harvested from the femurs of three male Sprague-Dawley rats (200-250 g) following an approved IACUC protocol at the University of Kansas. The rBMSCs were first harvested in minimum essential medium-α (MEM-α, ThermoFisher) with 10% fetal bovine serum (FBS, MSC qualified, ThermoFisher) and 1% antibiotic-antimycotic (ThermoFisher) and then cultured in this medium for 1 week to ensure no mycotic contamination from harvesting. The rBMSCs were then cultured in MEM-α supplemented with 10% FBS and 1% penicillin/streptomycin (ThermoFisher) until the cells reached passage 4 for cell encapsulation into the hydrogels.

Description of Experimental Groups

The four formulations tested for the cell-based analyses using crosslinked hydrogels were 3% (by weight) MeHA, 3% MeHA + 5% DCC, 3% MeHA + 10% DCC, and 3% MeHA + 10% DVC. Because native extracellular matrix is incorporated into the pastes, acellular formulations of the same four groups were prepared and analyzed with the cellular groups to quantify the acellular biochemical content and to analyze the effect of cells encapsulated in the networks. The 10% concentration was chosen for DCC and DVC because it was the percentage that yielded a moderate yield stress (e.g., 100 Pa) without affecting the ability to crosslink the paste when exposed to UV light. Both the MeHA and MeHA + 10% DCC groups were tested with and without exposure to 10 ng/mL human transforming growth factor-β_3 (TGF-β_3, PeproTech Inc., Rocky Hill, NJ). For the rheological testing prior to crosslinking, additional groups of 2.5% DCC, 5% DCC, and 10% DCC, all of which did not contain MeHA, were tested. DCC and DVC alone cannot be crosslinked into a hydrogel network, which is why these three DCC groups were only tested rheologically.

Preparation of Hydrogel Pastes, Cell Encapsulation, and Hydrogel Culture Conditions

Hydrogel pastes were made first by measuring out the desired weight percents of MeHA, DVC, or DCC into a mini-centrifuge tube. All materials for cellular analyses were then sterilized with ethylene oxide prior to use and were handled under sterile conditions thereafter. All gels were mixed in two stages (e.g., in photoinitiator solution overnight and then more photoinitiator or cell suspension the day of testing) because some of the samples

required mixing with cells and the time it took for MeHA to dissolve to ensure mixture homogeneity (i.e., overnight) was deemed too long for adequate cell survival. Therefore, cell mixtures were added the next day after the MeHA was given a chance to dissolve in half of the final solution. For acellular rheological testing, sterile 0.01M PBS containing 0.05% (w/v) Irgacure (I-2959) photoinitiator was added until the concentration of MeHA and DCC was twice the desired concentration. The samples were mixed, centrifuged, and placed in 4 ºC overnight to allow time for the MeHA to dissolve. Prior to testing, more photoinitiator solution was added until the desired concentration was reached and the samples were again mixed and centrifuged to remove air bubbles. For example, to make a 3% MeHA solution, 12 mg MeHA and 200 µL photoinitiator solution were mixed and allowed to dissolve overnight and then another 200 µL photoinitiator solution was added to make the final concentration at 3% MeHA. For cellular testing, the samples were mixed with 0.1% (w/v) Irgacure photoinitiator in PBS until the concentration of MeHA and DCC was twice the desired final concentration, and then the solutions were centrifuged and stored at 4 ºC overnight. Passage 4 rBMSCs were then suspended at 20 million cells/mL in incomplete chondrogenic medium consisting of high glucose DMEM (ThermoFisher) with 4.5 g/L D-glucose supplemented with 10% FBS, 1% non-essential amino acids, 1% sodium pyruvate, 50 µg/mL ascorbic acid, and 0.25 mg/mL penicillin/streptomycin. This cell solution was then added to the hydrogel paste solutions until the desired concentration of MeHA and DCC or DVC was reached and the final cell concentration and photoinitiator concentrations were 10 million cells/mL and 0.05%, respectively. The solutions were then either tested rheologically or crosslinked with UV light and further characterized as solids.

For gels undergoing crosslinking, hydrogel precursor pastes were loaded into 2 mm thick molds between glass slides and exposed to 312 nm UV light at 3.0 mW/cm^2 in a UV crosslinker (Spectrolinker XL-100, Spectronics Corporation, Westbury, NY) for 2.5 min on each side. Each gel was then cut using a 4 mm biopsy punch and placed in one well of a 24 well, non-tissue culture-treated plate (Corning Incorporated, Corning, NY). Each gel was exposed to 1 mL of incomplete chondrogenic medium or 1 mL of complete chondrogenic medium, which consisted of incomplete chondrogenic medium plus 0.1 mg/mL dexamethasone and 10 ng/mL TGF-β_3. The medium was replaced every other day throughout the 6 weeks of culture.

Rheological Testing of Hydrogel Precursors

Prior to crosslinking the hydrogels, the precursor solutions were loaded into a 3 mL syringe and extruded onto a glass slide to macroscopically observe shape retention. The gels were extruded in a wavy line appearance to observe whether the formulations maintained their shape after crosslinking.

Using an AR-2000 rheometer (TA instruments, New Castle, DE), the oscillatory shear stress of the precursor solutions (n=5) was measured over an oscillatory shear stress sweep of 1-600 Pa at 37 ºC, where the rheometer was equipped with a 20 mm diameter roughened plate and a roughened Peltier plate cover using a gap of 500 µm. Frozen rBMSCs that were thawed and cultured to passage 4 were used to make cellular samples for rheological testing. The pastes were then created as previously mentioned for *in vitro* culture. The yield stress was interpolated from the oscillatory stress at which the storage

(G') and loss (G'') modulus crossed.[142] An oscillatory shear stress sweep of 0.1-10 Pa was performed to assess the linear viscoelastic region of the solutions to determine the value of the storage modulus of each solution.

Mechanical Testing of Crosslinked Hydrogels

The gels were allowed to swell to equilibrium for 1 day in either complete or incomplete chondrogenic medium and mechanical testing was performed at 1 day and 6 weeks. The geometric mean diameter of the gels were first determined using forceps and a stereomicroscope (20x magnification) and the height of each gel was measured directly with a RSA-III dynamic mechanical analyzer (DMA, TA instruments, New Castle, DE). The gels (n=5) were compressed on the DMA at a rate of 0.01 mm/s until mechanical failure and the modulus was calculated as the slope under the linear portion of the stress-strain curve (i.e., 0-10% strain).

Swelling Degree and Volume

To calculate the swelling degree, the swollen gels (swollen to equilibrium) were weighed after 1 day of swelling and then frozen and lyophilized. The dry weight was recorded after lyophilization and the swelling degree was calculated as the ratio of total wet mass to dry mass. The volume of the gels was recorded at 1 day and after 6 weeks of culture and was calculated from the diameter and height of the gels recorded during mechanical testing.

Biochemical Content Analysis

The biochemical content of the MeHA, DVC, and DCC and the biochemical content of the gels at 1 day, 3 weeks, and 6 weeks were quantified (n=5). The gels were digested overnight in a 1.5 mL papain mixture consisting of 125 mg/mL papain from papaya latex), 5 mM N-acetyl cysteine, 5 mM EDTA, and 100 mM potassium phosphate buffered saline at 65 ºC. Because some gels remained undigested, the remaining undigested gels were removed from the digestion medium and redigested overnight at 37 ºC in 0.5 mL hyaluronidase (Sigma-Aldrich, at a concentration of 500 U/mL) in 0.1M PBS. Then 1 mL of fresh papain mixture was added to the hyaluronidase solution and allowed to digest overnight at 65 ºC. Both the first and second digestion solutions were stored at -20 ºC. Prior to biochemical analysis, all digestion solutions were allowed to thaw to room temperature and then vortexed and centrifuged at 10,000 rpm for 10 min to pellet fragments of polymers. The supernatant was then used to quantify biochemical contents. According to manufacturer instructions and using a Cytation 5 Cell-Imaging Multi-Mode reader (Bio-Tek, Winooski, VT), DNA content was quantified with the PicoGreen assay (Molecular Probes, Eugene, OR), glycosaminoglycan (GAG) content was determined with the dimethylmethylene (DMMB) assay (Biocolor, Newtownabby, Northern Ireland) using a chondroitin sulfate standard, and hydroxyproline content was quantified with a hydroxyproline detection kit (Sigma-Aldrich). To obtain the total biochemical content for each gel, each of the two digestions for each gel was quantified and later added together. GAG and hydroxyproline contents were not normalized to DNA and are rather shown in total because of the gels' inherent initial DNA contents.

Gene Expression Analysis

RNA was isolated and purified using Qiagen QIAshredders and an RNeasy Kit (Valencia, CA) according to the manufacturer's guidelines (n=6). A high capacity cDNA reverse transcription kit (Applied Biosystems, Foster City, CA) was used to convert isolated RNA into cDNA. Real-time quantitative polymerase chain reaction (qPCR) was performed using a RealPlex MasterCycler (Eppendorf, Hauppauge, NY) and using TaqMan gene expression assays from Applied Biosystems for Sox-9 (Rn01751070_m1), aggrecan (Rn00573424_m1), collagens type I (Rn01463848_m1) and II (Rn01637087_m1), and GAPDH (Rn01775763_g1). The $2^{-\Delta\Delta Ct}$ method was used to quantify relative expression levels for each gene where the MeHA gels at day 1 were designated as the calibrator group and GAPDH expression was used as the endogenous control.[80] Last, RNA from DVC and DCC (i.e., no rBMSCs) was isolated, converted to DNA, and then PCR was performed with the same previously mentioned TaqMan assays, where it was confirmed that all gene expression observed in the study was due to rBMSCs.

Histological Analysis

Gels at 1 day and cellular gels at 6 weeks were fixed in 10% formalin for 15 min and then embedded in Optimal Temperature Cutting (OCT) medium (TissueTek, Torrance, CA) overnight at 37 °C, frozen at -20 °C, and were sectioned at a thickness of 10 μm using a cryostat (Microm HM-550 OMP, Vista, CA). The sections were stained with the standard Hematoxylin and Eosin (H&E) stain, which stains the nuclei purple and the cytoplasm,

connective tissues, and other extracellular substances red or pink. The sections were stained with the standard Safranin-O/Fast Green stain, which stains negatively charged GAGs orange. The sections were stained immunohistochemically using primary antibodies that target both rat and porcine tissues for collagen I (ThermoFisher, NB600408, 1:200 dilution), collagen II (Abcam, ab34712, 1:200 dilution), and aggrecan (ThermoFisher, MA3-16888, 1:100 dilution). Prior to primary antibody incubation, the slides were fixed in chilled acetone (-20 °C), treated with proteinase K (Abcam), and exposed to 0.3% hydrogen peroxide (Abcam) to suppress endogenous peroxidase activity. Sections were blocked with serum according to the Vectastain ABC kit (Vector Laboratories, Burlingame, CA) following the manufacturer's instructions and then incubated with primary antibody. Following incubation with the primary antibodies, the sections were exposed to biotinylated secondary antibodies (horse anti-rabbit or mouse) and ABC reagent according to the manufacturer's protocol. The antibodies were visualized using the ImmPact DAB peroxidase substrate (Vector), rinsed in DI water, counter stained with VECTOR hematoxylin QS stain, and then dehydrated and mounted. Negative controls consisted of substituting primary antibody exposure with exposure to a rabbit IgG isotype control (for collagen I and II, Abcam, ab27478) at an antibody concentration calculated to be the same used for the corresponding antibodies and omitting the primary antibody for aggrecan.

Statistical Analysis

GraphPad Prism 6 statistical software (GraphPad Software, Inc., La Jolla, CA) was used to compare experimental groups using a one-factor ANOVA (for analyses with one time point) or a two-factor ANOVA (for analyses with two or more time points) followed by a Sidak's *post hoc* test (for two-way ANOVAs with two time points only) or a *Tukey's post hoc* test (for all other ANOVAs), where $p \leq 0.05$ was considered significant. In addition, standard box plots were constructed to eliminate outliers. All quantitative results are reported as mean ± standard deviation within text or as mean + standard deviation within figures.

RESULTS

Characterization of MeHA, DVC, and DCC Microparticles

Analyzing the ratio of the relative peak area of methacrylate protons to methyl protons of MeHA revealed the MeHA had a 1.2% degree of methacrylation and the DNA and hydroxyproline contents were determined to be 9.2 ± 3.7 ng DNA/mg MeHA and 0.74 ± 0.14 µg hydroxyproline/mg MeHA, respectively (Figure 4.1A-C). Because the GAG assay only detects sulfated GAGs, and hyaluronic acid is a non-sulfated GAG, the GAG content of MeHA was not detected. The DNA, GAG, and hydroxyproline contents of DVC were determined to be 1151 ± 51 ng DNA/mg dry DVC, 252 ± 16 µg GAG/mg dry DVC, and 56.1 ± 3.9 µg hydroxyproline/mg dry DVC, respectively (Figure 4.1A-C). Following decellularization and cryogrinding to create DCC powder, there was a 44% reduction in DNA, a 23% reduction in GAG, and a 23% reduction in hydroxyproline ($p<0.05$) (Figure

4.1A-C). In prior work it was established that no significant reduction in biochemical content were observed between native cartilage and cartilage that was cryoground,[128] so the prior mentioned reductions are in reference to DVC powder.

SEM imaging revealed that DVC and DCC microparticles were approximately 45 µm in diameter or smaller and were noted to be heterogeneous in size and morphology (Figure 4.1D). The DCC microparticles were observed to have smoother surfaces overall in comparison to the DVC microparticles (Figure 4.1D). Under higher magnification, observing the surface morphology revealed a grain-like appearance to the surface of the DCC microparticles that was not observed on the DVC microparticles (Figure 4.1D).

Macroscopic Observation and Rheological Testing of Hydrogel Precursor Pastes

Macroscopic observation of hydrogel precursor formulations revealed non-Newtonian and paste-like behavior in precursors containing at least 5% DCC (Figure 4.2). Shape retention after extrusion through a 3 mL syringe, which was indicated by the fluid retaining the diameter of the syringe orifice after extrusion and after crosslinking, was noted in the 10% DCC and MeHA + DVC acellular groups (Figure 4.2). The remaining solutions spread out to 2-3 times the diameter of the syringe orifice. All formulations containing MeHA were able to be crosslinked to maintain extrusion shape.

Solutions exhibiting a measurable yield stress were the 10% DCC, MeHA + 10% DCC, and MeHA + DVC formulations (Figure 4.3A). The 10% DCC had a yield stress of 143 ± 33 Pa, while adding MeHA to 10% DCC reduced the yield stress to 92 ± 88 Pa, although the reduction was not significant. The yield stress of the MeHA + DVC group

was 2.7 and 1.7 times greater than that of the MeHA + 10% DCC and 10% DCC groups, respectively ($p<0.05$) (Figure 4.3A).

All of the groups exhibited viscoelastic behavior, as indicated by a measurable storage modulus. However, the storage modulus of the MeHA + DVC group was significantly higher than all of the other groups at 1240 ± 520 Pa, which was 58, 2.4, 2.6, and 8.8 times higher than the MeHA + 5% DCC, 10% DCC, MeHA + 10% DCC, and the cellular MeHA + 10% DCC cellular groups, respectively, which were the groups that had a storage modulus greater than 20 Pa ($p<0.05$) (Figure 4.3B).

Mechanical Testing of Crosslinked Hydrogels

One day after crosslinking, all of the groups except for the acellular MeHA group had a compressive modulus significantly higher than that of the MeHA group ($p<0.05$), which had a compressive modulus of 1.94 ± 0.13 kPa (Figure 4.4). The compressive modulus of the MeHA + DVC group was 6.82 ± 0.79 kPa (Figure 4.4), which was 3.5, 2.2, and 1.8 times larger than the MeHA, MeHA + 5% DCC, and MeHA + 10% DCC groups, respectively ($p<0.05$). Furthermore, the modulus of the MeHA + DVC group was 2.3 and 1.7 times larger than that of the MeHA + TGF-β_3 and MeHA + 10% DCC + TGF-β_3 groups, respectively. Finally, the moduli of the MeHA + DVC and MeHA + TGF-β_3 groups were 1.7 and 1.6 times respectively larger than their acellular controls ($p<0.05$).

At 6 weeks, the MeHA + 5% DCC acellular group, both cellular groups composed of MeHA + 10% DCC, and the DVC groups had at least 4 times larger compressive moduli than that of the MeHA group, which had a compressive modulus of 0.31 ± 0.13 kPa

($p<0.05$). The MeHA + DVC group had a compressive modulus of 2.964 ± 0.056 kPa, which was 9.1 times larger than that of the MeHA group ($p<0.05$), but was not significantly different from the MeHA + 10% DCC + TGF-β_3 group. The modulus of the MeHA + 10% DCC + TGF-β_3 group was 2.55 ± 0.39 kPa, which was 2 times larger than its acellular control ($p<0.05$). The MeHA + DVC acellular group had a compressive modulus of 2.40 ± 0.44 kPa, which was 1.9 times larger than that of the MeHA + 10% DCC group ($p<0.05$) (Figure 4.4).

Over the 6 week culture period, all of the groups had a significant reduction in their compressive moduli ($p<0.05$). However, while the acellular MeHA, MeHA, and MeHA + TGF-β_3 groups experienced 90%, 83%, and 73% respective reductions in their compressive moduli over the culture period ($p<0.05$), all of the other groups experienced less than 65% reductions in their respective compressive moduli ($p<0.05$). At 6 weeks, the compressive modulus of the MeHA + 10% DCC + TGF-β_3 was 37% less than its original value at 1 day ($p<0.05$), while the modulus of its respective acellular group was 64% less than its original value ($p<0.05$) (Figure 4.4).

Swelling and Volume Analysis of Crosslinked Hydrogel Pastes

After swelling to equilibrium for 24 hours, the swelling degree of the MeHA group was 34 ± 13 (Figure 5A). The only groups that had significantly smaller swelling degrees were the MeHA + 10% DCC acellular group and the MeHA + DVC acellular and cellular groups, which had swelling degrees of 17.9 ± 3.1, 15.6 ± 1.3, and 13.27 ± 0.88, respectively ($p<0.05$) (Figure 4.5A).

At 1 day after crosslinking, none of the gel volumes deviated significantly from the MeHA group, which had a volume of 40.5 ± 2.7 µL ($p<0.05$) (Figure 4.5B). However, at 6 weeks after crosslinking, the MeHA group had a volume of 82.7 ± 11.6 µL. The volumes of the MeHA + 5% DCC, MeHA + 10% DCC, and MeHA + DVC were 26%, 31.5%, and 43% lower than that of the MeHA group, respectively ($p<0.05$) (Figure 5B). In addition, the volume of the MeHA + TGF-β_3 group was 20.5% and 21.2% lower than that of the MeHA acellular and cellular groups, respectively ($p<0.05$). The DVC group was not significantly different from the MeHA + 10% DCC + TGF-β_3 group, but the volume of the MeHA + 10% DCC + TGF-β_3 group was 31% less and 20% less than the MeHA + TGF-β_3 and the MeHA + 10% DCC groups, respectively.

Over the 6 week culture period, the volumes of all gels, with the exception of the MeHA + 10% DCC + TGF-β_3 and the acellular MeHA + DVC groups, increased significantly ($p<0.05$). The volume of the MeHA group increased by 2.1 times compared to its original volume, while the volumes of the MeHA + TGF-β_3, the MeHA + 5% DCC, and the MeHA + 10% DCC groups only increased by 49%, 47%, and 45%, respectively ($p<0.05$) (Figure 4.5B).

Biochemical Content of Crosslinked Hydrogels

All of the cellular groups had significantly higher DNA contents than their respective acellular groups at all time points ($p<0.05$). At one day after crosslinking, the MeHA + 10% DCC group had 570 ± 130 ng DNA per gel, and the only gels with a significantly different DNA content from this group were the MeHA + 10% DCC + TGF-

β_3 and MeHA + DVC groups, which had DNA contents 45% and 82% higher per gel, respectively ($p<0.05$) (Figure 4.6A). There was no significant difference between the MeHA + 10% DCC + TGF-β_3 and MeHA + DVC groups, however. At 3 weeks after crosslinking, the MeHA + DVC group had a DNA content of 386 ± 73 ng DNA per gel, which was 36%, 49%, and 35% less than the MeHA + TGF-β_3, MeHA + 5% DCC, and MeHA + 10% DCC + TGF-β_3 groups, respectively ($p<0.05$) (Figure 4.6A). There was no significant difference between the MeHA + DVC group and the MeHA + 10% DCC group, however. After 6 weeks of culture, the MeHA + 5% DCC group contained 1.8 times more DNA than the MeHA + 10% DCC group ($p<0.05$) (Figure 4.6A). However, no other cellular groups were significantly different from the MeHA + 10% DCC group. Over the course of the 6 week culture period, all of the cellular groups had a significant reduction in DNA content ($p<0.05$), where the DNA content in the MeHA, MeHA + TGF-β_3, MeHA + 5% DCC, MeHA + 10% DCC, MeHA + 10% DCC + TGF-β_3, and MeHA + DVC groups reduced by 45%, 31%, 16%, 43%, 38%, and 55% compared to their original DNA contents, respectively ($p<0.05$). The acellular groups did not have any significant reduction in DNA content over the culture period (Figure 4.6A).

All of the groups with DCC and DVC had significantly higher initial GAG contents at day 1 than that of the MeHA group ($p<0.05$), which had a GAG content of 15.5 ± 4.6 µg GAG per gel. Compared to the MeHA group, the GAG contents of the MeHA + 5% DCC, MeHA + 10% DCC, and MeHA + DVC groups were 4.9, 6.3, 6.7, and 12.9 times larger, respectively (Figure 4.6B). At day 1, the GAG content of the MeHA + DVC group was 16.6% higher than its respective acellular group ($p<0.05$). Furthermore, the GAG content

of the MeHA + DVC group was 15, 2.1, and 1.9 times larger than the MeHA + TGF-β_3, MeHA + 10% DCC, and the MeHA + 10% DCC + TGF-β_3 groups, respectively. At 3 weeks, all of the groups with DCC and DVC contained significantly larger GAG contents than the MeHA group ($p<0.05$), which had a GAG content of 12.5 ± 4.6 µg GAG per gel. The GAG contents of the MeHA + 5% DCC, MeHA + 10% DCC, and MeHA + DVC groups were 3.2, 4, 3.6, and 4.1 times larger than that of MeHA, respectively (Figure 4.6B). In addition, the GAG content of the MeHA + DVC group was 52% less than its respective acellular control ($p<0.05$). Furthermore, there were no significant differences among the MeHA + DVC, the MeHA + 10% DCC + TGF-β_3, and the MeHA + 10% DCC groups. At 6 weeks, again all of the groups with DCC and DVC contained significantly larger GAG contents than the MeHA group ($p<0.05$), which had a GAG content of 1.7 ± 1.2 µg GAG per gel. Compared to the MeHA group, the GAG content of the MeHA + 5% DCC, MeHA + 10% DCC, and MeHA + DVC groups were 17, 24, 20, and 29 times larger, respectively (Figure 4.6B). The GAG content of the MeHA + DVC group was 48% less than its respective acellular control ($p<0.05$), but there were no significant differences among the MeHA + DVC, the MeHA + 10% DCC + TGF-β_3, and the MeHA + 10% DCC groups. Over the 6 week culture period, all of the groups with DCC and DVC had significant reductions in GAG content, where the GAG contents of the MeHA + 5% DCC acellular and cellular groups, the MeHA + 10% DCC acellular, cellular, and TGF-β_3-exposed groups, and the acellular and cellular MeHA + DVC groups, reduced by 54%, 62%, 69%, 58%, 66%, 44%, and 75%, respectively.

Furthermore, all of the groups with DCC and DVC had significantly higher initial hydroxyproline contents at day 1 than that of the MeHA group ($p<0.05$), which had a hydroxyproline content of 2.57 ± 0.23 µg hydroxyproline per gel. Compared to the MeHA group, the hydroxyproline contents of the MeHA + 5% DCC, MeHA + 10% DCC, and MeHA + DVC groups were 15, 32, 34, and 43 times larger, respectively (Figure 4.6C). At day 1, the hydroxyproline content of the MeHA + DVC group was 1.3 times higher than that of the MeHA + 10% DCC group ($p<0.05$). Additionally, the MeHA + 10% DCC group contained 2.1 times the amount of hydroxyproline of the MeHA + 5% DCC group ($p<0.05$). At 3 weeks, all of the DCC and DVC groups contained significantly larger hydroxyproline contents than the MeHA group ($p<0.05$), which contained 1.90 ± 0.40 µg hydroxyproline per gel. Compared to the MeHA group, the hydroxyproline contents of the MeHA + 5% DCC, MeHA + 10% DCC, and MeHA + DVC groups were 16, 36, 33, and 29 times larger, respectively (Figure 4.6C). In addition, the hydroxyproline content of the MeHA + DVC group was 27.4% less than its respective acellular control ($p<0.05$) and the MeHA + 10% DCC group contained 2.2 times the amount of hydroxyproline found in the MeHA + 5% DCC group ($p<0.05$). However, there were no significant differences among the MeHA + DVC, the MeHA + 10% DCC, and the MeHA + 10% DCC + TGF-β_3 groups. At 6 weeks, again all of the groups with DCC and DVC contained significantly larger hydroxyproline contents than that of the MeHA group ($p<0.05$), which contained 1.64 ± 0.24 µg hydroxyproline per gel. Compared to the MeHA group, the hydroxyproline contents of the MeHA + 5% DCC, MeHA + 10% DCC, and MeHA + DVC groups were 21, 49, 34, and 38 times larger, respectively (Figure 4.6C). The hydroxyproline content of the MeHA +

10% DCC group was 2.4 and 1.5 times larger than the MeHA + 5% DCC and MeHA + 10% DCC + TGF-β_3 groups, respectively ($p<0.05$). However, there was no significant difference between the MeHA + DVC and the MeHA + 10% DCC + TGF-β_3 groups. Over the 6 week culture period, the groups that did not have a significant reduction in hydroxyproline content were all three MeHA groups, both MeHA + 5% DCC groups, and the MeHA + 10% DCC group. The hydroxyproline content of the MeHA + DVC group reduced to 56% of its original content over the 6 weeks ($p<0.05$).

Gene Expression

Throughout the entire culture period, the MeHA + 5% DCC and MeHA + 10% DCC groups never expressed collagen II. At 1 day, the rest of the groups did not have any significant differences. At 1 week, the MeHA + TGF-β_3 group did not express collagen II, and there were no significant differences in expression between the remaining groups. At 2 weeks, the only groups expressing collagen II were the MeHA + 10% DCC + TGF-β_3 and the MeHA + DVC groups, although the difference between them was not significant. At 3 weeks and 6 weeks, the only group expressing collagen II was the MeHA + DVC group, which had a relative collagen II expression that was 180 and 320 times larger than the calibrator group (i.e., MeHA group at day 1), respectively ($p<0.05$) (Figure 4.7A).

At 1 day, the DCC containing groups had at least 98% less collagen I expression than the MeHA group ($p<0.05$) (Figure 4.7B). By 2 weeks, the relative collagen I expression of MeHA + DVC increased to 304 times the MeHA group value. However, that expression significantly decreased by 86% at 3 weeks, but was still 99 times larger than

the relative expression of the MeHA group. Although the collagen I expression reduced significantly from 1 day to 1 week for both the cellular and acellular MeHA groups ($p<0.05$), the collagen I expression for these and all groups but the MeHA + DVC groups remained steady the rest of the 6 weeks.

The MeHA + TGF-β_3 and MeHA + DVC groups had significantly higher Sox-9 expression than the groups containing DCC from 1 day to 3 weeks, where the relative expression was 2 and 1.3 times the MeHA group, respectively at day 1, and was 3.7 and 3 times larger than the MeHA group at 3 weeks ($p<0.05$) (Figure 4.7C). At 6 weeks, the DVC group had significantly higher Sox-9 expression than all other groups, where its expression was 4.4 and 109 times higher than the MeHA + TGF-β_3 and the MeHA + 10% DCC + TGF-β_3 groups, respectively ($p<0.05$).

At day 1, the relative aggrecan expression of the DCC containing groups was significantly lower than the MeHA group, whereas the relative expression of MeHA + DVC group was 2 times higher than the MeHA group ($p<0.05$) (Figure 4.7D). Over the culture period, both the cellular and acellular MeHA groups significantly reduced their aggrecan expression, however the MeHA + DVC group remained significantly higher than MeHA and all DCC groups over the 6 weeks ($p<0.05$). Additionally, the MeHA + DVC group's relative aggrecan expression was 2, 17, 22, 34, and 410 times higher than that of MeHA at 1 day, 1 week, 2 weeks, 3 weeks, and 6 weeks, respectively ($p<0.05$). Lastly, the relative aggrecan expression of the MeHA + DVC group at 6 weeks was 80 and 585 times higher than that of the MeHA + TGF-β_3 and the MeHA + 10% DCC + TGF-β_3 groups, respectively.

Histological Evaluation

Saf-O staining did not reveal an increase in Saf-O staining intensity over the culture period. However, at 6 weeks, some nodular Saf-O staining was noted in the MeHA + TGF-β_3 group (Figure 4.8). All DCC and DVC containing groups stained for collagen II; however, no changes were noted in the location and intensity of collagen II staining over the culture period (Figure 4.8). Collagen I staining was noted again in all of the DCC and DVC containing groups. However, the intensity of collagen I staining decreased over the culture period for the MeHA + 5% DCC and MeHA + 10% DCC groups (Figure 4.8). The intensity of the collagen I staining appeared to increase slightly for the MeHA + DVC group. This slight increase in intensity was noted near and within the DVC microparticles. Aggrecan staining was noted in all DCC and DVC containing groups, where notably the aggrecan staining became more intense near the DCC and DVC microparticles in the MeHA + 10% DCC + TGF-β_3 and MeHA + DVC groups over the culture period (Figure 4.8).

DISCUSSION

We have introduced not only a method to overcome the drawbacks of implanting hydrogels *in situ* (i.e., leaking from the defect site), but in addition, we have introduced a method to induce chondrogenesis of cells encapsulated within the networks. Previous studies have explored the chondrogenic potential of DCC and DVC.[13, 14, 92, 109, 155, 161] Cheng *et al.*[14] reported using a porous cartilage matrix composed of homogenized and then

lyophilized DVC matrix, of which chondrogenesis was observed even without growth factor supplementation. However, these matrices succumbed to cell-mediated contraction, but when the matrices were further crosslinked with genipin, they found the materials did not exhibit contraction and were chondroinductive.[13] The same group infiltrated cartilage matrix with woven poly(ε-caprolactone) and observed cartilaginous matrix production.[92] Zheng *et al.*[161] reported using DCC to create nanofibrous ECM scaffolds that induced MSC chondrogenesis. Our group was the first to explore the short-term chondrogenic potential of DCC versus DVC.[128] However, for the first time in this current study, not only were DVC and DCC compared for their long-term chondrogenic potential, they were evaluated for their ability to exhibit a yield stress in hydrogel precursor solutions. In this current study, chondrogenesis was induced through incorporating native cartilage ECM into the MeHA/cartilage matrix gel networks, which furthermore resulted in the paste-like behavior and yield stress that was observed prior to crosslinking. The yield stress denotes the threshold where a solution transitions between an elastic solid and a pseudoplastic liquid, and exhibiting a yield stress is crucial because it will prevent the hydrogel precursor from flowing away, keeping the material at the site of interest until crosslinking. In a surgical context, a material that exhibits a yield stress would allow a surgeon to appropriately shape and contour the material to the defect site before crosslinking it in place. The paste-like precursor solutions were able to obtain yield stresses of over 200 Pa with MeHA mixed with DVC microparticles. For context, the yield stress for a common paste-like material such as toothpaste is approximately 200 Pa. However, we did not achieve toothpaste consistency with the incorporation of DCC microparticles although we still did note that

these materials did have a yield stress. Although at this point without further testing, it is uncertain why the DCC microparticles did not impart as high of a yield stress on the pastes as the DVC microparticles, the SEM images revealed subtle differences between the DCC and DVC, which may provide clues to understanding the observed rheological differences. A grain-like appearance was noted only on the DCC and that the DCC microparticles had in general, smoother surfaces than the DVC microparticles. Because it is known that decellularization can result in changes in matrix architecture and surface ligand landscape,[60] it is possible that these entities were altered in the decellularization process, and thus the decellularization process may have played a role in the reduction of yield stress that we observed. It was noted that the yield stress of DCC microparticles alone was higher than the yield stress of MeHA combined with the DCC, and this reduction in yield stress when MeHA and particles were combined differs from what was noted in previous work, where a 3.4-fold increase was observed in the yield stress of hyaluronic acid nanoparticles combined with MeHA in comparison to the nanoparticles alone, where the MeHA alone had no measurable yield stress.[5] That work suggested that the hyaluronic acid nanoparticles had some physical or chemical interactions with the MeHA in addition to the interactions with the other nanoparticles, whereas in the current study, the interactions between particles and MeHA were likely negligible. Of concern is that when rBMSCs were mixed in with the DCC group, the precursor had no measurable yield stress, although it still exhibited some viscoelastic behavior, evident by its measurable storage modulus and macroscopically observed non-Newtonian behavior. Last, although it was not performed in the current study, future quantification of syringeability would be of value.

In addition to DVC having superior rheological properties, the DVC invoked superior chondroinductivity in comparison to DCC microparticles. For collagen II, Sox-9, and aggrecan expression, the MeHA + DVC group repeatedly outperformed the DCC containing groups, even when the DCC groups were exposed to TGF-β_3. Interestingly, we only performed a mild decellularization by removing only 44% of the initial DNA, 23% of the initial GAG, and 23% of the initial hydroxyproline and even though the initial biochemical contents were not drastically altered, the cellular response to these materials was severely affected. The current finding of DVC outperforming DCC in chondroinduction is in contradiction to our previously reported increase in chondroinductivity of DCC over DVC,[128] but we hypothesize the differences between the previous and current study is that currently, rBMSCs were encapsulated within a 3D scaffold rather than studied in pellet culture, and the long term gene expression over a 6 week period rather than only 1 week as in the prior study was observed. Moreover, under biochemical and histological analysis, other than a slight increase in aggrecan staining near the cartilage microparticles over the 6 week culture period, significant tissue synthesis overall was not observed, which suggests that although the cells may have been chondroinduced, they were not actively secreting large amounts of cartilage matrix. However, it is possible that some of the matrix was being remodeled, so a net increase in the amount of staining could not be observed even though matrix secretion might have been present. Ultimately, without further testing, it still remains unclear as to whether decellularization is necessary for cartilage tissue engineering.

The question of whether or not decellularization is needed is complex and will depend upon each application of cartilage ECM. It has been established that cells exposed to a target ECM will more easily differentiate toward the target tissue,[44, 121] where one of the reasons for this ECM specific differentiation may be because native ECM may have the potential to retain the growth factors that will steer the differentiation toward the specific target tissue.[6] Decellularizing cartilage ECM may not only alter the matrix architecture, but it may furthermore remove some of these important growth factors, affecting the bioactivity of the cartilage ECM. Furthermore, altering the architecture may hinder growth factor retention. For example, proteoglycans, specifically aggrecan in cartilage matrix, are well known for how they affect the mechanical properties of tissues and found extensively in native cartilage matrix, are thought to be a reservoir of several growth factors,[17, 57] and thus, the preservation of these proteoglycans may be crucial to successful tissue regeneration. Therefore, although we are still at the beginning stages of determining the appropriate ECM processing protocol for cartilage tissue, it may prove to be ideal to use unaltered, non-decellularized cartilage tissue for certain applications. Applications such as cell-derived matrix, where cartilage ECM can be grown from a patient's own cells,[129] would not need to be decellularized since the tissue source would be autogenous. Additionally, through the successful use of allograft cartilage as evidenced by the success of current allograft products like Zimmer's DeNovo®, if the cartilage tissue would be used for articular cartilage applications, it may not need to be decellularized.

However, on the opposing side of whether or not to decellularize cartilage tissue are cases where cartilage is being used for bone regeneration via endochondral ossification.

In these applications where the cartilage will be more exposed to host immunogenic cells,[42] decellularization may be necessary. Additionally, decellularization may be necessary for cartilage derived from xenogeneic sources. In the current study, we used porcine cartilage as proof of concept for comparing DCC to DVC. However, ultimately it may or may not be desired to use xenograft sources for future work. Using xenografts comes with its own challenges, such as the need to remove the alpha-Gal epitope, a carbohydrate found within xenograft ECM that is known to cause graft failure if not successfully removed.[129]

Although graft failure can be caused through biochemical entities, it is possible for graft failure to occur biomechanically. For this reason, we tested the mechanical and swelling properties of DCC and DVC-incorporated hydrogel networks after crosslinking. Native cartilage is approximately 80% water, which equates to a swelling degree of approximately 5, and has an elastic compressive modulus ranging from 240-1000 kPa.[2, 76, 85] However, it must be noted that the biomechanical properties can vary depending on parameters such as the method of testing, the strain rate of testing, and cartilage zone depth.[49] In this work, the swelling degree was significantly lowered from over 30 to between 10 and 20 by incorporating 10% DCC or DVC. For tissue engineering, it is neither desired for scaffold constructs to swell from the defect site, nor is it desirable for the constructs to shrink within the defect site, because in both instances it can cause disintegration of the scaffold with host tissue, and thus may hinder cartilage regeneration.[13] In the current study, it was noted that the inclusion of DVC resulted in the gels retaining their original volumes throughout culture. However, it was noted that the elastic compressive moduli obtained in the current study (ranging from approximately 2 to 8 kPa

at day 1) were nowhere near that of native cartilage. Including DCC and DVC with MeHA significantly increased the compressive modulus and encapsulation of DVC and cells together significantly increased the compressive modulus. Therefore, in the current study, although incorporating DVC and DCC may prove to be beneficial for tissue engineering, to ultimately obtain mechanical properties to that of native cartilage ECM, it may be necessary to increase the degree of methacrylation or to change the photocrosslinkable polymer to a polymer that has an inherently higher compressive modulus.[114]

CONCLUSION

ECM-based materials are gaining widespread attention in the regenerative medicine field and they continue to show great promise toward cartilage regeneration applications. In the current study, cartilage matrix microparticles not only induced cells to differentiate toward a chondrogenic lineage, but they concurrently provided the hydrogel precursor solutions with a yield stress (i.e., paste-like consistency), which translates to a tremendous advantage for material placement in clinical applications. Additionally, although significant emphasis has been placed on the necessity to decellularize ECM components that are used in regenerative medicine products, we challenged that paradigm by providing the first direct comparison of the long-term bioactivity of DCC and DVC and thereby demonstrating that DVC may be superior in promoting chondrogenesis over DCC. Moreover, DVC consistently outperformed all TGF-β_3-exposed groups in aggrecan and collagen II gene expression, which may present significant advantages in cost and

regulatory approval of chondroinductive strategies for cartilage regeneration.[127] Certainly future work will need to address improving the mechanical properties and overall matrix production, where *in vivo* studies will be paramount, because immunogenicity as well as how biomechanical stimulation of DCC and DVC may affect chondroinductivity and therefore, hyaline-like cartilage regeneration can be tested. Furthermore, the reproducibility and shelf life of these materials must be tested since the heterogeneity of cartilage matrix and differences in the quality of cartilage ECM from one hog to another may vary and may affect the ability to reproduce similar particles every time. Overall, the results of this study suggest that devitalized cartilage may be a promising chondroinductive material for some cartilage tissue engineering strategies.

CHAPTER 5: APPROACHING THE COMPRESSIVE MODULUS OF ARTICULAR CARTILAGE WITH A DECELLULARIZED CARTILAGE-BASED HYDROGEL[§]

ABSTRACT

ECM-based materials are appealing for tissue engineering strategies because they may promote stem cell recruitment, cell infiltration, and cell differentiation without the need to supplement with additional biological factors. Cartilage ECM has recently shown potential to be chondroinductive, particularly in a hydrogel-based system, which may be revolutionary in orthopedic medicine. However, hydrogels composed of natural materials are often mechanically inferior to synthetic materials, which is a major limitation for load-bearing tissue applications. The objective was therefore to create an unprecedented hydrogel composed entirely of native cartilage ECM that was both mechanically more similar to native cartilage tissue and capable of inducing chondrogenesis. Porcine cartilage was decellularized, solubilized, and then methacrylated and UV photocrosslinked to create methacrylated solubilized decellularized cartilage (MeSDCC) gels. Methacrylated gelatin (GelMA) was employed as a control for both biomechanics and bioactivity. Rat bone marrow-derived mesenchymal stem cells were encapsulated in these networks, which were cultured *in vitro* for 6 weeks, where chondrogenic gene expression, the compressive modulus, swelling, and histology were analyzed. One day after crosslinking, the elastic compressive modulus of the 20% MeSDCC gels was 1070 ± 150 kPa. Most notably, the

---

[§]To be submitted as **Beck E.C.**, Barragan M., Tadros M.H., Gehrke S.H., and Detamore M.S., Approaching the Compressive Modulus of Articular Cartilage With a Decellularized Cartilage-Based Hydrogel, *Biomaterials*, 2015.

stress strain profile of the 20% MeSDCC gels fell within the 95% confidence interval range of native porcine cartilage. Additionally, MeSDCC gels significantly upregulated chondrogenic genes compared to GelMA as early as day 1 and supported extensive matrix synthesis as observed histologically. Given that these gels approached the mechanics of native cartilage tissue, supported matrix synthesis, and induced chondrogenic gene expression, MeSDCC hydrogels may be promising materials for cartilage tissue engineering applications. Future efforts will focus on improving fracture mechanics as well to benefit overall biomechanical performance.

INTRODUCTION

Arthritis is one of the leading causes of disability among US adults.[94] Some of the current clinical treatments include autologous chondrocyte implantation, mosiacplasty, and microfracture.[3, 50] However, not only do these treatments involve high risk of donor site morbidity and/or the need for multiple surgeries, these treatments still lack the ability to regenerate fully functional cartilage tissue.[13, 64, 127] Tissue engineering approaches are therefore striving to fully regenerate cartilage tissue by utilizing a bioactive and bioresorbable construct that provides the necessary cues to facilitate cell growth, differentiation, and tissue integration, while providing the mechanical integrity and support to allow the tissue to sustain its load bearing function.[50]

Hydrogels have several advantages in cartilage tissue engineering, which include ease of formation, the ability to fine tune mechanical properties, the ability to encapsulate cells, and vast array of conjugation options for degradability, bioactivity, etc.[9, 23, 33]

Hydrogels can be made from both synthetic (e.g., polyethylene glycol) and natural materials (e.g., collagen, gelatin), where both have their own inherent advantages and disadvantages. Synthetic materials have the advantage of the ability to more readily control the composition and mechanical properties of the hydrogel compared to hydrogels composed of natural materials, but natural materials have the additional advantage of providing biochemical cues and signals to facilitate cell attachment, growth, and differentiation.[148]

One such natural material that is gaining attention in tissue engineering approaches is naturally derived extracellular matrix.[129] ECM materials can either be obtained from cell-derived matrices that are secreted during *in vitro* culture or they can be derived directly from native tissue,[6, 11, 13, 22, 116, 156] and often they have been decellularized to remove cellular components and nucleic acids that may have the potential to cause an adverse immunological response.[129] We and other groups have already established that decellularized cartilage has chondroinductive potential,[11, 15, 41, 73, 115, 128] and we recently reported the chondroinductive potential of decellularized cartilage (DCC) in pellet culture,[128] where we observed increased chondroinductivity of rat bone marrow stem cells (rBMSCs) exposed to DCC as compared to those cells only exposed to TGF-β_3.[128]

Therefore, in this study we endeavored to create a material that was entirely composed of DCC to potentially make the material inherently chondroinductive, and we furthermore endeavored to design a material would have the mechanical properties necessary to be load-bearing. Several studies have made gels entirely out of ECM by first solubilizing the ECM, where the solubilized matrix would form a gel at body

temperature.[40, 41, 43, 120] One group even utilized solubilized cartilage matrix gels for drug delivery, where they noted that the gel maintained enough structural integrity under physiological conditions to be a stable drug depot.[70] We tried using solubilized cartilage hydrogels, but the gels that formed were too compliant and left opportunity for improvement for load-bearing applications. Methods of crosslinking unsolubilized cartilage have been reported, including crosslinking cartilage ECM with genipin, dehydrothermal treatment, ultraviolet irradiation, and carbodiimide chemistry.[13, 109] Using these methods, cartilage scaffolds were able to be crosslinked and maintained some mechanical integrity throughout culture where cell mediated contraction was able to be controlled depending on the method of crosslinking. However, the authors of these previous studies noted that the constructs would require additional reinforcements to attain functional biomechanical properties and additionally, a sole ECM content of 10% was used to make the gels. In the current study, we sought to overcome this limitation through solubilizing and further crosslinking cartilage tissue. The rationale for solubilizing the cartilage tissue was to provide more control over mechanical properties through the ability to more finely tune the solid content of the hydrogel. Furthermore, solubilizing the cartilage may free up more reactive sites for crosslinking on the cartilage ECM, which may help reinforce the biomechanical properties of the solubilized cartilage once it is crosslinked. Therefore, based on our experience of functionalizing GAGs such as hyaluronic acid and chondroitin sulfate with glycidyl methacrylate,[5, 63] which allows the hydrogel to be formed through photocrosslinking, we decided to methacrylate solubilized, decellularized cartilage ECM. Earlier in 2015, one pioneering study reported methacrylating solubilized cartilage

matrix to make photocrosslinkable hydrogels, demonstrating for the first time that native tissues can be crosslinked to form hydrogels.[141] However, in that study, the solubilized cartilage matrix was mixed with methacrylated gelatin (GelMA) and the biomechanics of the hydrogels, evaluated via the compressive modulus, still fell short of native cartilage tissue. Garrigues *et al.*[41] cleverly reinforced solubilized cartilage ECM through combining it with poly(ε-caprolactone) and then electrospinning it into a scaffold. However, the Young's moduli of the cartilage-containing electrospun scaffolds were approximately 10 kPa, which again fall short of the biomechanics of native cartilage tissue. In this current study, the goal was to create the first hydrogel entirely composed of solubilized cartilage ECM without additional reinforcements. We hypothesized that this MeSDCC hydrogel would have a compressive modulus comparable to native cartilage and would be chondroinductive. Therefore, solubilized cartilage hydrogels were photocrosslinked and their mechanics as well as chondroinductive potential were analyzed.

METHODS AND MATERIALS

Tissue Retrieval, Devitalization, and Decellularization

Ten porcine knees obtained from Berkshire hogs (castrated males that were approximately 7-8 months old and 120 kg) were purchased from a local abattoir (Bichelmeyer Meats, Kansas City, KS). Articular cartilage from the knee and hip joints was carefully removed and collected using scalpels. The cartilage was then rinsed twice in DI water and stored at -20 ºC. After freezing overnight, the cartilage was thawed and then coarsely ground with dry ice using a cryogenic tissue grinder (BioSpec Products,

Bartlesville, OK). Coarse grinding was performed to reduce diffusion distances during the decellularization process. The dry ice was then allowed to evaporate overnight in the freezer, at which point the cartilage was referred to as devitalized cartilage (DVC),[129] and then the DVC was packed into dialysis tubing (3500 MWCO) and decellularized using an adapted version of our previously established method using osmotic shock, detergent, and enzymatic washes.[20] The packets were placed under gentle agitation (70 rpm) in a hypertonic salt solution (HSS) overnight at room temperature. The packets were then subjected to 220 rpm agitation with two reciprocating washes of triton X-100 (0.01% v/v) followed with HSS to permeabilize intact cellular membranes. The tissue was then treated overnight with benzonase (0.0625 KU ml^{-1}) at 37 ºC and then with sodium-lauroylsarcosine (NLS, 1% v/v) overnight to further lyse cells and denature cellular proteins. After NLS exposure, the tissue was washed with ethanol (40% v/v) at 50 rpm and then was subjected to organic exchange resins at 65 rpm to extract the organic solvents. The tissue was then washed in saline-mannitol solution at 50 rpm followed by two hours of rinsing with DI water at 220 rpm. The tissue was then removed from the packets and was then frozen and lyophilized. The cartilage was then cryoground into a fine powder with a freezer-mill (SPEX SamplePrep, Metuchen, NJ) and was lyophilized overnight. The decellularized cartilage powder was then filtered using a 45 µm mesh (ThermoFisher Scientific, Waltham, MA) to remove large particles and then frozen until use.

Synthesis and Characterization of MeSDCC and GelMA

DCC powder was first solubilized using an adapted protocol from a previously reported method.[119] DCC powder was first mixed in 0.1M HCl at a concentration of 10mg DCC per 1 mL HCl. Pepsin was then added at a concentration of 1mg/mL and the solution was stirred at 200 rpm for 2 days at room temperature. The solution was then brought back to physiological pH, verified with litmus paper, by adding 1M NaOH. The solubilized DCC powder (SDCC) was then centrifuged at 10,000 x *g* for 3 min and the supernatant was frozen and lyophilized and used to make methacrylated SDCC (MeSDCC).

MeSDCC was prepared by reacting SDCC with 20 fold molar excess glycidyl methacrylate (Sigma-Aldrich, St. Louis, MO) in the presence of trimethylamine and tetrabutyl ammonium bromide (Sigma-Aldrich). The reaction solution was a 1:3 acetone:water mixture, which was stirred at 200 rpm at a concentration of 1 g SDCC for every 150 mL solution. The molar excess was approximated based on reacting one glycidyl methacrylate group to every monomer present in the solution and with the assumption that all monomers were hyaluronic acid. The reaction continued stirring for 6 days, the MeSDCC was then precipitated in excess acetone, dialyzed for 2 days in DI water, and then lyophilized. Methacrylated gelatin (GelMA) was made with the same protocol used to make MeSDCC, except Type A gelatin from porcine skin (Sigma-Aldrich) was used in the reaction instead of SDCC. Methacrylation was confirmed using ^{1}H NMR (Avance AV-III 500, Bruker).

Rat Bone Marrow Stem Cell Harvest and Culture

Rat bone marrow stems cells (rBMSCs) were harvested from both femurs of five male Sprague-Dawley rats (200-250 g) following an approved University of Kansas IACUC protocol (AUS #175-08). The rBMSCs were first harvested in minimum essential medium-α (MEM-α, ThermoFisher) supplemented with 10% fetal bovine serum (FBS, MSC qualified, ThermoFisher) and 1% antibiotic-antimycotic (anti-anti, ThermoFisher) and were then cultured in this medium for one week to ensure no mycotic contamination from harvesting. After 1 week of culture, the anti-anti was substituted for 1% penicillin/streptomycin (ThermoFisher) and the cells were cultured in this medium until they reached passage 4 for cell encapsulation into the hydrogels.

Description of Experimental Groups

Formulations tested in the 6 week culture were both cellular and acellular formulations of 10% GelMA, 10% MeSDCC, and 20% MeSDCC (w/v). In addition, acellular GelMA was tested at a concentration of 20% under mechanical compression and swelling at day 1. Acellular formulations were prepared and analyzed with the cellular groups to quantify the acellular biochemical content and to analyze the effect of cells encapsulated in the networks. A concentration of 10% for GelMA and MeSDCC was chosen as it was a concentration previously reported in literature, and it was verified in our preliminary studies by evaluation of a wide range of concentrations.[141] A concentration of 20% was chosen as that is the approximate concentration of dry mass in native cartilage matrix.[85]

Preparation of Hydrogels, Cell Encapsulation, and Hydrogel Culture Conditions

Hydrogels were made by first measuring out the desired weight percents of either GelMA or MeSDCC into a 50 mL centrifuge tube. The tubes with the weighed materials were then sterilized with ethylene oxide prior to use and from then on were handled under sterile conditions. All gels were mixed in two stages (e.g., in photoinitiator solution overnight and then more photoinitiator or cell suspension the day of testing). This two-stage mixing process was used because some of the samples required mixing with cells and the time it took for MeSDCC to dissolve to ensure mixture homogeneity (i.e., overnight) was deemed too long for adequate cell survival. Therefore, cell suspensions were added the next day after the MeSDCC was given a chance to dissolve in half of the final solution. For acellular testing, the first stage of mixing involved adding sterile 0.01 M PBS containing 0.05% (w/v) Irgacure (I-2959) photoinitiator until the concentration of MeSDCC or GelMA was twice the desired concentration. The acellular samples were then mixed, centrifuged at 3000 rpm, and stored at 4 ºC overnight to allow time for the MeSDCC to dissolve. Prior to testing, more photoinitiator solution was added to the acellular samples until the desired concentration was reached. The samples were then mixed again and centrifuged to remove air bubbles. For example, to make a 10% MeSDCC solution, 40 mg MeSDCC and 200 µL photoinitiator solution were mixed and allowed to dissolve overnight, and then another 200 µL photoinitiator solution was added to make the final concentration at 10% MeSDCC. For cellular testing, the first stage of mixing involved adding 0.1% (w/v) Irgacure photoinitiator in PBS until the concentration of MeSDCC or

GelMA was twice the desired final concentration, and then the solutions were centrifuged and stored at 4 ºC overnight. Passage 4 rBMSCs were then suspended at 10 million cells/mL in incomplete chondrogenic medium consisting of high glucose DMEM (ThermoFisher) with 4.5 g/L D-glucose supplemented with 10% FBS, 1% non-essential amino acids, 1% sodium pyruvate, 50 μg/mL ascorbic acid, and 0.25 mg/mL penicillin/streptomycin. We refer to incomplete chondrogenic medium as medium that did not contain growth factors. The cell suspension in incomplete chondrogenic medium was then added to the cellular samples until the desired concentration of MeSDCC or GelMA was reached and the final cell concentration and photoinitiator concentration was 5 million cells/mL and 0.05%, respectively. Both cellular and acellular solutions were then loaded into 2 mm thick molds between glass slides and exposed to 312 nm UV light at 3.0 mW/cm^2 in a UV crosslinker (Spectrolinker XL-100, Spectronics Corporation, Westbury, NY) for 2.5 min on each side. Each gel was then cut using a 4mm biopsy punch and placed in one well of a 24 well, non-tissue culture-treated plate (Corning Incorporated, Corning, NY). Each gel was exposed to 1 mL of incomplete chondrogenic medium, which was replaced every other day throughout the 6 weeks of culture.

Mechanical Testing of Crosslinked Hydrogels and Native Cartilage

The gels were allowed to swell to equilibrium for 24 hours in incomplete chondrogenic medium and mechanical testing was performed at 1 day and 6 weeks. The geometric mean diameter of the gels was first determined using forceps and a stereomicroscope (20x magnification) and the height of each gel was measured directly

with a RSA-III dynamic mechanical analyzer (DMA, TA instruments, New Castle, DE). The gels (n=5) were compressed until mechanical failure at a rate of 0.01 mm/s (i.e., 0.6% strain/s) until and the compressive modulus was calculated as the slope of the linear portion of the stress-strain curve (i.e., 4-10% strain).

To compare the compressive modulus to that of native porcine cartilage, cylindrical samples of native articular cartilage obtained from the load-bearing region of the femoral head of the same porcine tissue harvested to make MeSDCC, were cut to the same height as the gel samples using scalpels and were then cut to the appropriate diameter using a 4 mm biopsy punch. Methacrylated hyaluronic acid (MeHA) gels were tested on the DMA as a control. MeHA was prepared by reacting hyaluronic acid (MW 1 MDa, Lifecore Biomedical, Chaska, MN) with 20 fold molar excess glycidyl methacrylate (Sigma-Aldrich) in the presence of triethylamine and tetrabutyl ammonium bromide (Sigma-Aldrich) in a 50:50 water:acetone mixture stirring at 200rpm for 12 days. MeHA was then dialyzed against deionized (DI) water for two days and was frozen and lyophilized. The degree of methacrylation was determined to be 1.2% using ^{1}H NMR (Avance AV-III 500, Bruker) by calculating the ratio of the relative peak area of methacrylate protons to methyl protons.[63] MeHA was mixed to a 3% concentration using the same two step procedure as described prior and samples were cut using a 4 mm biopsy punch and were allowed to swell to equilibrium for 24 hours before testing on the DMA.

Swelling Degree and Volume

Gels were swollen to equilibrium for 24 hours and the swollen weight was recorded. The gels were then frozen and lyophilized. The dry weight was then recorded and the swelling degree was calculated as the ratio of total wet mass to dry mass. Gel volume was calculated at 1 day and 6 weeks from the diameter and height of the gels that were recorded during mechanical testing.

Biochemical Content Analysis

The biochemical content of the initial DVC, DCC, SDCC, MeSDCC, and GelMA materials as well as the biochemical content of the gels at 1 day, 3 weeks, and 6 weeks of culture were quantified (n=5). The materials and gels were digested in a 1.5 mL papain mixture consisting of 125 mg/mL papain from papaya latex), 5 mM N-acetyl cysteine, 5 mM EDTA, and 100 mM potassium phosphate buffered saline at 65 ºC overnight. The digestion solutions were stored at -20 ºC until further testing. Prior to biochemical analysis, all digestion solutions were allowed to thaw to room temperature and then vortexed and centrifuged at 10,000 rpm for 10 min to pellet polymer fragments and the supernatant was then used to quantify biochemical contents. Using a Cytation 5 Cell-Imaging Multi-Mode reader (Bio-Tek, Winooski, VT), the DNA content was quantified with the PicoGreen assay (Molecular Probes, Eugene, OR), the glycosaminoglycan (GAG) content was analyzed with the dimethylmethylene (DMMB) assay (Biocolor, Newtownabby, Northern Ireland), and hydroxyproline content was determined with a hydroxyproline detection kit (Sigma-Aldrich), all according to the manufacturer's instructions. GAG and

hydroxyproline contents were not normalized to DNA and are rather shown in total because of the gels' inherent initial GAG and hydroxyproline contents.

Gene Expression Analysis

Using Qiagen QIAshredders and an RNeasy Kit (Valencia, CA) according to the manufacturer's guidelines, RNA was isolated and purified (n=6). The isolated RNA was converted into cDNA using a high capacity cDNA reverse transcription kit (Applied Biosystems, Foster City, CA). Real-time quantitative polymerase chain reaction (qPCR) was performed using a RealPlex MasterCycler (Eppendorf, Hauppauge, NY) and TaqMan gene expression assays from Applied Biosystems, which included Sox-9 (Rn01751070_m1), aggrecan (Rn00573424_m1), collagens type I (Rn01463848_m1) and II (Rn01637087_m1), and GAPDH (Rn01775763_g1). The $2^{-\Delta\Delta Ct}$ method was used to quantify relative expression levels for each gene where the 10% GelMA gels at day 1 were designated as the calibrator group and GAPDH expression was used as the endogenous control.[80] Finally, RNA from DVC and DCC only (i.e., no rBMSCs) was isolated, converted to DNA, and then PCR was performed with the same previously mentioned TaqMan assays, where it was confirmed that all gene expression observed in the study was that of the rBMSCs.

Histological Analysis

Both cellular and acellular gels at day 1 and cellular gels from 6 weeks were analyzed histologically. These gels were first fixed in 10% formalin for 15 min, were

embedded in Optimal Temperature Cutting (OCT) medium (TissueTek, Torrance, CA) overnight at 37 °C, and were then frozen at -20 °C. Sections were cut at a thickness of 10 µm using a cryostat (Micron HM-550 OMP, Vista, CA). The sections were then stained with the standard Hematoxylin and Eosin (H&E) stain, which stains the cytoplasm, connective tissues, and other extracellular substances red or pink and stains the nuclei purple. The sections were stained for GAGs with the standard Safranin-O/Fast Green (Saf-O) stain, where the GAGs stain orange in color. Lastly, the sections were stained immunohistochemically using primary antibodies that target both rat and porcine tissues for collagen I (ThermoFisher, NB600408, 1:200 dilution), collagen II (Abcam, ab34712, 1:200 dilution), and aggrecan (ThermoFisher, MA3-16888, 1:100 dilution). Prior to primary antibody incubation, the slides were first fixed in chilled acetone (-20 °C) and then treated with proteinase K (Abcam). The slides were then exposed to 0.3% hydrogen peroxide (Abcam) to suppress endogenous peroxidase activity. The sections were then blocked with serum according to the manufacturer's instructions in the Vectastain ABC kit (Vector Laboratories, Burlingame, CA) and were then incubated with primary antibody. Then the sections were exposed to biotinylated secondary antibodies (horse anti-rabbit and mouse) and ABC reagent according to manufacturer protocol. The antibodies were visualized using the ImmPact DAB peroxidase substrate (Vector), and then the sections were rinsed in DI water, counter stained with VECTOR hematoxylin QS stain, and then dehydrated and mounted. Exposure to a rabbit IgG isotype control (for collagen I and II, Abcam, ab27478) at an antibody concentration calculated to be the same used for the

corresponding antibodies or omitting the primary antibody (for aggrecan) was used as the negative control.

Statistical Analysis

Statistics were performed on GraphPad Prism 6 statistical software (GraphPad Software, Inc., La Jolla, CA). A one-factor ANOVA was used for analyses with one time point and a two-factor ANOVA was used for analyses with two or more time points. Both ANOVAs were followed by either a Sidak's *post hoc* test (for two-way ANOVAs with two time points only) or a *Tukey's post hoc* test (for all other ANOVAs), where $p \leq 0.05$ was considered significant. In addition, outliers were eliminated by constructing standard box plots. All quantitative results are reported as mean ± standard deviation within the text or as mean + standard deviation within the figures. Select significant differences between groups are highlighted in the Results section, with complete statistically significant differences reported in the figures.

RESULTS

Characterization of Initial DVC, DCC, MeSDCC, and GelMA DNA and Matrix Content

Success of the methacrylation procedure for both MeSDCC and GelMA was confirmed via ^{1}H NMR by the emergence of methacrylate peaks between 5 and 6.5 ppm (Figure 5.1A-B). The success of the methacrylation procedure was further confirmed with the formation of crosslinked GelMA and MeSDCC gels (Figure 5.1C). The DNA, GAG,

and hydroxyproline contents of DVC were determined to be 1151 ± 51 ng DNA/mg dry DVC, 252 ± 17 µg GAG/mg dry DVC, and 56.1 ± 3.9 µg hydroxyproline/mg dry DVC, respectively (Figure 5.2). Following decellularization and cryogrinding, there was a 44% reduction in DNA, a 23% reduction in GAG, and a 23% reduction in hydroxyproline ($p<0.05$) (Figure 5.2). After solubilizing and after methacrylating, the DNA content further reduced to 4% and 1.7% of that of the original DVC DNA content, respectively ($p<0.05$), although there were no significant reductions in GAG content through the solubilization and methacrylation procedure. Following solubilization, the hydroxyproline content was reduced by 25% compared to DCC, and then increased by 59% after the methacrylation procedure compared to SDCC ($p<0.05$). The DNA, GAG, and hydroxyproline contents of GelMA were 10.10 ± 0.81 ng DNA/mg dry GelMA, 8 ± 15 µg GAG/mg dry GelMA, and 71.9 ± 1.0 µg hydroxyproline/mg dry GelMA, respectively (Figure 5.2).

Mechanical Testing of Crosslinked Hydrogels

One day after crosslinking, the compressive modulus of the 10% GelMA was 55 ± 10 kPa, whereas that of the 10% MeSDCC and 20% MeSDCC groups were 5.3 and 20 times larger, respectively ($p<0.05$) (Figure 5.3A). Furthermore, the compressive modulus of the 20% MeSDCC group was 3.7 times larger than that of the 10% MeSDCC group ($p<0.05$). In addition, the modulus of the 20% MeSDCC acellular group was 2.3 and 3.4 times larger than that of the 10% MeSDCC and 20% GelMA acellular groups, respectively ($p<0.05$).

Six weeks after crosslinking, the compressive modulus of the 20% MeSDCC group was 560 ± 310 kPa, which was 7.4 and 3.0 times larger than that of the 10% GelMA and 10% MeSDCC groups, respectively ($p<0.05$) (Figure 5.3A).

Over the 6 weeks of culture, the only groups that significantly deviated from their original compressive modulus were the 20% MeSDCC groups, where the modulus of the 20% MeSDCC acellular and cellular groups reduced by 30% and 48%, respectively ($p<0.05$) (Figure 5.3A). Additionally, the modulus of the 10% GelMA group increased by 37% over the 6 week culture period, although the increase was not significant.

The stress-strain profiles of native porcine cartilage samples were compared with that of the 20% MeSDCC, 20% GelMA acellular, and 3% MeHA groups, where the 95% confidence intervals were compared at each level of strain tested. The only stress-strain profile that fell within the 95% confidence interval of the native porcine cartilage was that of the 20% MeSDCC group until it began to fracture at 7.5% strain (Figure 5.3B).

Swelling and Volume Analysis

The only group that had a significantly different swelling degree than 10% GelMA, which had a swelling degree of 8.6 ± 1.2 after swelling to equilibrium, was the 10% MeSDCC acellular group, which had a swelling degree 56% higher than that of 10% GelMA ($p<0.05$) (Figure 5.4A). In addition, all 20% GelMA and MeSDCC groups had between 15% and 38% lower swelling degrees than that of the 10% MeSDCC cellular and acellular groups, where the swelling degrees of 20% GelMA, 20% MeSDCC acellular and

20% MeSDCC groups were 34%, 19%, and 15% lower than 10% MeSDCC ($p<0.05$) (Figure 5.4A).

At one day after crosslinking and swelling to equilibrium, the gel volumes of the 20% GelMA and all MeSDCC gels were significantly higher than that of 10% GelMA ($p<0.05$) (Figure 5.4B). The 10% MeSDCC group had a volume of 20.24 ± 0.47 µL, while the 20% MeSDCC group had a volume 9.6% greater. These 10% and 20% MeSDCC groups in turn had volumes that were 17% and 29% higher than that of 10% GelMA, respectively ($p<0.05$).

At 6 weeks after crosslinking, the volume of the 20% MeSDCC group was 21.8 ± 1.2 µL, which was 14% and 9.3% higher than that of 10% MeSDCC and 10% GelMA, respectively ($p<0.05$) (Figure 5.4B). In addition, the volume of the 20% MeSDCC group was 92% of its acellular control ($p<0.05$).

Over the course of the 6 weeks, the only group that had a significant change in volume was the 10% MeSDCC acellular group, which experienced an 11% reduction in volume ($p<0.05$).

Biochemical Content Analysis

As expected, all cellular groups had significantly higher DNA contents than their respective acellular groups at all time points ($p<0.05$) (Figure 5.6A). At 1 day after hydrogel formation, the 10% GelMA group contained 650 ± 160 ng DNA per gel, and the only gel with a significantly different DNA content was the 20% MeSDCC group, which had 21% more DNA per gel ($p<0.05$) (Figure 5.5A). At 3 weeks after crosslinking, the

20% MeSDCC group had a DNA content of 833 ± 88 ng DNA per gel, which was 3.2 and 1.7 times higher than that of the 10% GelMA and 10% MeSDCC groups, respectively ($p<0.05$) (Figure 5.5A). After 6 weeks of culture, the 20% MeSDCC group contained 660 ± 80 ng DNA per gel, which was 2.1 and 1.3 times higher than that of the 10% GelMA and 10% MeSDCC groups, respectively ($p<0.05$) (Figure 5.5A). Over the course of the 6 week culture period, all cellular groups had a significant reduction in DNA content ($p<0.05$), where the DNA content in the 10% GelMA, 10% MeSDCC, and 20% MeSDCC groups reduced by 51%, 30%, and 16%, respectively ($p<0.05$). The acellular groups did not have any significant reduction in DNA content over the culture period (Figure 5.5A).

Throughout the culture period, there was no detectable level of GAG in the 10% GelMA group (Figure 5.5B). At 1 day after crosslinking, the GAG content of the 10% MeSDCC group was 74 ± 23 µg GAG per gel, and the GAG content of the 20% MeSDCC group was 92% higher ($p<0.05$) (Figure 5.5B). At 3 weeks, the GAG content of the 10% MeSDCC group was 22.3 ± 7.6 µg GAG per gel, which was not significantly different from the 20% MeSDCC group (Figure 5.5B). In addition, the GAG content of the 20% MeSDCC group was 55% less than its respective acellular control ($p<0.05$). At 6 weeks, the GAG content of the 10% MeSDCC group was 23.7 ± 9.2 µg GAG per gel, and the GAG content of the 20% MeSDCC group was 4.1 times larger ($p<0.05$). In addition, the GAG content of the 10% MeSDCC group was 68% less than that of its respective acellular control ($p<0.05$). Over the 6 week culture period, both the 10% MeSDCC group and the 20% MeSDCC groups experienced 68% and 32% reductions in GAG content, respectively ($p<0.05$) (Figure 5.5B).

Finally, at 1 day, the initial hydroxyproline content of 10% GelMA was 108 ± 11 µg hydroxyproline per gel, where that of the 20% MeSDCC group was 66% higher ($p<0.05$) (Figure 5.5C). At 3 weeks, the 10% GelMA group contained 111 ± 19 µg hydroxyproline per gel, which was 53% higher than that of the 10% MeSDCC group and 22% lower than that of the 20% MeSDCC group ($p<0.05$). Furthermore, the 20% MeSDCC group contained 95% more hydroxyproline than that of the 10% MeSDCC group ($p<0.05$). At 6 weeks, the hydroxyproline content of the 10% GelMA group was 118 ± 17 µg per gel, which was 44% higher than that of the 10% MeSDCC group ($p<0.05$). Furthermore, the hydroxyproline content of the 20% MeSDCC group was 80% higher than that of the 10% MeSDCC group ($p<0.05$). Over the 6 week culture period, the only group that experienced a significant loss in hydroxyproline was the 20% MeSDCC group, where the hydroxyproline loss was 18% ($p<0.05$) (Figure 5.5C).

Gene Expression Analysis

At 1 day after crosslinking, the relative Sox-9 expression of 10% MeSDCC and 20% MeSDCC were 8.5 and 3.4 times larger than that of 10% GelMA ($p<0.05$) (Figure 5.6A). The relative Sox-9 expression of the 10% MeSDCC group was 2.5 times larger than that of the 20% MeSDCC group ($p<0.05$). At 1 week, the relative Sox-9 expression of the 10% GelMA group was 2.6 times larger than that of the 20% MeSDCC group ($p<0.05$). For the rest of the study, there were no significant differences in Sox-9 expression among groups within each time point. From 1 day to 1 week, the relative Sox-9 expression of the 10% GelMA group increased by a factor of 2.5 ($p<0.05$), but then decreased by 54% from

1 week to 2 weeks ($p<0.05$), and did not change significantly thereafter. From 1 day to 1 week, the relative Sox-9 expression of the 10% MeSDCC group decreased by 69% ($p<0.05$), and then further decreased by 80% from 1 week to 2 weeks ($p<0.05$). The relative Sox-9 expression of the 10% MeSDCC group did not change significantly after 2 weeks. Last, the relative Sox-9 expression of the 20% MeSDCC group decreased by 72% from 1 day to 1 week ($p<0.05$) and did not change significantly thereafter (Figure 5.6A).

The relative aggrecan expression of 10% MeSDCC and 20% MeSDCC were 6.5 and 2.8 times higher than that of 10% GelMA, respectively at 1 day ($p<0.05$) (Figure 5.6B). There were no significant differences among groups at each time point thereafter. By 1 week, the relative aggrecan expressions of 10% GelMA, 10% MeSDCC, and 20% MeSDCC were reduced by 85%, 96%, and 89%, respectively, compared to their expression levels at 1 day ($p<0.05$), and there were no significantly different changes in expression thereafter.

The 10% MeSDCC and 20% MeSDCC groups had 8.1 and 2.9 fold higher relative collagen II expressions at 1 day ($p<0.05$), and by 1 week, the relative aggrecan expression of the 10% MeSDCC group was 2.7 times higher than that of 10% GelMA ($p<0.05$). Furthermore, at one week, the relative collagen II expression of the 10% MeSDCC group was 2.7 times higher than that of the 20% MeSDCC group. There were no significant differences among groups at each time point thereafter and collagen II expression was not detected at all at 6 weeks (Figure 5.6C). Over the culture period, there were no significant changes in collagen II expression for the 10% GelMA group, but the relative collagen II expression of the 10% MeSDCC group decreased by 73% from 1 day to 1 week ($p<0.05$),

and then it did not change significantly thereafter. The relative collagen II expression of the 20% MeSDCC group decreased by 81% from 1 day to 1 week ($p<0.05$), was not detectable at 2 weeks, but was detectable at 3 weeks, although the expression level at 3 weeks was not significantly different from the expression level detected at 1 week (Figure 5.6C).

The relative collagen I expressions of the 10% MeSDCC and 20% MeSDCC groups were 23% and 67% lower than that of the 10% GelMA group at day 1, respectively ($p<0.05$) (Figure 5.6D). There were no significant differences among groups observed thereafter within each time point in the culture period. From 1 day to 1 week, the relative collagen expression levels of the 10% GelMA, 10% MeSDCC, and 20% MeSDCC groups decreased by 94%, 93%, and 72%, respectively ($p<0.05$), and did not change significantly thereafter (Figure 5.6D).

Histological Analysis

H&E staining revealed regions of tissue growth within the 10% MeSDCC and 20% MeSDCC groups at 6 weeks. Saf-O did not stain for GAGs in any of the 10% GelMA stains; however, an increase in Saf-O staining intensity was notably observed over the 6 week culture period in the 10% and 20% MeSDCC groups, particularly in the regions surrounding rBMSCs (Figure 5.7). All MeSDCC groups stained for collagen II, although no increase in collagen II staining intensity was observed for those groups. However, the 10% GelMA group had an increase in collagen II staining intensity over the culture period (Figure 5.7). Collagen I staining was noted in the 10% GelMA group, although there were

no significant changes in staining over the culture period and minimal collagen I staining was observed in the other groups (Figure 5.7). Finally, the 10% GelMA and the 20% MeSDCC groups had a slight increase in aggrecan staining over the culture period (Figure 5.7).

DISCUSSION

In the current study, we were the first to create hydrogels derived entirely from solubilized cartilage ECM and test their chondroinductivity. ECM-based materials are attractive for tissue engineering strategies because they can potentially aid in stem cell recruitment, cell infiltration, and cell differentiation without supplementing with additional biological factors.[6, 10, 104] However, one of the major limitations of using natural polymers in hydrogels is their reduced mechanical integrity.[133] While native human articular cartilage has an elastic compressive modulus ranging from 240-1000 kPa,[2, 76, 85] the compressive modulus of hydrogels composed of natural materials are typically an order of magnitude less than native cartilage tissue.[133] However, it must be noted that biomechanical properties of cartilage can vary depending on parameters such as the method of testing, the strain rate of testing, and cartilage zone depth.[49] Although certainly other mechanical properties have been explored and analyzed in cartilage tissue engineering, including the aggregate modulus, hydraulic permeability, and fracture stress,[133, 150] in the current study the compressive modulus and the overall stress-strain profile of the gel constructs were the primary emphases. Gels composed entirely of crosslinked solubilized cartilage matrix were created that had a compressive modulus in the same range of values

reported for native cartilage. The 20% MeSDCC gels had a compressive modulus of 1070 ± 150 kPa after one day of culture, which was more than 3 fold higher than that of the 20% GelMA acellular group. Furthermore, when the 95% confidence intervals of the stress strain profiles of the 20% MeSDCC gels were compared to native porcine cartilage, it was found that the stress strain profile of the 20% MeSDCC gels actually fell within the confidence interval of native cartilage, and they were the only gels to do so. Although the 20% gels fractured early at 7.5% strain, the fact that they fell within the stress strain profile of native cartilage tissue was promising. Clinically, these results could potentially translate to a surgeon being able to inject the paste into a cartilage defect and then crosslink the paste into a gel, allowing the patient to walk after the procedure. Certainly the early fracture stress needs to be addressed, however.[150] Modifications to the hydrogel may be made such as increasing the solid content or methacrylation efficiency, to improve the fracture stress. At this stage, due to not knowing the exact biochemical content of MeSDCC, the degree of methacrylation could not be calculated through the NMR spectra, so this is one limitation of using MeSDCC as a hydrogel material. However, the ability to modulate the mechanical properties through the solid content is a tremendous advantage compared to crosslinking cartilage particles, where the solid content would be confined due to particles only crosslinking in the vicinity of other particles.

The mechanical properties of MeSDCC hydrogels may be able to be improved through mechanical stimuli *in vivo*, as mechanical stimulation alone is known to induce chondrogenesis.[140] Therefore, once the material is implanted *in vivo*, there could be less of a decrease in the compressive modulus long-term like what was observed after 6 weeks of

in vitro culture in the current study. However, superior matrix synthesis was observed in the MeSDCC gels over the GelMA gels even *in vitro* via hematoxylin and eosin staining and Saf-O staining, even though the biochemical content analysis did not show an increase in the amount of matrix produced. This could be due to the cells assisting in the biodegradation and remodeling of the ECM, whereby even though some matrix is being lost, new matrix is simultaneously being formed. Low overall matrix production is consistent with findings from Visser *et al.;*[141] however, they observed an increase in collagen I expression when exposed to MeSDCC as opposed to the current study, where a decrease in collagen I expression was noted while exposed to MeSDCC in reference to GelMA gels.

Compared to GelMA gels, a significant increase in collagen II, Sox-9, and aggrecan expression was observed in the MeSDCC gels. Although a significant reduction in all chondrogenic gene expression was noted after 1 day, this reduction does not necessarily mean aggrecan and collagen II synthesis stopped. GelMA is widely used in the field of tissue engineering for its low cost, its abundant cell adhesion sites, and for its ability to support chondrocyte differentiation.[114, 141] Therefore, it is possible that all gels had sufficient cartilage ECM production and the low chondrogenic gene expression levels were low only in reference to GelMA at day 1, the calibrator group. Through collagen II IHC analysis for example, the GelMA gels were noted to have an increase in collagen II staining at 6 weeks compared to day 1, even though the collagen II expression after 1 day was significantly reduced. Because the MeSDCC gels contained so much collagen II initially, it was difficult to discern any new collagen II production, but at least the relative level of

collagen II staining remained the same throughout culture. It must be noted that an increase in matrix synthesis and an increase in chondrogenic gene expression at day 1 was observed without any growth factor supplementation. ECM-based materials, like these MeSDCC hydrogels, are attractive for regenerative medicine because of their ability to potentially aid in stem cell recruitment, infiltration, and differentiation without supplementing with additional biological factors.[6, 10, 104, 129] The ability to cause some differentiation shows great promise in using these materials for cartilage tissue engineering and may even make these gels more economical than using other natural materials such as hyaluronic acid or gelatin.[127]

Of note was the limited removal of DNA in a mild decellularization process, which may need to be addressed in future work if it is deemed that a higher degree of decellularization is required for successful cartilage regeneration *in vivo*. However, non-decellularized products, such as Zimmer's DeNovo® product, rely on the immunoprivileged environment and so far there have been no reports to the best of our knowledge of allograft rejection or disease transmission even though the product is composed of living allogeneic cells. Additionally, although the DeNovo® product is composed of human juvenile cartilage, it has been observed to create hyaline-like cartilage in goats, where no T-cell-mediated response was noted.[1] Furthermore, even though the decellularization process in the current study only removed 44% of the DNA, the DNA content of the SDCC and MeSDCC was reduced to 4% and 1.7% of that of the original DVC DNA content, respectively ($p<0.05$). At this stage, it is unknown whether the solubilization and methacrylation process were removing DNA, or if the DNA was

modified to a degree where the PicoGreen assay could no longer detect the DNA. Due to the low pH and pepsin exposure during the solubilization process, the DNA would likely be denatured to a single-stranded state and would in addition, be hydrolyzed and further degraded.[88] Furthermore, the dialysis step after methacrylation would likely remove these degraded DNA segments and low molecular weight nucleotides and amino acids, leaving behind higher molecular weight methacrylated GAGs and collagen. Future work will certainly need to address how solubilization and methacrylation affect cartilage DNA and other biochemical contents and how they affect the retained growth factors. However, depending on the application of MeSDCC gels, decellularization may not even be necessary.

In addition to mechanics and gene expression, the swelling and volume of the materials were analyzed throughout culture. One major concern of using hydrogels for tissue engineering is cell-mediated contraction of the gel construct throughout culture.[13, 141] Contraction of gels can cause disintegration with host tissue, which could potentially hinder successful cartilage regeneration and may even dislodge the hydrogel from the defect site. In the current study, however, the only gels that had a significant reduction in volume were the 20% MeSDCC gels, where the gels only reduced in volume by 2%, which is unlikely a concern for cartilage tissue engineering applications. In addition to volume, the swelling of the materials is important as well due to a drastic increase in swelling after surgical placement is undesirable. The swelling degree was significantly lowered by increasing the amount of material in the hydrogels from 10% to 20%, which is to be expected since additional material would increase the solid content.

CONCLUSION

We created crosslinkable hydrogels composed entirely of native cartilage ECM. The cartilage was first solubilized and then methacrylated to create photocrosslinkable gels. Compared to the traditional GelMA hydrogels, these MeSDCC gels supported rBMSC growth, ECM production, caused significant upregulation of chondrogenic genes at 1 day after crosslinking, and remarkably, the mechanics of the MeSDCC gels were characteristically similar to that of native porcine cartilage until their failure. The concentration of MeSDCC was found to affect chondroinduction and mechanical properties, where the 20% MeSDCC gels were superior in mechanical performance and promoting ECM synthesis, while the 10% MeSDCC gels were superior in chondroinduction. Future work will address improving the fracture mechanics, and chondrogenesis and immune compatibility *in vivo*. In the current study, we have shown that MeSDCC may prove to be a promising biomaterial for cartilage tissue engineering applications.

CHAPTER 6: CHONDROINDUCTIVE HYDROGEL PASTES COMPOSED OF NATURALLY DERIVED DEVITALIZED CARTILAGE[**]

ABSTRACT

Hydrogels have several advantages for cartilage tissue engineering, but hydrogel precursors are liquid solutions that are prone to leaking from the defect site once implanted *in vivo*. In prior work, we addressed this drawback by adding hyaluronic acid nanoparticles to traditional photocrosslinkable polymers to induce paste-like behavior in hydrogel precursors, and the hydrogel precursors could then be crosslinked to form rigid hydrogel networks. In the current study, the objective was not only to create a hydrogel precursor that exhibited a yield stress, but to additionally create a chondroinductive biomaterial for cartilage tissue engineering applications. Given that cartilage extracellular matrix (ECM) has recently become known for its chondroinductive potential, devitalized cartilage ECM (DVC) were mixed with DVC that had been solubilized and methacrylated (MeSDVC) as a new two-component hydrogel precursor solution. Precursors composed of 10% MeSDVC and 10% MeSDVC with 10% DVC were evaluated rheologically and then photocrosslinked and further characterized as solids. The crosslinked gels contained encapsulated rat bone marrow stem cells (rBMSCs) and were cultured *in vitro* for 6 weeks in incomplete chondrogenic medium (i.e., no growth factors), where the MeSDVC + DVC gels were exposed to both incomplete and complete (i.e., addition of TGF-β_3) chondrogenic

---

[**]To be submitted as **Beck E.C.**, Barragan M., Tadros M.H., Kieweg, S.L., and Detamore M.S., Chondroinductive Hydrogel Pastes Composed of Naturally Derived Devitalized Cartilage, *Annals of Biomedical Engineering*, 2015.

media. The compressive modulus, gene expression, biochemical content, swelling, and histology of the gels were analyzed. Prior to crosslinking, non-Newtonian behavior was observed in all hydrogel precursors and a yield stress of over 1800 Pa was observed when MeSDVC and DVC particles were combined. The DVC-containing gels repeatedly outperformed the MeSDVC-only group in chondrogenic gene expression, especially at 6 weeks, where the relative collagen II expression of the DVC-containing groups with and without TGF-β_3 exposure was 40 and 78 fold higher, respectively, than that of MeSDVC alone. Of translational relevance, DVC-containing groups did not have any significant cell-mediated contraction, while the MeSDVC gels contracted 18% over the culture period. Future work will address the combinations of DVC and MeSDVC that yield mechanics closer to that of native cartilage tissue and will test for chondrogenesis *in vivo*. Overall, these two cartilage-derived components are promising materials for cartilage tissue engineering applications.

INTRODUCTION

Hydrogels have several advantages for cartilage tissue engineering, including the ease of formation, the ability to encapsulate cells, and the ability to fine tune mechanical properties.[9, 23, 33] Although hydrogels are promising materials for cartilage regeneration, they cannot be molded into a defect site by a surgeon because hydrogel precursors are liquid solutions that are prone to leaking after placement.[110, 135] To address this drawback, we recently published a method to achieve paste-like hydrogel precursor solutions by combining hyaluronic acid nanoparticles with traditional crosslinked hyaluronic acid

hydrogels, known as methacrylated hyaluronic acid (MeHA).[5] This paste-like behavior was induced by incorporating hyaluronic acid nanoparticles,[5] where the MeHA mixed with hyaluronic acid nanoparticles were together referred to as hydrogel pastes prior to crosslinking. The hydrogel pastes were then crosslinked to form a rigid traditional hydrogel structure. In this current study, in an effort to introduce bioactivity to the hydrogel itself, the two components of the hydrogel paste, both the MeHA and nanoparticles were substituted with components made from naturally derived cartilage extracellular matrix (ECM).

Materials derived from ECM are attractive for regenerative medicine because they may promote stem cell recruitment, infiltration, and differentiation without the need to supplement with additional biological factors.[6, 10, 104] We and other groups have recently established that cartilage ECM has chondroinductive potential,[11, 15, 41, 73, 115, 128] where we observed that rat bone marrow stem cells (rBMSCs) exposed to cartilage ECM outperformed those cells exposed to TGF-β_3 in chondroinductivity.[128] ECM materials in general can be obtained from cell-derived matrices, which are ECM materials secreted during *in vitro* culture, or they can be obtained from native tissue.[6, 11, 13, 22, 116, 156] Additionally, ECM materials are generally either decellularized to remove cellular components and nucleic acids or they are devitalized to kill but not necessarily remove cells within the matrix.[129]

Decellularization processes are known to inevitably cause some disruption to the matrix architecture, orientation, and surface landscape.[60] Therefore, in this current work, only unaltered DVC was studied. The objective was to create a hydrogel paste that was

entirely derived from DVC that was capable of inducing chondrogenesis. Prior studies have made traditional hydrogels entirely out of ECM by first solubilizing the ECM, and the solubilized matrix could then form a gel at body temperature.[40, 41, 43, 120] One group even used solubilized cartilage matrix as a depot for delivering drugs, where the gel maintained enough structural integrity under physiological conditions to sufficiently deliver bioactive molecules.[70] When we tried using this thermoresponsive method to create solubilized cartilage hydrogels, the gels that formed were too compliant and left opportunity for improvement for load-bearing applications, so methods to further crosslink the cartilage were desired. The crosslinking of unsolubilized cartilage has been reported, including crosslinking cartilage ECM with genipin, dehydrothermal treatment, ultraviolet irradiation, or carbodiimide chemistry.[13, 109] Using these methods, cartilage scaffolds were crosslinked and maintained some mechanical integrity throughout culture. Furthermore, cell mediated contraction was able to be controlled depending on the method of crosslinking. However, the authors noted that the constructs would need added reinforcements to achieve functional biomechanical properties. In the current study, these added reinforcements were attained by first solubilizing and then further crosslinking the cartilage tissue. Solubilizing the cartilage tissue allows for more fine-tuning of mechanical properties through allowing the control of the solid content of the hydrogel. Furthermore, solubilizing cartilage can remove particles that may cause premature gel fracture and it may open up more reactive sites on the cartilage ECM for crosslinking, which may help reinforce the ECM-based gels once they are crosslinked.

Therefore, with prior experience with functionalizing GAGs, such as hyaluronic acid and chondroitin sulfate with glycidyl methacrylate,[5, 63] which allows photocrosslinking of the hydrogel material, in the current study, the solubilized cartilage ECM was methacrylated. One pioneering study recently reported methacrylating solubilized cartilage matrix to make photocrosslinkable hydrogels, and they demonstrated for the first time that native tissues can be crosslinked forming hydrogels.[141] However, in that study, the solubilized cartilage matrix was reinforced with methacrylated gelatin (GelMA). In another study, solubilized cartilage ECM was cleverly reinforced by combining it with poly(ε-caprolactone) and then electrospinning it into a scaffold,[41] although the biomechanics of the scaffolds in that study still fell short of that of native cartilage tissue. The purpose of the current study was to create, for the first time, a hydrogel entirely composed of cartilage ECM without the use of GelMA and to additionally mix the methacrylated cartilage ECM with particles to give the hydrogel precursor a yield stress before crosslinking. We hypothesized that the hydrogel precursors containing DVC particles would exhibit a yield stress, and would be more chondroinductive than that of the methacrylated cartilage alone.

METHODS AND MATERIALS

Tissue Retrieval, Devitalization, and Cryogrinding

Twenty porcine knees were purchased from a local abattoir (Bichelmeyer Meats, Kansas City, KS). The knees came from Berkshire hogs, which were castrated males that were approximately 7-8 months old and 120 kg in weight. Articular cartilage from both the

knee and hip joints was carefully removed and collected using scalpels and was then rinsed twice in deionized (DI) water and stored at -20 ºC. After freezing overnight, the cartilage was thawed, mixed with dry ice and coarsely ground using a cryogenic tissue grinder (BioSpec Products, Bartlesville, OK). The dry ice was allowed to evaporate overnight in the freezer, where the cartilage was then referred to as devitalized cartilage (DVC), and then the DVC was lyophilized. The DVC was then cryoground into a fine powder using a freezer-mill (SPEX SamplePrep, Metuchen, NJ) and was lyophilized again overnight. The DVC powder was then filtered using a 106 µm mesh (ThermoFisher Scientific, Waltham, MA) to remove large particles and then frozen until use.

Synthesis and Characterization of MeSDVC

DVC powder was first solubilized using an adapted protocol from our previously reported method.[119] First, DVC powder was mixed in 0.1M HCl at a concentration of 10 mg DVC per 1 mL HCl. Pepsin was then added to the solution at a concentration of 1 mg/mL. The mixture was then stirred at 200 rpm at room temperature. After 2 days of stirring, the solution was then brought back to physiological pH by adding 1M NaOH. This solubilized DVC powder (SDVC) was then centrifuged at 10,000 *x g* for 3 min to pellet any unsolubilized particulates and the supernatant was frozen and lyophilized and later used to make methacrylated SDVC (MeSDVC).

MeSDVC was created by reacting SDVC with 20 fold molar excess glycidyl methacrylate (Sigma-Aldrich, St. Louis, MO) in the presence of trimethylamine and tetrabutyl ammonium bromide (Sigma-Aldrich) in a 1:3 acetone:water mixture at a

concentration of 1 g SDVC for every 150 mL solution. This solution was then stirred at 200 rpm for 6 days. The molar excess was approximated based on reacting one glycidyl methacrylate group to every monomer present in the solution and with the assumption that all monomers were hyaluronic acid. After 6 days, the MeSDVC was then precipitated in excess acetone, was dialyzed for 2 days in DI water, and then was lyophilized. Successful methacrylation was confirmed using ^{1}H NMR (Avance AV-III 500, Bruker).

Rat Bone Marrow Stem Cell Harvest and Culture

Following an approved IACUC protocol at the University of Kansas (AUS #175-08), rat bone marrow stems cells (rBMSCs) were harvested from the femurs of two male Sprague-Dawley rats (200-250 g). The rBMSCs were first cultured for one week in minimum essential medium-α (MEM-α, ThermoFisher) supplemented with 10% fetal bovine serum (FBS, MSC qualified, ThermoFisher) and 1% antibiotic-antimycotic (anti-anti, ThermoFisher) to ensure no mycotic contamination from harvesting. After 1 week of culture, the anti-anti was substituted for 1% penicillin/streptomycin (ThermoFisher), in which the cells were then cultured until they reached passage 4 for cell encapsulation into the hydrogels.

Description of Experimental Groups

Both acellular and cellular crosslinked formulations of 10% MeSDVC and 10% MeSDVC 10% DVC (w/v) were tested for 6 weeks *in vitro* along with one cellular group composed of 10% MeSDVC 10% DVC that was exposed to 10 ng/mL human transforming

growth factor-β_3 (TGF-β_3, PeproTech Inc., Rocky Hill, NJ). In addition, one acellular group composed of 20% MeSDVC was tested at day 1 after crosslinking. The acellular formulations were analyzed along with the cellular groups to quantify the acellular biochemical content and to analyze the effect of cells encapsulated in the networks. Ten percent MeSDVC was chosen as it was a concentration previously reported in literature for methacrylated gelatin (GelMA) gels.[141] A concentration of 20% MeSDVC was chosen as that is the approximate concentration of dry mass in native cartilage matrix.[85] Prior to crosslinking, the aforementioned cellular and acellular groups (except the growth factor group) and additional groups of 5% DVC and 10% DVC were tested rheologically. However, DVC alone cannot be crosslinked into a hydrogel network, which is why these two DVC groups were only tested rheologically.

Preparation of Hydrogel Pastes, Cell Encapsulation, and Hydrogel Culture Conditions

Hydrogel pastes were created by first measuring the desired weight percents of MeSDVC and DVC in a mini-centrifuge tube. All materials used for future cell encapsulation were then sterilized with ethylene oxide prior to use and were handled under sterile conditions thereafter. The pastes were mixed in two stages (e.g., in photoinitiator solution overnight and then more photoinitiator solution or cell suspension the day of testing) due to the longer time it took for MeSDVC to dissolve (i.e., overnight) to ensure mixture homogeneity. This length of time was deemed too long for adequate cell survival for the groups incorporating cells. Therefore, cell mixtures were added the day after the MeSDVC was mixed and given a chance to dissolve in half of the final solution. For

rheological testing of acellular groups, two stages of mixing was performed to maintain the same mixing process for both cellular and acellular groups. Sterile 0.01M PBS containing 0.05% (w/v) Irgacure (I-2959) photoinitiator was added to the acellular groups until the concentration of MeSDVC and DVC was twice the desired concentration. The samples were then mixed, centrifuged at 3000 rpm, and stored at 4 ºC overnight to allow the MeSDVC to adequately dissolve. Prior to rheological testing, more photoinitiator solution was added until the desired final concentration of materials was reached. The samples were then again mixed and centrifuged to remove air bubbles. For example, to make a 10% MeSDVC solution, 40 mg MeSDVC and 200 µL photoinitiator solution were mixed and allowed to fully dissolve overnight and then another 200 µL photoinitiator solution was added to make the final concentration at 10% MeSDVC the following day. For cellular testing, the samples were first mixed with 0.1% (w/v) Irgacure photoinitiator in PBS until the concentration of MeSDVC and DVC was twice the desired final concentration, and then the solutions were centrifuged and stored at 4 °C overnight just like the acellular groups. The following day however, passage 4 rBMSCs were then suspended at 20 million cells/mL in incomplete chondrogenic medium consisting of high glucose DMEM (ThermoFisher) with 4.5 g/L D-glucose supplemented with 10% FBS, 1% non-essential amino acids, 1% sodium pyruvate, 50 µg/mL ascorbic acid, and 0.25 mg/mL penicillin/streptomycin. This cell suspension was then added to the hydrogel paste solutions until the desired concentration of MeSDVC and DVC was reached and the final cell concentration and photoinitiator concentration were 10 million cells/mL and 0.05%, respectively. These solutions were then either tested rheologically or they were crosslinked

with UV light and further characterized as solids. For pastes undergoing crosslinking, the paste solutions were loaded into 2 mm thick molds between glass slides and exposed to 312 nm UV light at 3.0 mW/cm^2 in a UV crosslinker (Spectrolinker XL-100, Spectronics Corporation, Westbury, NY) for 2.5 min on each side for a total of 5 min. Using a 4 mm biopsy punch, each gel was cut and placed in one well of a 24 well, non-tissue culture-treated plate (Corning Incorporated, Corning, NY). Each gel was then exposed to 1 mL of incomplete chondrogenic medium or 1 mL of complete chondrogenic medium, which consisted of incomplete chondrogenic medium and 0.1 mg/mL dexamethasone and 10 ng/mL TGF-β_3. The medium was replaced every other day throughout the 6 week study.

Rheological Testing of Hydrogel Precursors

Prior to crosslinking the hydrogel precursor pastes, the precursor solutions were shaped into spheres to demonstrate their shaping capabilities, and they were then loaded into a 3 mL syringe and extruded onto a glass slide to macroscopically observe shape retention. The gels were extruded in a wavy line appearance to observe whether the formulations could maintain shaping after crosslinking.

The oscillatory shear stress of the precursor solutions (n=5) was measured over an oscillatory shear stress sweep of 1-2500 Pa at 37 °C using an AR-2000 rheometer (TA instruments, New Castle, DE) and a gap of 500 µm. The rheometer was equipped with a 20 mm diameter roughened plate and a roughened Peltier plate cover. Frozen rBMSCs that were thawed and cultured to passage 4 were used to make the cellular samples for rheological testing. The pastes for rheological testing were created as previously mentioned

for the *in vitro* culture. The yield stress was interpolated from the point at which the storage (G') and loss (G'') modulus crossed.[142] Additionally, an oscillatory shear stress sweep of 0.1-10 Pa was performed to assess the linear viscoelastic region of the hydrogel precursors to determine the storage modulus of each solution.

Mechanical Testing of Crosslinked Hydrogels

After swelling to equilibrium for 24 hours in either complete or incomplete chondrogenic medium, mechanical testing was performed. In addition, the groups in the 6 week study were tested at 6 weeks as well. First, the geometric mean diameter of the gels was determined using forceps and a stereomicroscope (20x magnification) and then the height of each gel was measured directly using a RSA-III dynamic mechanical analyzer (DMA, TA instruments, New Castle, DE). The gels (n=5) were then compressed at a rate of 0.01 mm/s until mechanical failure. The compressive modulus was calculated as the slope of the linear portion of the stress-strain curve (i.e., 5-15% strain).

Swelling Degree and Volume

Gels that were swollen to equilibrium were weighed 1 day after crosslinking and were then frozen and lyophilized (n=5). The dry weight was then recorded and the swelling degree was calculated as the ratio of total wet mass to dry mass. From the diameter and height readings recorded during mechanical testing, the volume of each gel (n=5) was calculated at 1 day and after 6 weeks of culture.

Biochemical Content Analysis

The biochemical content of the starting materials, which include MeSDVC, SDVC, and DVC, and the biochemical content of the gels at 1 day, 3 weeks, and 6 weeks were quantified (n=5). The gels were each digested overnight in a 1.5 mL papain mixture consisting of 125 mg/mL papain from papaya latex), 5 mM N-acetyl cysteine, 5 mM EDTA, and 100 mM potassium phosphate buffered saline at 65 °C. The digested solutions were then frozen and stored at -20 °C. Prior to biochemical analyses, all digested gel solutions were thawed to room temperature and then vortexed and centrifuged at 10,000 rpm for 10 min to pellet fragments of polymers. The supernatant was then used to quantify DNA, GAG, and hydroxyproline contents. Using a Cytation 5 Cell-Imaging Multi-Mode reader (Bio-Tek, Winooski, VT) and according to manufacturer instructions, the DNA content was quantified with the PicoGreen assay (Molecular Probes, Eugene, OR), the glycosaminoglycan (GAG) content was determined with the dimethylmethylene blue (DMMB) assay (Biocolor, Newtownabby, Northern Ireland), and the hydroxyproline content was quantified using a hydroxyproline detection kit (Sigma-Aldrich). Neither the GAG or hydroxyproline contents were normalized to DNA and instead are shown in total because of the gels' inherent initial DNA contents (i.e., true normalization to DNA content of seeded cells is not possible).

Gene Expression Analysis

RNA was isolated and purified using Qiagen QIAshredders followed by an RNeasy Kit (Valencia, CA) according to manufacturer guidelines (n=6). Isolated RNA was

converted into cDNA using a high capacity cDNA reverse transcription kit (Applied Biosystems, Foster City, CA). Real-time quantitative polymerase chain reaction (qPCR) was performed using a RealPlex MasterCycler (Eppendorf, Hauppauge, NY) and TaqMan gene expression assays from Applied Biosystems for Sox-9 (Rn01751070_m1), aggrecan (Rn00573424_m1), collagens type I (Rn01463848_m1) and II (Rn01637087_m1), and GAPDH (Rn01775763_g1). Relative gene expression levels for each gene were calculated using the $2^{-\Delta\Delta Ct}$ method where the 10% MeSDVC gels at day 1 were designated as the calibrator group and GAPDH expression was used as the endogenous control.[80] Last, RNA from DVC only (i.e., no rBMSCs) was isolated, converted to DNA, and then PCR was performed with the same previously mentioned TaqMan assays, where it was confirmed that all gene expression observed in the study was that of the rBMSCs.

Histological Analysis

Cellular gels from day 1 and 6 weeks were fixed in 10% formalin for 15 min and then embedded in Optimal Temperature Cutting (OCT) medium (TissueTek, Torrance, CA) overnight at 37 °C. Then the gels were frozen at -20 °C and were sectioned at a thickness of 10 µm using a cryostat (Micron HM-550 OMP, Vista, CA). The sections were then stained with the standard Hematoxylin and Eosin (H&E) stain, which stains the cytoplasm, connective tissues, and other extracellular substances red or pink and the nuclei purple. In addition, sections were stained with the standard Safranin-O/Fast Green (Saf-O) stain, which stains negatively charged GAGs orange. Last, the sections were stained immunologically using primary antibodies that target both rat and porcine tissues for

collagen I (ThermoFisher, NB600408, 1:200 dilution), collagen II (Abcam, ab34712, 1:200 dilution), and aggrecan (ThermoFisher, MA3-16888, 1:100 dilution). The slides were first fixed in chilled acetone (-20 °C), treated with proteinase K (Abcam), and exposed to 0.3% hydrogen peroxide to suppress endogenous peroxidase activity. Then the sections were blocked with serum according to the Vectastain ABC kit (Vector Laboratories, Burlingame, CA) following the manufacturer's instructions and were then incubated with primary antibody. Following primary antibody incubation, the sections were exposed to biotinylated secondary antibodies (horse anti-rabbit and mouse) and ABC reagent according to the manufacturer protocol. Antibodies were visualized using the ImmPact DAB peroxidase substrate (Vector). The sections were then rinsed in DI water, counter stained with VECTOR hematoxylin QS stain, and then were dehydrated and mounted. Negative controls consisted of omitting the primary antibody (for aggrecan) or substituting with a rabbit IgG isotype control (for collagen I and II, Abcam, ab27478) at an antibody concentration calculated to be the same used for the corresponding antibodies.

Statistical Analysis

Using GraphPad Prism 6 statistical software (GraphPad Software, Inc., La Jolla, CA), experimental groups were compared using a one-factor ANOVA (for analyses with one time point) or a two-factor ANOVA (for analyses with two or more time points) followed by either a Sidak's *post hoc* test (for two-way ANOVAs with two time points only) or a *Tukey's post hoc* test (for all other ANOVAs), where $p \leq 0.05$ was considered significant. Standard box plots were constructed to eliminate outliers. All quantitative

results are reported as mean ± standard deviation within the text or as mean + standard deviation within the figures. Furthermore, unless otherwise stated, all groups discussed in the Results section are cell-encapsulated.

RESULTS

Characterization of MeSDVC, SDVC, and DVC particles

Success of the methacrylation procedure MeSDVC was confirmed via ^{1}H NMR by the emergence of methacrylate peaks between 5 and 6.5 ppm (Figure 6.1). The DNA content of the DVC particles was 1170 ± 68 ng DNA per mg dry DVC, where the SDVC and MeSDVC had DNA contents that were 92% and 97% less than DVC, respectively ($p<0.05$) (Figure 6.2A). The GAG content of the DVC particles was 380 ± 57 µg GAG per mg dry DVC, and the SDVC and MeSDVC had GAG contents that were 44% and 41% less than that of DVC, respectively ($p<0.05$) (Figure 6.2B). Last, the hydroxyproline content of DVC was 48.60 ± 0.58 µg hydroxyproline per mg dry DVC, where the hydroxyproline content of SDVC was 26% lower than that of DVC ($p<0.05$) (Figure 6.2C). The hydroxyproline content of MeSDVC was not significantly different from that of DVC, but was 41% higher than that of SDVC ($p<0.05$).

Macroscopic Observation and Rheological Testing of Hydrogel Precursors

Macroscopic observation of hydrogel precursors revealed non-Newtonian and paste-like behavior in all precursors (Figure 6.3). Furthermore, all solutions except the 5% DVC and 10% DVC groups were able to be shaped and molded into a sphere, where it was

noted that the pastes incorporating particles were easier to shape and manipulate because the solutions containing only MeSDVC were sticky. Shape retention after extrusion through a 3 mL syringe was indicated by the fluids that retained the diameter of the syringe orifice. All pastes exhibited shape retention except the 5% DVC group, which spread out over 2 times the diameter of the syringe orifice. Furthermore, all formulations containing MeSDVC were able to be crosslinked to maintain extrusion shape (Figure 6.3).

Additionally, all solutions exhibited a yield stress (Figure 6.4A). The yield stress of 10% MeSDVC acellular group was 725 ± 55 Pa, where the difference in yield stress compared to its respective cellular group was not significant. The 5% DVC and 10% DVC groups had yield stresses that were 96% and 92% lower, respectively, than that of 10% MeSDVC ($p<0.05$), while the MeSDVC + DVC acellular group had a yield stress that was 94% higher than that of 10% MeSDVC ($p<0.05$) (Figure 6.4A). Furthermore, when cells were mixed into the MeSDVC + DVC group, the yield stress was not significantly different from the acellular group, but it was 62% higher than that of the 20% MeSDVC acellular group ($p<0.05$).

All solutions exhibited viscoelastic behavior, which was indicated by a measurable storage modulus, although the storage modulus of the 5% DVC was the lowest at 1.33 ± 0.80 Pa (Figure 6.4B). The storage modulus of the 10% MeSDVC acellular group was 773 ± 84 Pa. The only groups that were significantly different from the 10% MeSDVC acellular group were the acellular and cellular MeSDVC + DVC groups, where their storage moduli were 5.7 and 7.2 times higher than that of the 10% MeSDVC acellular group, respectively

($p<0.05$). Last, the storage modulus of the MeSDVC + DVC cellular group was 2 times higher than that of the 20% MeSDVC acellular group ($p<0.05$).

Mechanical Testing of Crosslinked Hydrogel Pastes

One day after crosslinking, the compressive modulus of the 10% MeSDVC acellular group was 135 ± 37 kPa (Figure 6.5). None of the groups were significantly different from the 10% MeSDVC acellular group except the 20% MeSDVC acellular group, which had a modulus of 675 ± 130 kPa ($p<0.05$).

Six weeks after crosslinking, the compressive modulus of the 10% MeSDVC acellular group was 32 ± 12 kPa, although there were no significant differences compared to other groups (Figure 6.5). However, over the 6 weeks of culture, while most of the groups did not deviate significantly from their original compressive modulus, the compressive modulus of the 10% MeSDVC acellular and cellular groups reduced by 77% and 86%, respectively ($p<0.05$).

Swelling and Volume Analysis of Crosslinked Hydrogel Pastes

The only group that had a significantly lower swelling degree than that of the 10% MeSDVC group, which had a swelling degree of 10.5 ± 3.5 after swelling to equilibrium, was the 20% MeSDVC acellular group, where its swelling degree was 36% lower than that of the 10% MeSDVC group ($p<0.05$) (Figure 6.6A).

At one day after crosslinking and swelling to equilibrium, the gel volume of the 10% MeSDVC group was 19.26 ± 0.54 µL, where the volumes of the MeSDVC + DVC

cellular, acellular, and TGF-β_3 exposed groups were 17%, 20%, and 17% higher, respectively ($p<0.05$) (Figure 6.6B). Furthermore, the volume of the MeSDVC + DVC group was 22.6 ± 1.7 µL and it was not significant from its respective acellular and growth factor exposed group.

At 6 weeks after crosslinking, again all three of the MeSDVC + DVC groups had significantly higher volumes than that of the 10% MeSDVC group ($p<0.05$) (Figure 6.6B). The volume of the 10% MeSDVC group was 15.8 ± 2.1 µL, while the volume of the cellular MeSDVC + DVC group was 36% larger ($p<0.05$).

Over the course of 6 weeks, the only groups that had a significant change in volume were the 10% MeSDVC acellular and cellular groups, where they each decreased in volume by 27% and 18%, respectively ($p<0.05$) (Figure 6.6B). The volumes of all three MeSDVC + DVC groups remained constant throughout the 6 week study.

Biochemical Content of Crosslinked Hydrogel Pastes

All cellular groups had significantly higher DNA contents than their respective acellular groups at all time points ($p<0.05$) (Figure 6.7A). At 1 day after crosslinking, the 10% MeSDVC group contained 680 ± 170 ng DNA per gel, and both the MeSDVC + DVC cellular and growth factor exposed groups contained 26% and 28% more DNA, respectively, ($p<0.05$). At 3 weeks after crosslinking, the 10% MeSDVC group had a DNA content of 386 ± 37 ng DNA per gel, which was not significantly different from any of the other cellular groups (Figure 6.7A). After 6 weeks of culture, the 10% MeSDVC group contained 241 ± 18 ng DNA per gel, which was 42% lower than the DNA content of the

MeSDVC + DVC + TGF-β_3 group ($p<0.05$) (Figure 6.7A). Over the course of the 6 week culture period, all cellular groups had a significant reduction in DNA content ($p<0.05$), where after 3 weeks the DNA content in the 10% MeSDVC, MeSDVC + DVC, and the MeSDVC + DVC + TGF-β_3 groups decreased by 43%, 43%, and 49%, respectively ($p<0.05$). By 6 weeks, the DNA contents of the 10% MeSDVC and MeSDVC + DVC groups were significantly lower than their 3 week values, where their total reductions in DNA over the entire culture period was 65% and 72%, respectively ($p<0.05$). There was not a significant reduction in DNA content for the growth factor exposed group after 3 weeks. Finally, the acellular groups did not have any significant reduction in DNA content over the culture period (Figure 6.7A).

At one day after crosslinking, the GAG content of the 10% MeSDVC group was 86 ± 15 µg GAG per gel, where that of the MeSDVC + DVC group was 3.9 fold higher ($p<0.05$) (Figure 6.7B). Additionally, the MeSDVC + DVC and the TGF-β_3 exposed groups contained 45% and 27% more GAG than their acellular control ($p<0.05$). At 3 weeks, the GAG content of the 10% MeSDVC was 40.7 ± 2.5 µg GAG per gel, whereas that of the MeSDVC + DVC group was 4.7 fold higher ($p<0.05$) (Figure 6.7B). At 6 weeks, the GAG content of the 10% MeSDVC group was 25.2 ± 3.0 µg GAG per gel, whereas that of the MeSDVC + DVC group was 3.7 fold higher ($p<0.05$). In addition, the GAG content of the MeSDVC + DVC + TGF-β_3 group was 75% larger than that of the MeSDVC + DVC group ($p<0.05$). From day 1 to 3 weeks, the GAG contents of the 10% MeSDVC, the MeSDVC + DVC, and the MeSDVC + DVC + TGF-β_3 group decreased by 53%, 43%, and 26%, respectively ($p<0.05$). By 6 weeks, the GAG contents of the MeSDVC + DVC

and the MeSDVC + DVC + TGF-β_3 groups decreased by 72% and 44%, respectively, compared to their original GAG contents ($p<0.05$).

Finally, at day 1, the initial hydroxyproline content of the 10% MeSDVC group was 66.4 ± 2.8 μg hydroxyproline per gel, whereas that of the MeSDVC + DVC group was 2.7 fold higher ($p<0.05$) (Figure 6.7C). At 3 weeks, the MeSDVC + DVC group contained 144 ± 21 μg hydroxyproline per gel, which was 2 times higher than that of the 10% MeSDVC group and 22% lower than that of the MeSDVC + DVC + TGF-β_3 group ($p<0.05$). At 6 weeks, the hydroxyproline content of the MeSDVC + DVC group was 114 ± 11 μg hydroxyproline per gel, which was 89% higher than that of the 10% MeSDVC group and 28% lower than that of the MeSDVC + DVC + TGF-β_3 group ($p<0.05$). The only group that experienced a loss in hydroxyproline content from day 1 to 3 weeks was the MeSDVC + DVC group, where at 3 weeks the hydroxyproline content was 81% of its original content at day 1 ($p<0.05$). By 6 weeks, all three of the DVC-incorporating groups experienced a significant loss in hydroxyproline, where the hydroxyproline contents for the MeSDVC + DVC and the MeSDVC + DVC + TGF-β_3 groups were 64% and 95% of their original contents at day 1 ($p<0.05$).

Gene Expression Analysis

At 1 day after crosslinking, the relative Sox-9 expression of 10% MeSDVC was 9.4 times larger than that of the MeSDVC + DVC group ($p<0.05$) (Figure 6.8A). Furthermore, growth factor exposure had no significant effect on Sox-9 expression compared to the MeSDVC + DVC group. At 1 week, the relative Sox-9 expression of the 10% MeSDVC

group was 73% larger than that of the TGF-β_3 exposed group ($p<0.05$). At 2 weeks, the relative Sox-9 expression of the MeSDVC + DVC group was 89% larger than that of the 10% MeSDVC group and 37% smaller than that of the TGF-β_3 exposed group ($p<0.05$). At 3 weeks, the relative Sox-9 expression of the MeSDVC + DVC group was 5.2 fold higher than that of the 10% MeSDVC group ($p<0.05$). At 6 weeks, the relative Sox-9 expression of the MeSDVC + DVC group was 15 and 5.6 times larger than that of the 10% MeSDVC and the TGF-β_3 exposed groups, respectively ($p<0.05$) (Figure 6.8A). From 1 day to 3 weeks, the relative Sox-9 expression of the 10% MeSDVC group decreased by 82% ($p<0.05$), but did not change significantly thereafter. From 1 day to 1 week, the relative Sox-9 expression of the MeSDVC + DVC group increased by a factor of 6.6 ($p<0.05$), and did not change significantly thereafter. Finally, the relative Sox-9 expression of the MeSDVC + DVC + TGF-β_3 group increased by a factor of 6.6 from 1 day to 1 week ($p<0.05$), increased by a factor of 2.9 from 1 week to 2 weeks ($p<0.05$), decreased by 54% from 2 weeks to 3 weeks ($p<0.05$), and then decreased again by 87% from 3 weeks to 6 weeks ($p<0.05$) (Figure 6.8A).

The relative aggrecan expression of 10% MeSDVC was 42 times higher than that of the MeSDVC + DVC group at day 1 ($p<0.05$) (Figure 6.8B). There were no significant differences among groups at 1 week. At 2 weeks, the relative aggrecan expression of the MeSDVC + DVC group was 2.8 times higher than that of 10% MeSDVC and 41% lower than that of the TGF-β_3 exposed group ($p<0.05$). At 3 weeks, the relative aggrecan expression of the MeSDVC + DVC group was 8.6 times higher than that of the 10% MeSDVC group ($p<0.05$). At 6 weeks, there was no detectable aggrecan expression in the

TGF-β_3 exposed group. However, the relative aggrecan expression of the MeSDVC + DVC group was 53 times higher than that of the 10% MeSDVC group ($p<0.05$). From day 1 to 1 week, the relative aggrecan expression of the 10% MeSDVC group decreased by 94% ($p<0.05$), and did not change significantly thereafter. The relative aggrecan expression of the MeSDVC + DVC group increased by a factor of 3.3 from 1 day to 1 week ($p<0.05$), and did not change significantly thereafter. Last, from 1 day to 2 weeks, the relative aggrecan expression of the MeSDVC + DVC + TGF-β_3 group increased by a factor of 5.9 ($p<0.05$), and then decreased by 45% from 2 weeks to 3 weeks ($p<0.05$) (Figure 6.8B).

There were no significant differences between groups for collagen II expression from day 1 through 6 weeks (Figure 6.8C). Additionally, there was no detectable collagen II expression in the DVC-incorporated groups at 2 and 3 weeks, and there was no detectable collagen II expression in the 10% MeSDVC group at week 3. However, at 6 weeks, the relative collagen II expressions of the MeSDVC + DVC and the TGF-β_3 exposed groups were 78 and 40 fold higher than that of the 10% MeSDVC group, respectively ($p<0.05$). Due to many groups not having detectable collagen II expression throughout the culture period, for observing differences within groups throughout the culture period, only differences from day 1 to 6 weeks were reported here. From 1 day to 6 weeks, the relative collagen II expression for 10% MeSDVC did not change significantly. However, the relative collagen II expression for the MeSDVC + DVC and the MeSDVC + DVC + TGF-β_3 groups increased by a factor of 131.1 and 92.9, respectively ($p<0.05$) (Figure 6.8C).

The relative collagen I expression of the 10% MeSDVC group at 1 day was 17.9 fold higher than that of the MeSDVC + DVC group ($p<0.05$) (Figure 6.8D). The relative

collagen I expression of the 10% MeSDVC group was 84% and 92% less than that of the MeSDVC + DVC group at 1 week and 2 weeks, respectively ($p<0.05$). At 3 weeks and at 6 weeks, there were no significant differences among groups. From 1 day to 1 week, the relative collagen I expression of the 10% MeSDVC group decreased by 98% ($p<0.05$) and did not change significantly thereafter. Finally, the relative collagen I expression level for the DVC-incorporating groups did not change significantly throughout the culture period (Figure 6.8D).

Histological and Immunohistochemical Evaluation

At 6 weeks, there were no discernable changes in any of the constructs other than the DVC-containing groups appeared to have a decreased cell density compared to their respective cell densities at day 1. However, throughout culture, the cells remained evenly distributed. Saf-O stained MeSDVC and DVC particles a dark red/orange color and the staining intensity of the DVC particles appeared to fade over the 6 weeks in culture (Figure 6.9). All groups stained for collagen II, where the collagen II staining for the DVC-incorporated groups was slightly darker at 6 weeks compared to 1 week (Figure 6.9). The 10% MeSDVC group had a slight increase in collagen I staining over the culture period, whereas the DVC-incorporating groups had a slight decrease in collagen I staining (Figure 6.9). The MeSDVC + DVC group had the least amount of collagen I staining at 6 weeks. Aggrecan staining revealed a slight increase in aggrecan deposition in the 10% MeSDVC gels over the 6 week culture period (Figure 6.9). Additionally, the MeSDVC + DVC group had an increase in aggrecan staining over the course of the 6 weeks (Figure 6.9). Finally,

no discernable changes in aggrecan staining was observed at 6 weeks for the MeSDVC + DVC + TGF-β_3 group compared to its aggrecan staining at day 1 (Figure 6.9).

DISCUSSION

To the best of our knowledge, we were the first group to create a covalently crosslinked hydrogel composed entirely of cartilage ECM and we are the first to additionally add cartilage matrix particles to give the hydrogel precursor a yield stress before crosslinking. Although the major focuses of hydrogel technologies are on hydrogels in their crosslinked form, our group additionally focuses on the fluid behavior of the hydrogel precursor solutions by fabricating colloidal gels instead, which are dynamically paste-like materials prior to crosslinking that can be molded into place and will 'set' after placement.[147] Colloidal gels are cohesive through disruptable particle interactions, we have previously shown that these gels are capable of successfully filling tissue defects, delivering bioactive signals, and promoting new tissue formation in non-load bearing cranial defect applications.[25, 144-146] Preliminary work demonstrated that these colloidal gels did not retain their integrity over time in culture and recently, we published a method to combine colloidal gel systems with traditional crosslinked hyaluronic acid hydrogels to form a hydrogel suitable for load-bearing applications that exhibits a yield stress prior to crosslinking.[5] This yield stress, the threshold level where a solution transitions from an elastic solid to a pseudoplastic liquid, is crucial as it will enable a surgeon to mold and shape the material into the defect site without the concern that the material will flow or

leak from the defect, which is a major concern for traditional hydrogel precursor solutions.[110, 135]

In prior work from our group, only the colloidal solutions employing particulates were observed to exhibit a yield stress,[5] and therefore in the current study, it was hypothesized that particulates would be necessary to achieve a paste-like precursor solution. All samples tested in the current study, including the non-particulate samples composed of MeSDVC, were noted to have a yield stress. Ten percent MeSDVC alone had a yield stress of over 700 Pa, and when it was combined with 10% DVC particles, which had a yield stress of only 58 Pa, the combined materials had a yield stress of over 1800 Pa. This synergistic effect was similarly noted in prior work,[5] which suggests that there may be some physical or chemical interactions between DVC and MeSDVC. For context, toothpaste, a common paste-like material, has a yield stress of approximately 200 Pa. Additionally, when cells were mixed in with the materials, the cells did not significantly affect the yield stress value, which is advantageous because these materials can be mixed with cells if necessary in a surgical context and would still allow for appropriate shaping and contouring. Although the MeSDVC + DVC precursor solutions are easily molded, shaped, and extruded through a syringe, there may be applications where the yield stress may need to be reduced. In this case, the concentrations of MeSDVC and DVC can be altered. Furthermore, future quantification of syringeability would be of value.

This is not the first time yield stress has been reported in hydrogel precursors for tissue engineering purposes. One group used a dual component, “dock-and-lock”, self-assembling gelation mechanism to create shear-thinning, self-healing, and injectable

hydrogels.[81] Elder *et al.*[32] reported a method to modify the viscosity of hyaluronic acid hydrogel precursors by attaching peptides that self-assemble into β-sheets onto the hyaluronic acid. Although methods to induce yield stress in hydrogel precursor solutions have been reported, to the best of our knowledge, this current study is the first example of inducing yield stress in hydrogel precursors with ECM-based materials.

ECM-materials were used in the current study to not only impart a yield stress on the materials, but to further make the material inherently chondroinductive. A few other groups have recently reported the chondroinductivity of cartilage ECM.[11, 15, 41, 73, 115, 128] For example, Cheng *et al.*[14] developed a porous cartilage matrix composed of homogenized and then lyophilized cartilage matrix, which induced chondrogenic differentiation even without growth factor supplementation. However, these matrices contracted *in vitro*, so the cartilage matrix was then further crosslinked with genipin and found the crosslinking degree affected matrix synthesis and cell-mediated contraction. Although at a 0.05% genipin concentration, they found that the materials did not exhibit contraction and were chondroinductive.[13] Rowland *et al.*[109] further studied the crosslinking of these matrices, where it was reported that the crosslinking method affected the chondrogenesis and matrix synthesis of MSCs. Visser *et al.*[141] solubilized cartilage ECM and functionalized it with methacrylate groups, and demonstrated for the first time that hydrogels could be formed from ECM materials. However, these materials were not found to significantly affect the chondrogenic differentiation of MSCs. In the current study, compared to MeSDVC alone, an upregulation of Sox-9 and aggrecan was noted at two weeks when rBMSCs were exposed to DVC particles, with or without TGF-β_3 supplementation. Furthermore, at 6

weeks, the DVC particle groups with and without TGF-β_3 had a relative collagen II expression that was 40 and 78 fold higher, respectively, than that of MeSDVC alone ($p<0.05$). Additionally, collagen II expression of the DVC particle groups significantly increased over the culture period, whereas the relative collagen II expression of the MeSDVC group alone did not change. Although a significant increase was not observed in matrix production of the cells either histologically or through biochemical analysis, which could be a result of simultaneous bioabsorption and remodeling of the ECM, a slight increase in collagen II staining was observed in the DVC particle groups, in agreement with the gene expression data. A slight increase in aggrecan staining was noted in the 10% MeSDVC group, and this group was noted to have a significantly higher aggrecan gene expression than the other groups at day 1. Although the TGF-β_3 group had no discernable changes in aggrecan staining over the 6 weeks, it had the highest aggrecan gene expression at 2 weeks. Even though at weeks 1 and 2, the relative collagen I expression in the DVC particle groups was higher, at day 1, the relative collagen I expression in the DVC particle groups was significantly lower. Furthermore, collagen I staining actually increased slightly in the MeSDVC group over the culture period, while it decreased in the DVC particle groups. Overall, the gene expression and histological data pointed toward the DVC particles as an important component for upregulating chondrogenic genes, even though the particles are not necessary for inducing a yield stress in these MeSDVC and DVC systems.

Not only are the particles likely necessary for chondrogenesis, but they are successful in reducing hydrogel contraction. Hydrogel contraction is a major concern for tissue engineering because it can cause disintegration with host tissue, which could

potentially hinder successful cartilage regeneration and may even dislodge the hydrogel from the defect site.[13, 141] In prior work, Guilak and colleagues observed how the crosslinking degree and method of crosslinking affected gel contraction.[13, 109] However, in the current study, we observed that the inclusion of particles affected gel contraction and swelling. In the current study, gels composed only of MeSDVC contracted by 18% over the culture period, but the gels containing DVC particles did not have a significant change in volume.

Another important feature for hydrogels in cartilage tissue engineering is their ability to withstand mechanical loading and one major disadvantage of using natural materials is their decreased mechanical integrity.[133] The compressive modulus of hydrogels composed of natural materials are typically an order of magnitude less than that of native cartilage tissue,[133] which has a compressive elastic modulus ranging from 240-1000 kPa.[2] However, the biomechanical properties of cartilage can vary depending on parameters such as the method of testing, the cartilage zone depth, and the strain rate of testing.[49] In the study performed by Visser *et al.*,[141] the solubilized cartilage matrix was reinforced with methacrylated gelatin (GelMA); however, the biomechanics of the hydrogels, evaluated via the compressive modulus, still fell short of native cartilage tissue. Another group used poly(ε-caprolactone) to reinforce solubilized cartilage ECM by combining them and then electrospinning them into a scaffold.[41] However, the Young's moduli of these scaffolds were only approximately 10 kPa. In the current study, although we only observed compressive moduli in the range from 70-170 kPa for all of the 10% MeSDVC and MeSDVC + DVC groups, we did observe a compressive modulus of approximately 675

kPa in the acellular 20% MeSDVC group, which is on the same order of magnitude as native articular cartilage. Because there was such a difference in the modulus from 20% MeSDVC to MeSDVC + DVC even though both gels had a solids content of 20%, future work will be necessary to determine ratios of DVC particles and MeSDVC that still allow for sufficient chondrogenesis and reduced contraction, while maintaining the appropriate biomechanics. Furthermore, it is possible that once these materials are implanted *in vivo*, the biomechanical stimulation may help increase matrix synthesis and improve the mechanical properties.[140]

Even though DVC particles may hinder the biomechanical performance and are not necessarily needed to induce a yield stress if using MeSDVC as a hydrogel material, we have still demonstrated that the particles are likely contributing to enhanced chondrogenesis and the elimination of hydrogel contraction. Because the DVC particles contain mostly unaltered cartilage ECM, other than the DVC particles are cryoground, they may retain more of the bioactivity of the cartilage matrix than MeSDVC since MeSDVC is altered cartilage ECM, where it contained 97% less DNA and 41% fewer GAGs than DVC. Proteoglycans, specifically aggrecan in cartilage matrix, are found extensively in native cartilage matrix and are thought to be a reservoir of several growth factors.[17, 57] It can therefore be hypothesized that some of the growth factors inducing chondrogenesis within cartilage ECM may have been altered or removed in the processing of MeSDVC are retained in DVC.

Of interest is that the processing of MeSDVC appears to have removed much of the DNA content. It is uncertain at this time whether or not the DNA was altered and unable

to be detected via the PicoGreen assay, or if the MeSDVC process actually decellularizes the tissue as well and future work will certainly need to address this issue. The low pH exposure during the solubilization process would likely denature the DNA to a single-stranded state, and would in addition hydrolyze and further degrade the DNA.[88] Furthermore, the dialysis step after methacrylation would likely remove these degraded DNA segments and low molecular weight nucleotides and amino acids, leaving behind higher molecular weight methacrylated GAGs and collagen. Furthermore, a recent study found that pepsin, although previously known to only digest protein, is in addition, capable of digesting nucleic acids.[79] These results are consistent with our findings since there was no mass loss during the solubilization/pepsin digestion process. Therefore, future work will certainly need to address what immunological effects may occur by digesting tissues in pepsin. Currently, it is unknown whether decellularizing of cartilage tissue is necessary or to what exact degree cells must be removed to enable the material to be implanted *in vivo* without an adverse immunological response. For example, Zimmer's DeNovo® product, which is composed of living, allogeneic human cells, has no reports of allograft rejection or disease transmission and it has been observed to create hyaline-like cartilage in goats, where no T-cell-mediated response was noted.[1] Therefore, because cartilage tissue may be immunoprivileged for osteoarthritis applications, and because decellularization can result in changes in matrix architecture and surface ligand landscape,[60] decellularization may not even be necessary for some cartilage tissue engineering applications.

In addition, it must be noted that the inclusion of cells may or may not be necessary for future clinical application of these materials. It is possible that a cell source could come

from the subchondral bone if microfracture is performed prior to implanting the acellular pastes. Therefore, future work will also consider the ability of cells to migrate into and remodel the pastes to determine whether or not cell encapsulation is necessary.

CONCLUSION

In this current study, we created a potentially chondroinductive hydrogel that is entirely composed of cartilage-derived ECM and we have shown that by mixing in DVC particles, we can modulate the yield stress of the hydrogel precursors and prevent contraction after crosslinking. Furthermore, these two-component gels induced chondrogenic gene expression after 2 weeks compared to MeSDVC gels alone, and they had reduced cell-mediated contraction. Future work will address combinations of DVC and MeSDVC components that yield mechanics closer to that of native tissue and will further address tissue integration and regeneration *in vivo*. Ultimately, the combination of these two cartilage-derived components is promising for cartilage tissue engineering applications.

CHAPTER 7: CONCLUSION

Hydrogels are a promising class of tissue regenerative materials for several reasons, including their high water content, 3D structure, and tunable mechanical properties.[9, 23, 33] However, hydrogels in their precursor form (i.e., prior to crosslinking) are traditionally liquid solutions that lack a yield stress. The crux, therefore, of hydrogel technology for *in situ* implantation, is creating a hydrogel precursor that is capable of remaining within the defect site.[110, 135] As an alternative to traditional hydrogels, predecessors to this current thesis developed a new type of tissue engineering scaffold called a colloidal gel, which is a mechanically dynamic paste-like material that can be easily molded into place and will 'set' after placement.[147] It was found that these gels, composed of oppositely charged PLGA nanoparticles, could successfully fill tissue defects, deliver bioactive signals, and promote new tissue formation in non-load bearing cranial defect applications.[25, 144-146] A more recent predecessor found colloidal gels could be made out of solutions of hyaluronic acid (HA) nanoparticles.[37] These HA-based colloidal gels exhibited shear-thinning rheological behavior and had the ability to fully recover after compression to high strains even after physically destroying and reassembling the gel, which made them attractive for applications such as for cartilage regeneration.[37] Therefore, the work in the current thesis started with these HA-based colloidal gels and the primary objective was to develop a mechanically dynamic, "paste-like" hydrogel material that could retain its molded or extruded shape, would "set" after placement, and could withstand mechanical loading. Preliminary work with the HA-based colloidal gels demonstrated that they did not retain their integrity over time in culture, and therefore, although they were mechanically

dynamic, at their current state, they could be improved for cartilage tissue engineering applications.

When the HA nanoparticles were mixed with methacrylated hyaluronic acid (MeHA), a more traditional photocrosslinkable hydrogel material, the solutions exhibited a yield stress prior to crosslinking. Furthermore, it was found that if MeHA and linear HA (made with the same MW as the HA nanoparticles) were mixed, the solutions lacked a yield stress, which demonstrated that the nanoparticulate form of HA was necessary to achieve the paste-like behavior, although at this stage, the underlying mechanism causing this paste-like behavior is still unknown. Additionally, unlike the gels consisting of only HA nanoparticles that were previously found to disintegrate *in vitro*, the gels consisting of HA nanoparticles and MeHA were able to be photocrosslinked into mechanically stable hydrogels that could encapsulate cells that remained viable. However, gels were found to be mechanically weak after crosslinking in comparison to native articular cartilage tissue. Around the completion of this first study, our research group started working with cartilage extracellular matrix (ECM), as it was in the beginning stages of being explored as a chondroinductive material.[11, 15, 41, 73, 115] Therefore, the new objective of this current thesis became to improve the mechanics of the two-component hydrogel system after crosslinking so the hydrogels could withstand loads similar to that of native articular cartilage. Furthermore, the objective was to make the hydrogel chondroinductive by incorporating cartilage ECM, and ensure that the paste-like consistency prior to crosslinking was preserved.

The first new edition of the hydrogel two-component system in the current thesis replaced the HA nanoparticles with cartilage ECM microparticles. Furthermore, both devitalized (DVC) and decellularized (DCC) cartilage microparticles were tested in these hydrogel pastes to determine if decellularization affects long-term chondroinductivity. It is widely emphasized in the literature that improper decellularization of ECM-based tissues can result in detrimental inflammatory responses and ultimately hinder tissue regeneration.[59] However, cartilage ECM may be uniquely immunoprivileged in part because the ECM is so dense that it protects chondrocytes from T and natural killer cells that are released in graft rejection.[105] Therefore, the goal of this study was to compare the chondroinductive potential of DVC and DCC, especially since decellularization processes inevitably cause some disruption to the matrix architecture, orientation, and surface landscape,[60] which may ultimately limit or hinder the chondroinductive potential of the matrix. When DCC and DVC particles were mixed with MeHA, chondrogenic gene expression analysis found that the MeHA precursors containing DVC consistently outperformed the DCC-containing groups, even when compared to the groups exposed to TGF-β_3. Additionally, MeHA solutions containing DVC exhibited a higher yield stress compared to that of MeHA and DCC precursors. Overall, DVC appeared to be superior to DCC in both chondroinductivity and rheological performance of hydrogel precursors, which is contradictory to a prior study from our group that reported rat bone marrow stem cells (rBMSCs) exposed to DCC outperformed those cells exposed to DVC or TGF-β_3 in chondroinductivity.[128] However, it is hypothesized that the differences observed between this prior study, Sutherland *et al.*,[128] and the current thesis was a result of the scaffold

formulation since the current thesis evaluated rBMSCs encapsulated within a 3D hydrogel scaffold, whereas the Sutherland *et al.*[128] study was a pellet culture. Furthermore, Sutherland *et al.*[128] only evaluated short term gene expression over 1 week, while the current thesis observed the long term gene expression over 6 weeks. The current thesis work is the only long-term evaluation of DVC and DCC and although the long-term gene expression of cells exposed to DVC emphasizes that DVC may be superior in chondroinductivity *in vitro*, *in vivo* studies will be crucial to evaluate this concept further. *In vivo* studies will be able to not only compare chondroinductive potential, but will additionally be able to compare the immunological responses to these materials. Although *in vivo* studies are indeed suggested to study further the chondroinductive potential of DCC and DVC, the current thesis work did evaluate the materials implanted in a human cadaver. A hydrogel paste, consisting of MeHA and DCC, was implanted in a defect created in a human cadaver elbow joint and then were UV crosslinked *in situ*. The gels were able to be successfully molded into the defect and after crosslinking, the joint was able to be articulated without dislodging the gel (Figure 7.1), which suggested that these pastes indeed had potential for cartilage tissue engineering applications.

Because MeHA mixed with DCC still produced gels that were mechanically weak compared to native cartilage, it was then sought out to incorporate a crosslinkable material that would more closely match the mechanics of native cartilage tissue and be chondroinductive simultaneously. Therefore, the goal was to make a hydrogel out of cartilage ECM. Several studies had reported making gels out of ECM by first solubilizing the ECM, where the solubilized matrix would form a gel at body temperature.[40, 41, 43, 120]

Therefore, in this current thesis it was hypothesized that an *in situ*-gelling material may not only be chondroinductive, but it would additionally eliminate the need for photocrosslinking, a process which can be detrimental to cells and nearby tissues. However, preliminary testing in the current thesis determined that the gels that formed were compliant without further UV crosslinking, which left opportunity to improve the gels for load-bearing applications and it was decided to methacrylate the solubilized cartilage ECM, making photocrosslinkable MeSDCC (Methacrylated Solubilized Decellularized Cartilage). The elastic compressive modulus of the gels containing 20% MeSDCC were 1070 ± 150 kPa, which is similar to that reported for native articular cartilage. Furthermore, it was found that the stress-strain profiles of the 20% MeSDCC gels fell within the 95% confidence interval range for native porcine cartilage tissue. In addition, the MeSDCC gels significantly upregulated chondrogenic gene expression compared to a more traditionally used material, methacrylated gelatin. Finally, the MeSDCC gels supported extensive matrix synthesis. However, although the MeSDCC gels appeared to be more chondroinductive than methacrylated gelatin, it was noted that the chondrogenic potential could be improved. Specifically, it was noted in the study that there was no detectable levels of collagen II gene expression at 6 weeks and that aggrecan expression levels decreased over the culture period.

Given that in the current thesis it was found that DVC particles may be superior in promoting chondrogenesis to DCC particles, and because DVC particles induced significant collagen II expression long-term, in the final study of this current thesis, the DVC particles were mixed with methacrylated and solubilized DVC (MeSDVC), in an

attempt to create a hydrogel paste that could be crosslinked to form a gel that exhibited similar biomechanics to native cartilage tissue and could induce chondrogenesis. Prior to crosslinking, the MeSDVC and MeSDVC + DVC particle gels were found to exhibit a yield stress. However, the gels containing DVC repeatedly outperformed the MeSDVC group in chondrogenic gene expression and did not have any cell-mediated contraction, which is a phenomenon observed in the MeSDVC gels and is detrimental for hydrogels because it can hinder tissue regeneration and integration. Although the compressive moduli of the DVC-containing groups were much less than that of native cartilage and the 20% MeSDCC gels from work earlier on in this current thesis, overall, this two-component system has been shown to be chondroinductive, and mechanically, is a vast improvement over the HA-based hydrogels at the beginning of this thesis.

Because the compressive modulus of the MeSDVC + DVC gels were found to be much lower than that of the 20% MeSDCC and native cartilage, future work should definitely consider improving the overall mechanical performance of the MeSDVC + DVC gels. Interestingly, the compressive modulus of the 20% MeSDVC gels in aim 3 was found to be lower than that of 20% MeSDCC gels from aim 2 and overall the stress strain profiles were observed to be significantly different from each other (Figure 7.2). This difference could be due to a number of reasons although the exact reason for the difference is unknown at this time and would need further work to fully understand the cause. However, the difference could be due to one or a combination of the following reasons: (1) MeSDCC and MeSDVC were made from materials of the same breed of pig, and have similar biochemical contents, but they were made in different batches, so it is possible that there

could be some batch-to-batch variation in the methacrylation process, (2) even though we tried to control for the same breed of pig, there could be variations within the same breed of pigs since the MeSDCC was made from a completely separate batch of pigs than the MeSDVC was, and (3), because the decellularization process is known to cause changes in ECM, it is possible that something was changed through decellularization that ultimately affected the mechanics of the MeSDCC gels. However, the MeSDVC gels did not fracture early like the MeSDCC gels (Figure 7.2) and therefore, perhaps they would be more beneficial for future work. Because the compressive modulus of the 20% MeSDVC group was within the range of reported values for native articular cartilage, future work could explore varying the ratios of MeSDVC and DVC to obtain gels that more closely mimic native cartilage mechanically, while still being able to take advantage of the chondroinductive properties of DVC microparticles. Specifically, since MeSDVC alone already has a yield stress, the amount of DVC in the solutions may be able to be reduced such that there is still an associated chondrogenic response, but the mechanical properties are improved.

From the results of the current thesis, DVC is still considered to be necessary in the hydrogel pastes due to its superior chondroinductive properties compared to DCC and compared to methacrylated cartilage ECM alone. Because all three of my 6 week *in vitro* studies were performed similarly with the same kind of cells, and because each of the gels was tested against a GAPDH control, the PCR between studies can be compared and evaluated with the $2^{-\Delta\Delta Ct}$ method to approximate differences observed among groups of different experiments. Overall, although the 10% MeSDCC gels had significantly higher

aggrecan and Sox-9 expression at day 1 compared to the other groups, high levels of collagen II gene expression are only observed for the DVC-containing groups (Figure 7.3).

Therefore, in terms of deciding whether to use MeSDCC and MeSDVC, the mechanics as well as the chondroinductive properties must be considered. MeSDCC had more chondroinductive potential early on and did have a compressive modulus similar to that of native cartilage, and the DVC-containing gels, although weaker than the MeSDCC, were the only groups to induce collagen II expression. Therefore, in considering the next steps for the work in this current thesis, testing DVC in comparison to DCC *in vivo* should be held paramount. *In vivo* studies will help discern whether there is any immunological response to DVC and furthermore, they will ultimately be able to discern which of the two materials is superior in inducing chondrogenesis. After DVC and DCC are compared, it can then be decided how to incorporate either MeSDVC or MeSDCC. If MeSDCC is chosen to be pursued, the early fracture stress will need to be addressed and if MeSDVC is chosen to be pursued, the biomechanics will need to be improved upon. However, overall, the work of this current thesis has shown that a two component system is the most successful in creating a hydrogel precursor that is paste-like prior to crosslinking, and after crosslinking, can withstand native cartilage tissue loading, retain its original volume throughout culture, and is chondroinductive. Specifically, the MeSDVC/MeSDCC component has been shown to be initially chondroinductive while enabling the pastes to be crosslinked and withstand native cartilage tissue loading, while the DVC particles have been shown to be crucial for long-term chondrogenesis and gel volume retention. Therefore, the results of this current thesis suggest the combination of MeSDVC/MeSDCC

with DVC particles is the most promising for future work. This two-component hydrogel paste has been taken from an idea to providing promising results and producing numerous new avenues for research to consider for cartilage tissue engineering applications. Furthermore, this two-component hydrogel paste could be applied for other tissue engineering applications as well that cannot tolerate a liquid draining away from an irregularly shaped defect and this application does not necessarily need to apply to cartilage. The two components could be made from any tissue of interest, whether its bone, cartilage, muscle, skin, etc., and the two-components could be fabricated using similar methods as to what is reported in the current thesis. Therefore, this current thesis lays the foundation for an endless opportunity of future hydrogel research in the tissue engineering field.

REFERENCES

[1]Adkisson H. D., J. A. Martin, R. L. Amendola, C. Milliman, K. A. Mauch, A. B. Katwal, M. Seyedin, A. Amendola, P. R. Streeter, and J. A. Buckwalter. The potential of human allogeneic juvenile chondrocytes for restoration of articular cartilage. *The American journal of sports medicine*. 38:1324-1333, 2010.

[2]Armstrong C. and V. Mow. Variations in the intrinsic mechanical properties of human articular cartilage with age, degeneration, and water content. *The Journal of Bone & Joint Surgery*. 64:88-94, 1982.

[3]Athanasiou K. A. D., Eric M.; DuRaine, Grayson D.; Hu, Jerry C.; A. Hari Reddi. *Articular Cartilage*. Boca Raton, FL: CRC Press. 2013.

[4]Beck E., C. Berkland, S. Gehrke, and M. Detamore. *Novel Hyaluronic Acid Nanocomposite Hydrogel for Cartilage Tissue Engineering: Utilizing Yield Stress for Ease of Implantation*. in *ASME 2013 Summer Bioengineering Conference*. 2013: American Society of Mechanical Engineers.

[5]Beck E. C., B. L. Lohman, D. B. Tabakh, S. L. Kieweg, S. H. Gehrke, C. J. Berkland, and M. S. Detamore. Enabling Surgical Placement of Hydrogels Through Achieving Paste-Like Rheological Behavior in Hydrogel Precursor Solutions. *Annals of biomedical engineering*.1-8, 2015.

[6]Benders K., P. van Weeren, S. Badylak, D. Saris, W. Dhert, and J. Malda. Extracellular matrix scaffolds for cartilage and bone regeneration. *Trends Biotechnol*. 31:169-176, 2013.

[7]Benjamin M. and J. Ralphs. Fibrocartilage in tendons and ligaments—an adaptation to compressive load. *Journal of anatomy*. 193:481-494, 1998.

[8]Bian W., D. Li, Q. Lian, X. Li, W. Zhang, K. Wang, and Z. Jin. Fabrication of a bio-inspired beta-Tricalcium phosphate/collagen scaffold based on ceramic stereolithography and gel casting for osteochondral tissue engineering. *Rapid Prototyping Journal*. 18:68-80, 2012.

[9]Brigham M., A. Bick, E. Lo, A. Bendali, J. Burdick, and A. Khademhosseini. Mechanically robust and bioadhesive collagen and photocrosslinkable hyaluronic acid semi-interpenetrating networks. *Tissue Eng Part A*. 15:1645-1653, 2009.

[10]Burdick J. A., R. L. Mauck, J. H. Gorman, 3rd, and R. C. Gorman. Acellular biomaterials: an evolving alternative to cell-based therapies. *Sci Transl Med*. 5:176ps4, 2013.

[11]Cha M., S. Do, G. Park, P. Du, K.-C. Han, D. Han, and K. Park. Induction of re-differentiation of passaged rat chondrocytes using a naturally obtained extracellular matrix microenvironment. *Tissue Eng Part A*. 19:978-988, 2013.

[12]Cheng H., K. D. K. Luk, K. Cheung, and B. P. Chan. In vitro generation of an osteochondral interface from mesenchymal stem cell–collagen microspheres. *Biomaterials*. 32:1526-1535, 2011.

[13]Cheng N.-C., B. Estes, T.-H. Young, and F. Guilak. Genipin-crosslinked cartilage-derived matrix as a scaffold for human adipose-derived stem cell chondrogenesis. *Tissue Eng Part A*. 19:484-496, 2013.

[14]Cheng N.-C., B. T. Estes, H. A. Awad, and F. Guilak. Chondrogenic differentiation of adipose-derived adult stem cells by a porous scaffold derived from native articular cartilage extracellular matrix. *Tissue Engineering Part A*. 15:231-241, 2008.

[15]Cheng N.-C., B. T. Estes, T.-H. Young, and F. Guilak. Engineered cartilage using primary chondrocytes cultured in a porous cartilage-derived matrix. *Regenerative medicine*. 6:81-93, 2011.

[16]Chew S. Y., T. C. Hufnagel, C. T. Lim, and K. W. Leong. Mechanical properties of single electrospun drug-encapsulated nanofibres. *Nanotechnology*. 17:3880, 2006.

[17]Chun S. Y., G. J. Lim, T. G. Kwon, E. K. Kwak, B. W. Kim, A. Atala, and J. J. Yoo. Identification and characterization of bioactive factors in bladder submucosa matrix. *Biomaterials*. 28:4251-4256, 2007.

[18]Chung E. J., P. Kodali, W. Laskin, J. L. Koh, and G. A. Ameer. Long-term in vivo response to citric acid-based nanocomposites for orthopaedic tissue engineering. *Journal of Materials Science: Materials in Medicine*.1-8, 2011.

[19]Chung E. J., H. Qiu, P. Kodali, S. Yang, S. M. Sprague, J. Hwong, J. Koh, and G. A. Ameer. Early tissue response to citric acid–based micro-and nanocomposites. *Journal of Biomedical Materials Research Part A*. 96:29-37, 2011.

[20]Converse G., M. Armstrong, R. Quinn, E. Buse, M. Cromwell, S. Moriarty, G. Lofland, S. Hilbert, and R. Hopkins. Effects of cryopreservation, decellularization and novel extracellular matrix conditioning on the quasi-static and time-dependent properties of the pulmonary valve leaflet. *Acta Biomaterialia*. 8:2722-2729, 2012.

[21]Cool S., B. Kenny, A. Wu, V. Nurcombe, M. Trau, A. Cassady, and L. Grøndahl. Poly (3-hydroxybutyrate-co-3-hydroxyvalerate) composite biomaterials for bone tissue regeneration: In vitro performance assessed by osteoblast proliferation, osteoclast adhesion and resorption, and macrophage proinflammatory response. *Journal of Biomedical Materials Research Part A*. 82:599-610, 2007.

[22]Decaris M., B. Binder, M. Soicher, A. Bhat, and J. Leach. Cell-derived matrix coatings for polymeric scaffolds. *Tissue Eng Part A*. 18:2148-2157, 2012.

[23]DeKosky B., N. Dormer, G. Ingavle, C. Roatch, J. Lomakin, M. Detamore, and S. Gehrke. Hierarchically designed agarose and poly(ethylene glycol) interpenetrating network hydrogels for cartilage tissue engineering. *Tissue engineering. Part C, Methods*. 16:1533-1542, 2010.

[24]Deng M., R. James, C. Laurencin, and S. Kumbar. Nanostructured Polymeric Scaffolds for Orthopaedic Regenerative Engineering. *NanoBioscience, IEEE Transactions on*.1-1, 2011.

[25]Dennis S., M. Detamore, S. Kieweg, and C. Berkland. Mapping Glycosaminoglycan-Hydroxyapatite Colloidal Gels as Potential Tissue Defect Fillers. *Langmuir : the ACS journal of surfaces and colloids*. 2014.

[26]Detamore M. S. and A. N. Renth. Leveraging "Raw Materials" as Building Blocks and Bioactive Signals in Regenerative Medicine. *Tissue Engineering*. 2012.

[27]Dormer N. H., C. J. Berkland, and M. S. Detamore. Emerging techniques in stratified designs and continuous gradients for tissue engineering of interfaces. *Annals of biomedical engineering*. 38:2121-2141, 2010.

[28]Dormer N. H., K. Busaidy, C. J. Berkland, and M. S. Detamore. Osteochondral Interface Regeneration of Rabbit Mandibular Condyle With Bioactive Signal Gradients. *Journal of Oral and Maxillofacial Surgery*. 2011.

[29]Dormer N. H., M. Singh, L. Wang, C. J. Berkland, and M. S. Detamore. Osteochondral interface tissue engineering using macroscopic gradients of bioactive signals. *Annals of biomedical engineering*. 38:2167-2182, 2010.

[30]Dormer N. H., M. Singh, L. Zhao, N. Mohan, C. J. Berkland, and M. S. Detamore. Osteochondral interface regeneration of the rabbit knee with macroscopic gradients of bioactive signals. *Journal of Biomedical Materials Research Part A*. 2012.

[31]Dorozhkin S. V. Bioceramics of calcium orthophosphates. *Biomaterials*. 31:1465-1485, 2010.

[32]Elder A., N. Dangelo, S. Kim, and N. Washburn. Conjugation of β-sheet peptides to modify the rheological properties of hyaluronic acid. *Biomacromolecules*. 12:2610-2616, 2011.

[33]Elisseeff J., C. Puleo, F. Yang, and B. Sharma. Advances in skeletal tissue engineering with hydrogels. *Orthodontics & craniofacial research*. 8:150-161, 2005.

[34]Erisken C., D. M. Kalyon, and H. Wang. Functionally graded electrospun polycaprolactone and β-tricalcium phosphate nanocomposites for tissue engineering applications. *Biomaterials*. 29:4065-4073, 2008.

[35]Erisken C., D. M. Kalyon, and H. Wang. Viscoelastic and biomechanical properties of osteochondral tissue constructs generated from graded polycaprolactone and beta-tricalcium phosphate composites. *Journal of biomechanical engineering*. 132:091013, 2010.

[36]Erisken C., D. M. Kalyon, H. Wang, C. Ornek-Ballanco, and J. Xu. Osteochondral tissue formation through adipose-derived stromal cell differentiation on biomimetic polycaprolactone nanofibrous scaffolds with graded insulin and Beta-glycerophosphate concentrations. *Tissue Eng Part A*. 17:1239-52, 2011.

[37]Fakhari A., Q. Phan, and C. Berkland. Hyaluronic acid colloidal gels as self-assembling elastic biomaterials. *Journal of biomedical materials research. Part B, Applied biomaterials*. 2013.

[38]Fakhari A., Q. Phan, S. Thakkar, C. Middaugh, and C. Berkland. Hyaluronic acid nanoparticles titrate the viscoelastic properties of viscosupplements. *Langmuir : the ACS journal of surfaces and colloids*. 29:5123-5131, 2013.

[39]Filardo G., E. Kon, M. Delcogliano, G. Giordano, T. Bonanzinga, M. Marcacci, and S. Zaffagnini. Novel Nano-composite Multilayered Biomaterial for the Treatment of Patellofemoral Cartilage Lesions. *Patellofemoral Pain, Instabilty, and Arthritis: Clinical Presentation, Imaging, and Treatment*. 12:255, 2010.

[40]Freytes D. O., J. Martin, S. S. Velankar, A. S. Lee, and S. F. Badylak. Preparation and rheological characterization of a gel form of the porcine urinary bladder matrix. *Biomaterials*. 29:1630-1637, 2008.

[41]Garrigues N. W., D. Little, J. Sanchez-Adams, D. S. Ruch, and F. Guilak. Electrospun cartilage-derived matrix scaffolds for cartilage tissue engineering. *Journal of Biomedical Materials Research Part A*. 2014.

[42]Gawlitta D., K. E. Benders, J. Visser, A. S. van der Sar, D. H. Kempen, L. F. Theyse, J. Malda, and W. J. Dhert. Decellularized cartilage-derived matrix as substrate for endochondral bone regeneration. *Tissue Engineering Part A*. 21:694-703, 2014.

[43]Gershlak J. R., J. I. Resnikoff, K. E. Sullivan, C. Williams, R. M. Wang, and L. D. Black. Mesenchymal stem cells ability to generate traction stress in response to substrate stiffness is modulated by the changing extracellular matrix composition of the heart during development. *Biochemical and biophysical research communications*. 439:161-166, 2013.

[44]Gong J., O. Sagiv, H. Cai, S. H. Tsang, and L. V. Del Priore. Effects of extracellular matrix and neighboring cells on induction of human embryonic stem cells into retinal or retinal pigment epithelial progenitors. *Experimental eye research*. 86:957-965, 2008.

[45]Grayson W. L., P. H. G. Chao, D. Marolt, D. L. Kaplan, and G. Vunjak-Novakovic. Engineering custom-designed osteochondral tissue grafts. *Trends in biotechnology*. 26:181-189, 2008.

[46]Grogan S. P., C. Pauli, P. Chen, J. Du, C. B. Chung, S. D. Kong, C. W. Colwell Jr, M. Lotz, S. Jin, and D. D'Lima. In situ tissue engineering using magnetically guided 3D cell patterning. *Tissue Engineering*. 2012.

[47]Harley B. A., A. K. Lynn, Z. Wissner-Gross, W. Bonfield, I. V. Yannas, and L. J. Gibson. Design of a multiphase osteochondral scaffold III: Fabrication of layered scaffolds with continuous interfaces. *Journal of Biomedical Materials Research Part A*. 92:1078-1093, 2010.

[48]Harley B. A., A. K. Lynn, Z. Wissner-Gross, W. Bonfield, I. V. Yannas, and L. J. Gibson. Design of a multiphase osteochondral scaffold. II. Fabrication of a mineralized collagen–glycosaminoglycan scaffold. *Journal of Biomedical Materials Research Part A*. 92:1066-1077, 2010.

[49]Huang C.-Y., A. Stankiewicz, G. A. Ateshian, and V. C. Mow. Anisotropy, inhomogeneity, and tension–compression nonlinearity of human glenohumeral cartilage in finite deformation. *Journal of biomechanics*. 38:799-809, 2005.

[50]Hunziker E. Articular cartilage repair: basic science and clinical progress. A review of the current status and prospects. *Osteoarthritis and cartilage*. 10:432-463, 2002.

[51]Jha A., R. Hule, T. Jiao, S. Teller, R. Clifton, R. Duncan, D. Pochan, and X. Jia. Structural Analysis and Mechanical Characterization of Hyaluronic Acid-Based Doubly Cross-Linked Networks. *Macromolecules*. 42:537-546, 2009.

[52]Jha A., M. Malik, M. Farach-Carson, R. Duncan, and X. Jia. Hierarchically structured, hyaluronic acid-based hydrogel matrices via the covalent integration of microgels into macroscopic networks. *Soft matter*. 6:5045-5055, 2010.

[53]Jha A., X. Xu, R. Duncan, and X. Jia. Controlling the adhesion and differentiation of mesenchymal stem cells using hyaluronic acid-based, doubly crosslinked networks. *Biomaterials*. 32:2466-2478, 2011.

[54]Jia X. and K. Kiick. Hybrid multicomponent hydrogels for tissue engineering. *Macromolecular bioscience*. 9:140-156, 2009.

[55]Jia X., Y. Yeo, R. Clifton, T. Jiao, D. Kohane, J. Kobler, S. Zeitels, and R. Langer. Hyaluronic acid-based microgels and microgel networks for vocal fold regeneration. *Biomacromolecules*. 7:3336-3344, 2006.

[56]Johansen E. and H. F. Parks. Electron Microscopic Observations on the Three-Dimensional Morphology of Apatite Crystallites of Human Dentine and Bone'. *The Journal of biophysical and biochemical cytology*. 7:743-746, 1960.

[57]Kanematsu A., S. Yamamoto, M. Ozeki, T. Noguchi, I. Kanatani, O. Ogawa, and Y. Tabata. Collagenous matrices as release carriers of exogenous growth factors. *Biomaterials*. 25:4513-4520, 2004.

[58]Kaplan F., W. Hayes, T. Keaveny, A. Boskey, T. Einhorn, and J. Iannotti. Form and function of bone. *Orthopaedic Basic Science*.127-185, 1994.

[59]Keane T. J., R. Londono, N. J. Turner, and S. F. Badylak. Consequences of ineffective decellularization of biologic scaffolds on the host response. *Biomaterials*. 33:1771-1781, 2012.

[60]Keane T. J., I. T. Swinehart, and S. F. Badylak. Methods of tissue decellularization used for preparation of biologic scaffolds and in vivo relevance. *Methods*. 2015.

[61]Kew S., J. Gwynne, D. Enea, M. Abu-Rub, A. Pandit, D. Zeugolis, R. Brooks, N. Rushton, S. Best, and R. Cameron. Regeneration and repair of tendon and ligament tissue using collagen fibre biomaterials. *Acta Biomaterialia*. 2011.

[62]Khanarian N. T., N. M. Haney, R. A. Burga, and H. H. Lu. A functional agarose-hydroxyapatite scaffold for osteochondral interface regeneration. *Biomaterials*. 2012.

[63]Khanlari A., M. S. Detamore, and S. H. Gehrke. Increasing Cross-Linking Efficiency of Methacrylated Chondroitin Sulfate Hydrogels by Copolymerization with Oligo (Ethylene Glycol) Diacrylates. *Macromolecules*. 46:9609-9617, 2013.

[64]Kheir E., T. Stapleton, D. Shaw, Z. Jin, J. Fisher, and E. Ingham. Development and characterization of an acellular porcine cartilage bone matrix for use in tissue engineering. *Journal of biomedical materials research Part A*. 99:283-294, 2011.

[65]Kon E., M. Delcogliano, G. Filardo, G. Altadonna, and M. Marcacci. Novel nano-composite multi-layered biomaterial for the treatment of multifocal degenerative cartilage lesions. *Knee Surgery, Sports Traumatology, Arthroscopy*. 17:1312-1315, 2009.

[66]Kon E., M. Delcogliano, G. Filardo, M. Busacca, A. Di Martino, and M. Marcacci. Novel Nano-composite Multilayered Biomaterial for Osteochondral Regeneration. *The American journal of sports medicine*. 39:1180-1190, 2011.

[67]Kon E., M. Delcogliano, G. Filardo, M. Fini, G. Giavaresi, S. Francioli, I. Martin, D. Pressato, E. Arcangeli, and R. Quarto. Orderly osteochondral regeneration in a sheep model using a novel nano-composite multilayered biomaterial. *Journal of Orthopaedic Research*. 28:116-124, 2010.

[68]Kon E., M. Delcogliano, G. Filardo, D. Pressato, M. Busacca, B. Grigolo, G. Desando, and M. Marcacci. A novel nano-composite multi-layered biomaterial for treatment of osteochondral lesions: technique note and an early stability pilot clinical trial. *Injury*. 41:693-701, 2010.

[69]Kon E., A. Mutini, E. Arcangeli, M. Delcogliano, G. Filardo, N. Nicoli Aldini, D. Pressato, R. Quarto, S. Zaffagnini, and M. Marcacci. Novel nanostructured scaffold for osteochondral regeneration: pilot study in horses. *Journal of tissue engineering and regenerative medicine*. 4:300-308, 2010.

[70]Kwon J. S., S. M. Yoon, S. W. Shim, J. H. Park, K. J. Min, H. J. Oh, J. H. Kim, Y. J. Kim, J. J. Yoon, and B. H. Choi. Injectable extracellular matrix hydrogel developed using porcine articular cartilage. *International journal of pharmaceutics*. 454:183-191, 2013.

[71]Ladd M. R., S. J. Lee, J. D. Stitzel, A. Atala, and J. J. Yoo. Co-electrospun dual scaffolding system with potential for muscle–tendon junction tissue engineering. *Biomaterials*. 32:1549-1559, 2011.

[72]Lee J. M., B. S. Kim, H. Lee, and G. I. Im. In Vivo Tracking of Mesechymal Stem Cells Using Fluorescent Nanoparticles in an Osteochondral Repair Model. *Molecular Therapy*. 2012.

[73]Levorson E., O. Hu, P. Mountziaris, F. Kasper, and A. Mikos. Cell-derived polymer/extracellular matrix composite scaffolds for cartilage regeneration, part 2: construct devitalization and determination of chondroinductive capacity. *Tissue engineering. Part C, Methods*. 20:358-372, 2014.

[74]Li X., J. Xie, J. Lipner, X. Yuan, S. Thomopoulos, and Y. Xia. Nanofiber scaffolds with gradations in mineral content for mimicking the tendon-to-bone insertion site. *Nano letters*. 9:2763-2768, 2009.

[75]Lim J. and J. Temenoff. Tendon and ligament tissue engineering: Restoring tendon/ligament and its interfaces. *Fundamentals of Tissue Engineering and Regenerative Medicine*. 20:255, 2009.

[76]Little C. J., N. K. Bawolin, and X. Chen. Mechanical properties of natural cartilage and tissue-engineered constructs. *Tissue Engineering Part B: Reviews*. 17:213-227, 2011.

[77]Liu C., Z. Han, and J. Czernuszka. Gradient collagen/nanohydroxyapatite composite scaffold: Development and characterization. *Acta Biomaterialia*. 5:661-669, 2009.

[78]Liu X., X. Jin, and P. X. Ma. Nanofibrous hollow microspheres self-assembled from star-shaped polymers as injectable cell carriers for knee repair. *Nature Materials*. 10:398-406, 2011.

[79]Liu Y., Y. Zhang, P. Dong, R. An, C. Xue, Y. Ge, L. Wei, and X. Liang. Digestion of Nucleic Acids Starts in the Stomach. *Scientific reports*. 5, 2015.

[80]Livak K. J. and T. D. Schmittgen. Analysis of relative gene expression data using real-time quantitative PCR and the 2− ΔΔCT method. *methods*. 25:402-408, 2001.

[81]Lu H., M. Charati, I. Kim, and J. Burdick. Injectable shear-thinning hydrogels engineered with a self-assembling Dock-and-Lock mechanism. *Biomaterials*. 33:2145-2153, 2012.

[82]Lu H. and J. Jiang. Interface Tissue Engineeringand the Formulation of Multiple-Tissue Systems. *Tissue Engineering I*.91-111, 2006.

[83]Lu H. H. and J. P. Spalazzi. Biomimetic stratified scaffold design for ligament-to-bone interface tissue engineering. *Combinatorial Chemistry &# 38; High Throughput Screening*. 12:589-597, 2009.

[84]Lu H. H., S. D. Subramony, M. K. Boushell, and X. Zhang. Tissue engineering strategies for the regeneration of orthopedic interfaces. *Annals of biomedical engineering*. 38:2142-2154, 2010.

[85]Mansour J. M. Biomechanics of cartilage. *Kinesiology: the mechanics and pathomechanics of human movement*.66-79, 2003.

[86]Martin R. B., D. B. Burr, and N. A. Sharkey. *Skeletal tissue mechanics*: Springer Verlag. 1998.

[87]Matsusaki M., K. Kadowaki, K. Tateishi, C. Higuchi, W. Ando, D. A. Hart, Y. Tanaka, Y. Take, M. Akashi, and H. Yoshikawa. Scaffold-Free Tissue-Engineered Construct–Hydroxyapatite Composites Generated by an Alternate Soaking Process: Potential for Repair of Bone Defects. *Tissue Engineering Part A*. 15:55-63, 2008.

[88]McLennan A., A. Bates, P. Turner, and M. White. *BIOS Instant Notes in Molecular Biology*: Taylor & Francis. 2012.

[89]Mikos A. G., S. W. Herring, P. Ochareon, J. Elisseeff, H. H. Lu, R. Kandel, F. J. Schoen, M. Toner, D. Mooney, and A. Atala. Engineering complex tissues. *Tissue Engineering*. 12:3307-3339, 2006.

[90]Moffat K. L., I. Wang, S. A. Rodeo, and H. H. Lu. Orthopedic interface tissue engineering for the biological fixation of soft tissue grafts. *Clinics in sports medicine*. 28:157-176, 2009.

[91]Mohan N., N. H. Dormer, K. L. Caldwell, V. H. Key, C. J. Berkland, and M. S. Detamore. Continuous gradients of material composition and growth factors for effective regeneration of the osteochondral interface. *Tissue Engineering Part A*. 17:2845-2855, 2011.

[92]Moutos F. T., B. T. Estes, and F. Guilak. Multifunctional hybrid three-dimensionally woven scaffolds for cartilage tissue engineering. *Macromol Biosci*. 10:1355-64, 2010.

[93]Murat G., D. L. Hoang, and A. B. Jason. Shear-thinning hydrogels for biomedical applications. *Soft matter*. 8, 2012.

[94]Murphy L. and C. G. Helmick. The impact of osteoarthritis in the United States: a population-health perspective. *AJN The American Journal of Nursing*. 112:S13-S19, 2012.

[95]Nettles D. L., T. P. Vail, M. T. Morgan, M. W. Grinstaff, and L. A. Setton. Photocrosslinkable hyaluronan as a scaffold for articular cartilage repair. *Annals of biomedical engineering*. 32:391-397, 2004.

[96]Ngiam M., L. Nguyen, S. Liao, C. Chan, and S. Ramakrishna. Biomimetic nanostructured materials: Potential regulators for osteogenesis. *Ann. Acad. Med. Singap*. 40:213-220, 2011.

[97]Nirmala R., K. T. Nam, D. K. Park, B. Woo-il, R. Navamathavan, and H. Y. Kim. Structural, thermal, mechanical and bioactivity evaluation of silver-loaded bovine bone hydroxyapatite grafted poly (ε-caprolactone) nanofibers via electrospinning. *Surface and Coatings Technology*. 205:174-181, 2010.

[98]Panseri S., A. Russo, C. Cunha, A. Bondi, A. Di Martino, S. Patella, and E. Kon. Osteochondral tissue engineering approaches for articular cartilage and subchondral bone regeneration. *Knee Surgery, Sports Traumatology, Arthroscopy*.1-10, 2011.

[99]Poole A. R., T. Kojima, T. Yasuda, F. Mwale, M. Kobayashi, and S. Laverty. Composition and structure of articular cartilage: a template for tissue repair. *Clinical orthopaedics and related research*. 391:S26, 2001.

[100]Porter J. R., T. T. Ruckh, and K. C. Popat. Bone tissue engineering: a review in bone biomimetics and drug delivery strategies. *Biotechnology progress*. 25:1539-1560, 2009.

[101]Prata J., T. Barth, S. Bencherif, and N. Washburn. Complex fluids based on methacrylated hyaluronic acid. *Biomacromolecules*. 11:769-775, 2010.

[102]Qu D., J. Li, Y. Li, A. Khadka, Y. Zuo, H. Wang, Y. Liu, and L. Cheng. Ectopic osteochondral formation of biomimetic porous PVA-n-HA/PA6 bilayered scaffold and BMSCs construct in rabbit. *Journal of Biomedical Materials Research Part B: Applied Biomaterials*. 96:9-15, 2011.

[103]Ramalingam M., M. F. Young, V. Thomas, L. Sun, L. C. Chow, C. K. Tison, K. Chatterjee, W. C. Miles, and C. G. Simon Jr. Nanofiber scaffold gradients for interfacial tissue engineering. *Journal of Biomaterials Applications*. 2012.

[104]Renth A. N. and M. S. Detamore. Leveraging "raw materials" as building blocks and bioactive signals in regenerative medicine. *Tissue Eng Part B Rev*. 18:341-62, 2012.

[105]Revell C. M. and K. A. Athanasiou. Success rates and immunologic responses of autogenic, allogenic, and xenogenic treatments to repair articular cartilage defects. *Tissue Engineering Part B: Reviews*. 15:1-15, 2008.

[106]Rho J. Y., L. Kuhn-Spearing, and P. Zioupos. Mechanical properties and the hierarchical structure of bone. *Medical engineering & physics*. 20:92-102, 1998.

[107]Robinson R. A. An electron-microscopic study of the crystalline inorganic component of bone and its relationship to the organic matrix. *The Journal of Bone and Joint Surgery (American)*. 34:389-476, 1952.

[108]Rodrigues A. A., N. A. Batista, V. P. Bavaresco, V. Baranauskas, H. J. Ceragioli, A. C. Peterlevitz, J. R. L. Mariolani, M. H. A. Santana, and W. D. Belangero. In vivo evaluation of hydrogels of polyvinyl alcohol with and without carbon nanoparticles for osteochondral repair. *Carbon*. 2012.

[109]Rowland C., D. Lennon, A. Caplan, and F. Guilak. The effects of crosslinking of scaffolds engineered from cartilage ECM on the chondrogenic differentiation of MSCs. *Biomaterials*. 34:5802-5812, 2013.

[110]Rughani R. V., M. C. Branco, D. J. Pochan, and J. P. Schneider. De novo design of a shear-thin recoverable peptide-based hydrogel capable of intrafibrillar photopolymerization. *Macromolecules*. 43:7924-7930, 2010.

[111]Sahiner N., A. Jha, D. Nguyen, and X. Jia. Fabrication and characterization of cross-linkable hydrogel particles based on hyaluronic acid: potential application in vocal fold regeneration. *Journal of biomaterials science. Polymer edition*. 19:223-243, 2008.

[112]Sahoo S., T. K. H. Teh, P. He, S. L. Toh, and J. C. H. Goh. Interface Tissue Engineering: Next Phase in Musculoskeletal Tissue Repair. *Annals of the Academy of Medicine-Singapore*. 40:245, 2011.

[113]Samavedi S., C. Olsen Horton, S. A. Guelcher, A. S. Goldstein, and A. R. Whittington. Fabrication of a model continuously graded co-electrospun mesh for regeneration of the ligament-bone interface. *Acta Biomaterialia*. 2011.

[114]Schuurman W., P. A. Levett, M. W. Pot, P. R. van Weeren, W. J. Dhert, D. W. Hutmacher, F. P. Melchels, T. J. Klein, and J. Malda. Gelatin-Methacrylamide Hydrogels as Potential Biomaterials for Fabrication of Tissue-Engineered Cartilage Constructs. *Macromolecular bioscience*. 13:551-561, 2013.

[115]Schwarz S., A. F. Elsaesser, L. Koerber, E. Goldberg-Bockhorn, A. M. Seitz, C. Bermueller, L. Dürselen, A. Ignatius, R. Breiter, and N. Rotter. Processed xenogenic cartilage as innovative biomatrix for cartilage tissue engineering: effects on chondrocyte differentiation and function. *Journal of tissue engineering and regenerative medicine*. 2012.

[116]Schwarz S., L. Koerber, A. F. Elsaesser, E. Goldberg-Bockhorn, A. M. Seitz, L. Durselen, A. Ignatius, P. Walther, R. Breiter, and N. Rotter. Decellularized cartilage matrix as a novel biomatrix for cartilage tissue-engineering applications. *Tissue Eng Part A*. 18:2195-209, 2012.

[117]Seidi A. and M. Ramalingam. Impact of Gradient Biomaterials on Interface Tissue Engineering. *Journal of Biomaterials and Tissue Engineering*. 2:89-99, 2012.

[118]Seidi A., M. Ramalingam, I. Elloumi-Hannachi, S. Ostrovidov, and A. Khademhosseini. Gradient biomaterials for soft-to-hard interface tissue engineering. *Acta Biomaterialia*. 2011.

[119]Seif-Naraghi S. B., D. Horn, P. J. Schup-Magoffin, and K. L. Christman. Injectable extracellular matrix derived hydrogel provides a platform for enhanced retention and delivery of a heparin-binding growth factor. *Acta biomaterialia*. 8:3695-3703, 2012.

[120]Seif-Naraghi S. B., M. A. Salvatore, P. J. Schup-Magoffin, D. P. Hu, and K. L. Christman. Design and characterization of an injectable pericardial matrix gel: a potentially autologous scaffold for cardiac tissue engineering. *Tissue Engineering Part A*. 16:2017-2027, 2010.

[121]Sellaro T. L., A. K. Ravindra, D. B. Stolz, and S. F. Badylak. Maintenance of hepatic sinusoidal endothelial cell phenotype in vitro using organ-specific extracellular matrix scaffolds. *Tissue engineering*. 13:2301-2310, 2007.

[122]Singh M., N. Dormer, J. R. Salash, J. M. Christian, D. S. Moore, C. Berkland, and M. S. Detamore. Three-dimensional macroscopic scaffolds with a gradient in stiffness for functional regeneration of interfacial tissues. *Journal of Biomedical Materials Research Part A*. 94:870-876, 2010.

[123]Smith I. O. and P. X. Ma. Biomimetic Scaffolds in Tissue Engineering. *Tissue Engineering*.31-39, 2011.

[124]Smith L., Y. Xia, L. M. Galatz, G. M. Genin, and S. Thomopoulos. Tissue Engineering Strategies for the Tendon/Ligament-to-Bone Insertion. *Connective Tissue Research*. 2011.

[125]Sondi I. and B. Salopek-Sondi. Silver nanoparticles as antimicrobial agent: a case study on< i> E. coli</i> as a model for Gram-negative bacteria. *Journal of colloid and interface science*. 275:177-182, 2004.

[126]Spalazzi J. P., M. C. Vyner, M. T. Jacobs, K. L. Moffat, and H. H. Lu. Mechanoactive scaffold induces tendon remodeling and expression of fibrocartilage markers. *Clinical Orthopaedics and Related Research®*. 466:1938-1948, 2008.

[127]Sridharan B., B. Sharma, and M. S. Detamore. A Roadmap to Commercialization of Cartilage Therapy in the United States of America. *Tissue Engineering*. 2015.

[128]Sutherland A. J., E. C. Beck, S. C. Dennis, G. L. Converse, R. A. Hopkins, C. J. Berkland, and M. S. Detamore. Decellularized Cartilage May Be a Chondroinductive Material for Osteochondral Tissue Engineering. 2015.

[129]Sutherland A. J., G. L. Converse, R. A. Hopkins, and M. S. Detamore. The bioactivity of cartilage extracellular matrix in articular cartilage regeneration. *Advanced healthcare materials*. 4:29-39, 2015.

[130]Tampieri A., E. Landi, F. Valentini, M. Sandri, T. D'Alessandro, V. Dediu, and M. Marcacci. A conceptually new type of bio-hybrid scaffold for bone regeneration. *Nanotechnology*. 22:015104, 2011.

[131]Tampieri A., M. Sandri, E. Landi, D. Pressato, S. Francioli, R. Quarto, and I. Martin. Design of graded biomimetic osteochondral composite scaffolds. *Biomaterials*. 29:3539-3546, 2008.

[132]Tan H., C. Chu, K. Payne, and K. Marra. Injectable in situ forming biodegradable chitosan-hyaluronic acid based hydrogels for cartilage tissue engineering. *Biomaterials*. 30:2499-2506, 2009.

[133]Tatman P. D., W. Gerull, S. Sweeney-Easter, J. I. Davis, D.-H. Kim, and A. Gee. Multi-scale Biofabrication of Articular Cartilage: Bioinspired and Biomimetic Approaches. *Tissue Engineering*. 2015.

[134]Tezel A. and G. H. Fredrickson. The science of hyaluronic acid dermal fillers. *Journal of Cosmetic and Laser Therapy*. 10:35-42, 2008.

[135]Todd R. H. and S. K. Daniel. Hydrogels in drug delivery: Progress and challenges. *Polymer*. 49, 2008.

[136]Treacy M., T. Ebbesen, and J. Gibson. Exceptionally high Young's modulus observed for individual carbon nanotubes. 1996.

[137]Tsang K. Y., M. C. H. Cheung, D. Chan, and K. S. E. Cheah. The developmental roles of the extracellular matrix: beyond structure to regulation. *Cell and tissue research*. 339:93-110, 2010.

[138]Ulrich-Vinther M., M. D. Maloney, E. M. Schwarz, R. Rosier, and R. J. O'Keefe. Articular cartilage biology. *Journal of the American Academy of Orthopaedic Surgeons*. 11:421-430, 2003.

[139]Vavken P., U. Meyer, T. Meyer, J. Handschel, and H. Wiesman. Tissue engineering of ligaments and tendons. *Fundamentals of Tissue Engineering and Regenerative Medicine*.317-327, 2009.

[140]Villanueva I., C. A. Weigel, and S. J. Bryant. Cell–matrix interactions and dynamic mechanical loading influence chondrocyte gene expression and bioactivity in PEG-RGD hydrogels. *Acta biomaterialia*. 5:2832-2846, 2009.

[141]Visser J., P. A. Levett, N. C. te Moller, J. Besems, K. W. Boere, M. H. van Rijen, J. C. de Grauw, W. J. Dhert, P. R. van Weeren, and J. Malda. Crosslinkable Hydrogels Derived from Cartilage, Meniscus, and Tendon Tissue. *Tissue Engineering Part A*. 21:1195-1206, 2015.

[142]Wan Y. S., S. Wei-Heng, and A. A. Ilhan. Elastic and Yield Behavior of Strongly Flocculated Colloids. *Journal of the American Ceramic Society*. 82, 2004.

[143]Wang H., S. C. G. Leeuwenburgh, Y. Li, and J. A. Jansen. The Use of Micro-and Nanospheres as Functional Components for Bone Tissue Regeneration. *Tissue Engineering Part B: Reviews*. 2011.

[144]Wang Q., Z. Gu, S. Jamal, M. S. Detamore, and C. Berkland. Hybrid Hydroxyapatite Nanoparticle Colloidal Gels are Injectable Fillers for Bone Tissue Engineering. *Tissue Engineering Part A*. 19:2586-2593, 2013.

[145]Wang Q., S. Jamal, M. Detamore, and C. Berkland. PLGA-chitosan/PLGA-alginate nanoparticle blends as biodegradable colloidal gels for seeding human umbilical cord mesenchymal stem cells. *Journal of biomedical materials research. Part A*. 96:520-527, 2011.

[146]Wang Q., J. Wang, Q. Lu, M. Detamore, and C. Berkland. Injectable PLGA based colloidal gels for zero-order dexamethasone release in cranial defects. *Biomaterials*. 2010.

[147]Wang Q., L. Wang, M. S. Detamore, and C. Berkland. Biodegradable colloidal gels as moldable tissue engineering scaffolds. *Advanced Materials*. 20:236-239, 2008.

[148]Weiss P., A. Fatimi, J. Guicheux, and C. Vinatier. "Hydrogels for Cartilage Tissue Engineering," in *Biomedical Applications of Hydrogels Handbook*. 2010, Springer. 247-268.

[149]Woo S., M. Gomez, Y. Seguchi, C. Endo, and W. Akeson. Measurement of mechanical properties of ligament substance from a bone-ligament-bone preparation. *Journal of Orthopaedic Research*. 1:22-29, 1983.

[150]Xiao Y., E. A. Friis, S. H. Gehrke, and M. S. Detamore. Mechanical testing of hydrogels in cartilage tissue engineering: beyond the compressive modulus. *Tissue Eng Part B Rev*. 19:403-12, 2013.

[151]Xie J., X. Li, J. Lipner, C. N. Manning, A. G. Schwartz, S. Thomopoulos, and Y. Xia. “Aligned-to-random” nanofiber scaffolds for mimicking the structure of the tendon-to-bone insertion site. *Nanoscale*. 2:923-926, 2010.

[152]Xue D., Q. Zheng, C. Zong, Q. Li, H. Li, S. Qian, B. Zhang, L. Yu, and Z. Pan. Osteochondral repair using porous poly (lactide-co-glycolide)/nano-hydroxyapatite hybrid scaffolds with undifferentiated mesenchymal stem cells in a rat model. *Journal of Biomedical Materials Research Part A*. 94:259-270, 2010.

[153]Yang L., C. F. C. Fitié, K. O. Van Der Werf, M. L. Bennink, P. J. Dijkstra, and J. Feijen. Mechanical properties of single electrospun collagen type I fibers. *Biomaterials*. 29:955-962, 2008.

[154]Yang P. J. and J. S. Temenoff. Engineering orthopedic tissue interfaces. *Tissue Engineering Part B: Reviews*. 15:127-141, 2009.

[155]Yang Q., J. Peng, S. Lu, Q. Guo, B. Zhao, L. Zhang, and A. Wang. Evaluation of an extracellular matrix-derived acellular biphasic scaffold/cell construct in the repair of a large articular high-load-bearing osteochondral defect in a canine model. *Chinese Medical Journal*. 124:3930-3938, 2011.

[156]Yang Z., Y. Shi, X. Wei, J. He, S. Yang, G. Dickson, J. Tang, J. Xiang, C. Song, and G. Li. Fabrication and repair of cartilage defects with a novel acellular cartilage matrix scaffold. *Tissue Eng Part C Methods*. 16:865-76, 2010.

[157]Yunos D., Z. Ahmad, V. Salih, and A. Boccaccini. Stratified scaffolds for osteochondral tissue engineering applications: Electrospun PDLLA nanofibre coated Bioglass®-derived foams. *Journal of Biomaterials Applications*. 2011.

[158]Zhang Q., V. N. Mochalin, I. Neitzel, K. Hazeli, J. Niu, A. Kontsos, J. G. Zhou, P. I. Lelkes, and Y. Gogotsi. Mechanical properties and biomineralization of multifunctional nanodiamond-PLLA composites for bone tissue engineering. *Biomaterials*. 2012.

[159]Zhang R. and P. X. Ma. Porous poly (L-lactic acid)/apatite composites created by biomimetic process. 1999.

[160]Zhang X., D. Bogdanowicz, C. Erisken, N. M. Lee, and H. H. Lu. Biomimetic scaffold design for functional and integrative tendon repair. *Journal of Shoulder and Elbow Surgery*. 21:266-277, 2012.

[161]Zheng X., S. Lu, W. Zhang, S. Liu, J. Huang, and Q. Guo. Mesenchymal stem cells on a decellularized cartilage matrix for cartilage tissue engineering. *Biotechnology and Bioprocess Engineering*. 16:593-602, 2011.

[162]Zou B., Y. Liu, X. Luo, F. Chen, X. Guo, and X. Li. Electrospun fibrous scaffolds with continuous gradations in mineral contents and biological cues for manipulating cellular behaviors. *Acta Biomaterialia*. 2012.

APPENDIX A: Figures

CHAPTER 1: Figures 1.1-1.2

CHAPTER 2: Figure 2.1

CHAPTER 3: Figures 3.1-3.4

CHAPTER 4: Figures 4.1-4.8

CHAPTER 5: Figures 5.1-5.7

CHAPTER 6: Figures 6.1-6.9

CHAPTER 7: Figures 7.1-7.3

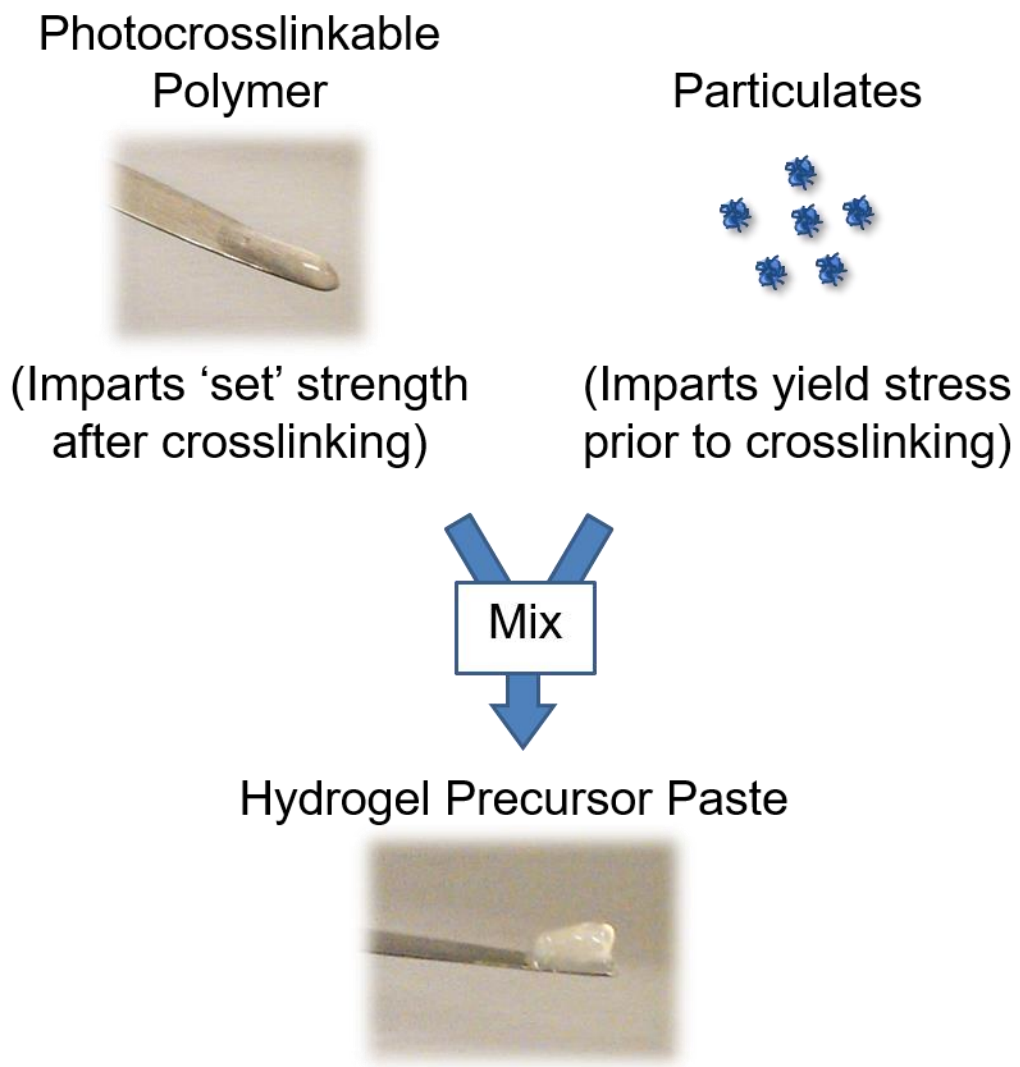

Figure 1.1: Conversion of Hydrogel Precursors into Hydrogel Precursor Pastes

Hydrogel pastes are created by mixing traditional photocrosslinkable polymers with particulates. The photocrosslinkable polymer gives the paste its 'set' strength after photocrosslinking while the particles impart a yield stress on the paste prior to crosslinking.

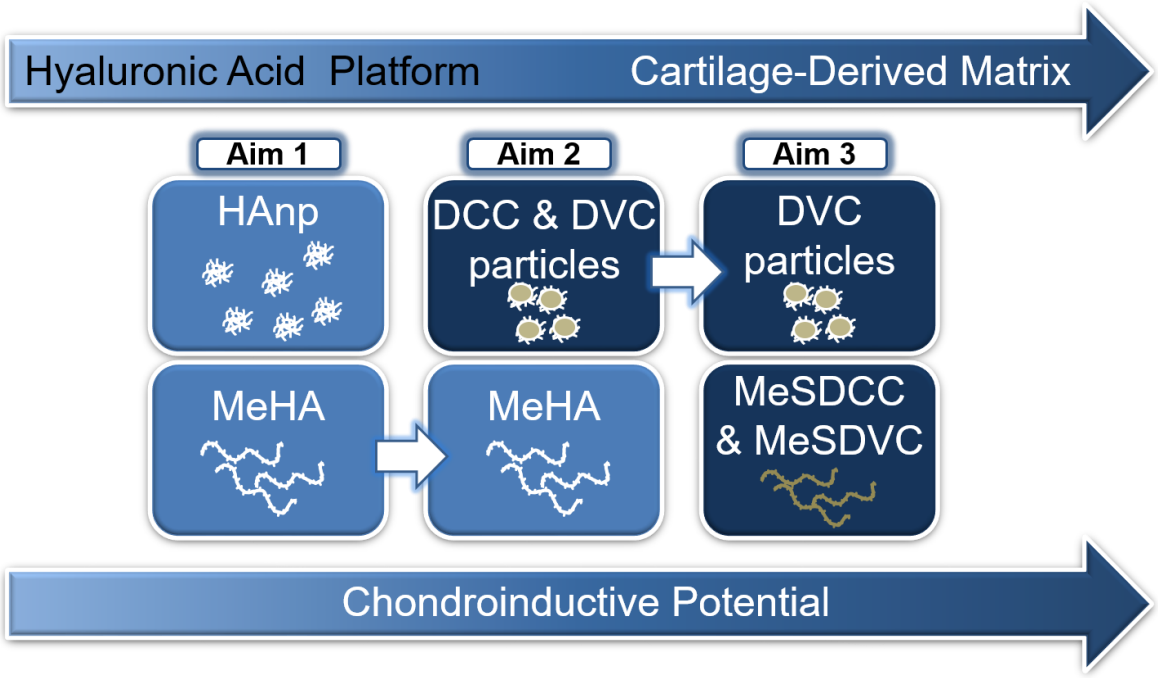

Figure 1.2: Schematic of the Progression of Thesis Aims

The two-component hydrogel pastes in aim 1 are hyaluronic acid nanoparticles (HAnp) and methacrylated hyaluronic acid (MeHA). In Aim 2, DCC and DVC particles replace the HAnp. In Aim 3, MeSDCC is evaluated alone as a hydrogel material and then two component pastes composed of DVC particles and MeSDVC were evaluated.

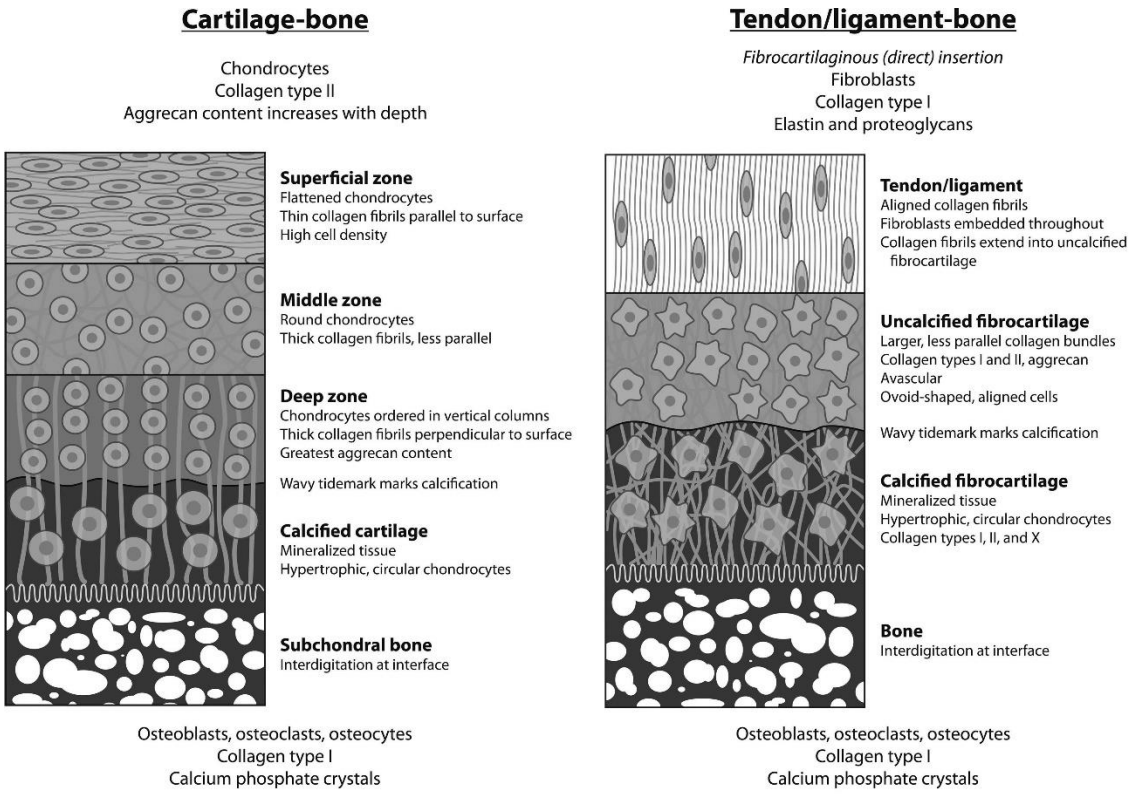

Figure 2.1: Structure and Components of Tissue Interfaces

This diagram depicts the cartilage–bone and tendon/ligament–bone interfaces and their compositions.

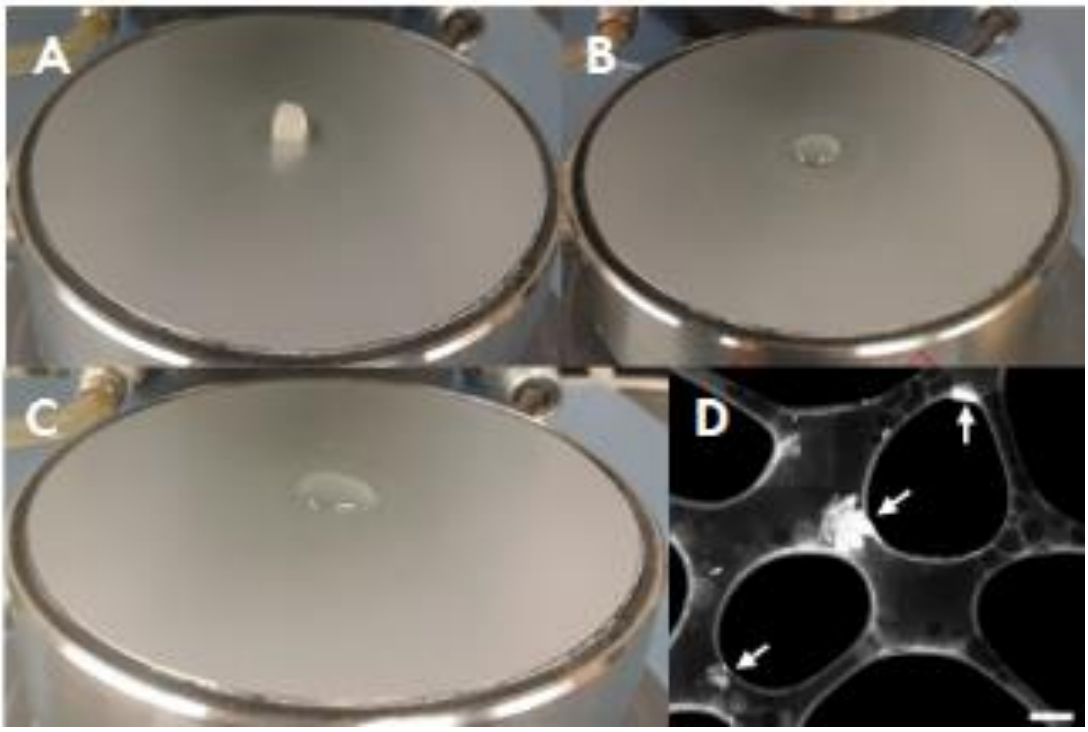

Figure 3.1: Hyaluronic Acid Nanoparticle (HAnp)-Incorporated Solutions Impart Paste-Like Gross Rheological Behavior

(A-C) Images of select experimental groups loaded onto the lower rheometer plate prior to rheological testing. (A) 4% Methacrylated hyaluronic acid (MeHA) with 15% HAnp gel solution with shape-retention, (B) 4% MeHA with 15% linear HA (HAlin) and (C) 4% MeHA formulations yielding low viscosity solutions absent of yield stress. Because there were no visible differences between the remaining linear HA groups and Figure 1B, and likewise, no visible differences between the remaining HAnp-containing solutions and Figure 1A, the photographs of these remaining experimental groups were omitted from this figure. (D) Scanning transmission electron microscopy (STEM) observation of HAnp. The scale bar is 200 nm and arrows point to individual HAnps.

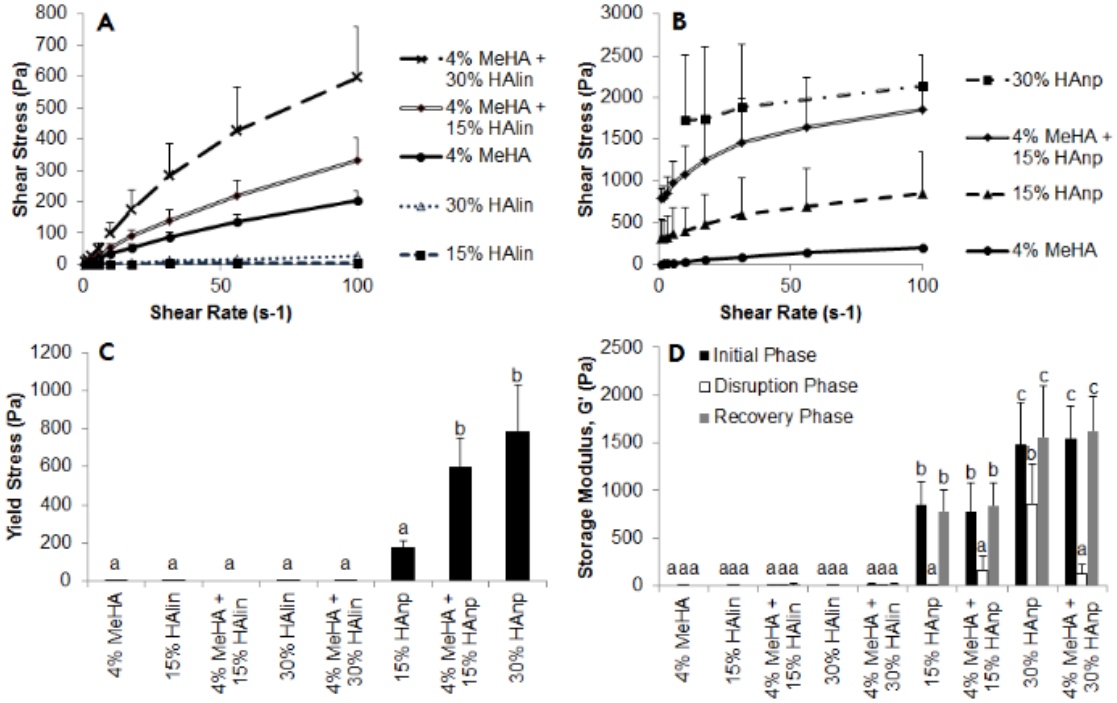

Figure 3.2: Rheological Behavior of Solutions Prior to Crosslinking

(A-B) Shear rate sweep of formulations without yield stress (A) and formulations with yield stress compared to 4% Methacrylated Hyaluronic Acid (MeHA) (B). Data points are mean + standard deviation (n=5) and the lines are used to connect the data points to discern between samples. For the 30% hyaluronic acid nanoparticle (HAnp) formulation, shear banding was observed at low shear rates so those data were excluded. (C) Yield stress obtained from fit to Herschel-Bulkley equation. (D) Storage modulus of formulations before, after, and during disruption. Data reported as mean + standard deviation (n=5). Formulations with different letters indicate statistically significant differences ($p<0.05$).

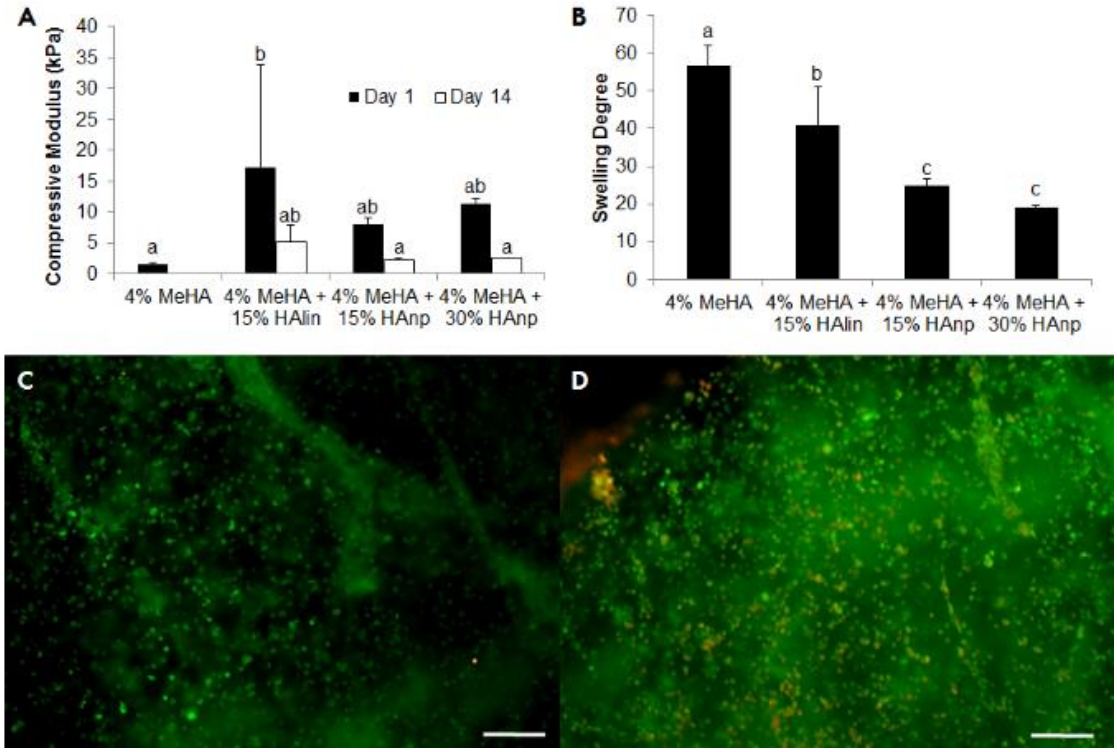

Figure 3.3: Characterization of Gels After Crosslinking

Compressive modulus (A) and swelling degree (B) of crosslinked gels. Data are reported as mean + standard deviation (n=6). Formulations with different letters indicate statistically significant differences ($p<0.05$). Live/Dead image analysis of cells encapsulated and cultured for 4 weeks within 4% Methacrylated Hyaluronic Acid (MeHA) (C) and 4% MeHA + 15% hyaluronic acid nanoparticles (HAnp) (D). Scale bars are 100 µm.

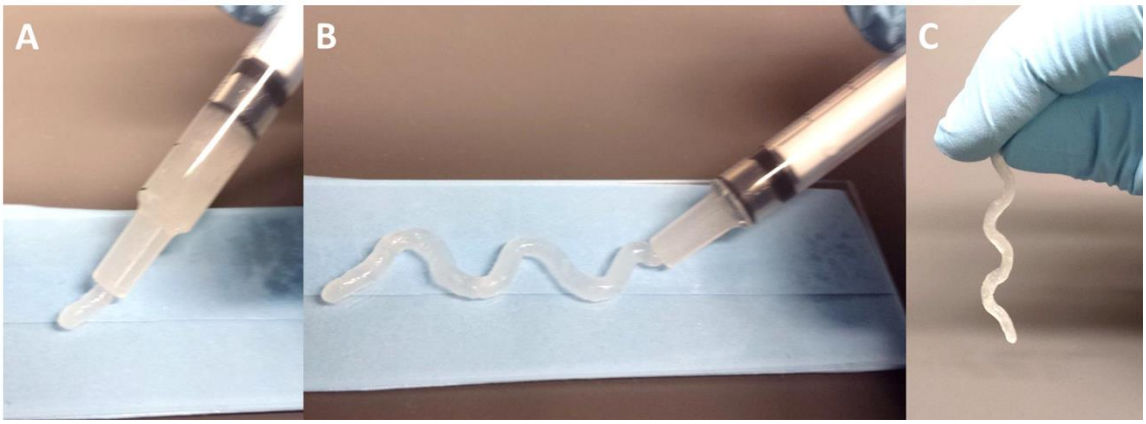

Figure 3.4: Hyaluronic Acid Nanoparticle (HAnp)-Incorporated Solutions Maintain Shaping Before and After Crosslinking

(A) A solution containing 4% MeHA with 15% HAnp can be readily loaded into a 1 mL syringe and extruded. (B) After extrusion, the HAnp-incorporated solution maintained extruded shaping, which demonstrates that this formulation could be implanted *in vivo* without the risk of leaking from the implantation site. (C) After photocrosslinking the HAnp-incorporated solution, the solution was a crosslinked hydrogel network that retained its original shaping.

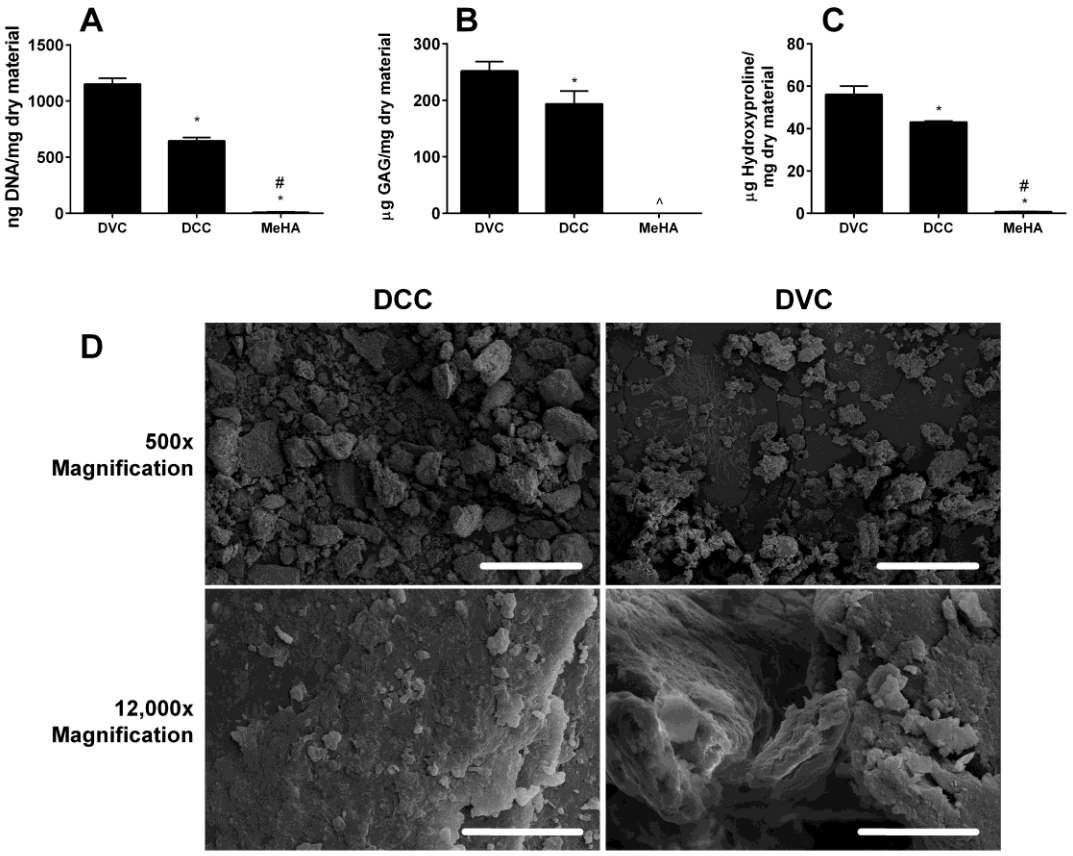

Figure 4.1: Biochemical Contents and SEM Images of Hydrogel Paste Components

A) PicoGreen content, B) GAG content, and C) Hydroxyproline content of DVC, DCC, and MeHA. Following decellularization, there was a 44% reduction in DNA, a 23% reduction in GAG, and a 23% reduction in hydroxyproline content. Data reported as mean + standard deviation (n=5); ^below detectable limit, *significantly different from DVC ($p<0.05$), #significantly different from DCC ($p<0.05$). D) SEM images of DCC and DVC microparticles under 500x and 12,000x magnifications. Under 500x magnification, the DCC microparticles were noted to have more smooth surfaces overall in comparison to the DVC microparticles and under 12,000x magnification, the surfaces of the DCC microparticles were noted to have a grain-like appearance that was non-existent in the DVC microparticles. Scale bars for the 500x and 12,000x magnifications are 100 µm and 5 µm, respectively.

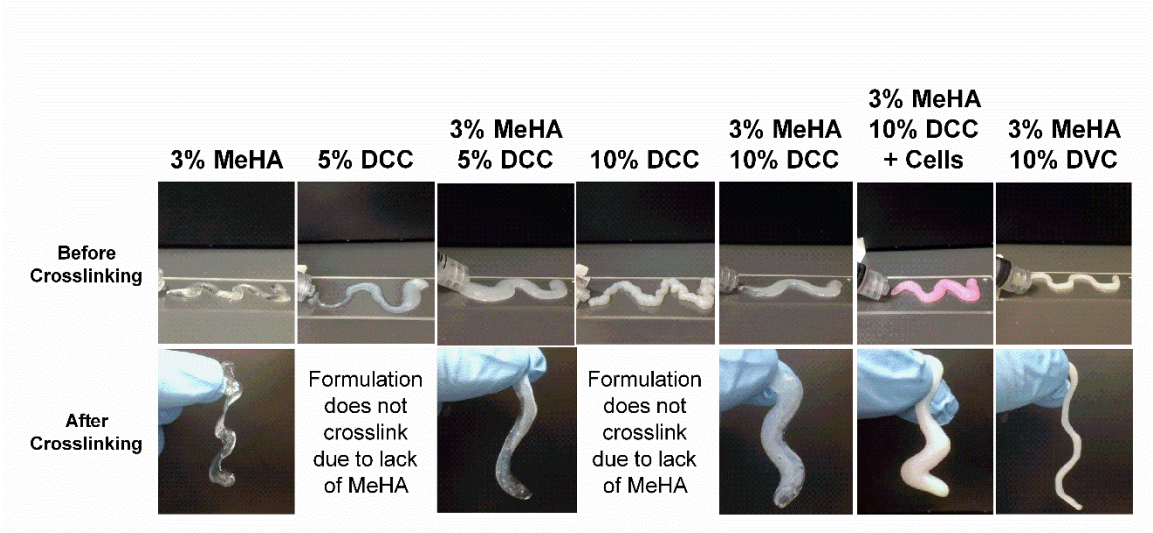

Figure 4.2: Macroscopic Rheological Evaluation of Hydrogel Precursors Before and After Crosslinking

All formulations were acellular unless noted. Non-Newtonian behavior was observed in solutions containing at least 5% DCC, whereas shape retention (indicated by the solution retaining extrusion orifice diameter) was only noted in 10% DCC and 3% MeHA + 10% DVC acellular formulations. All formulations containing MeHA retained their shape after crosslinking.

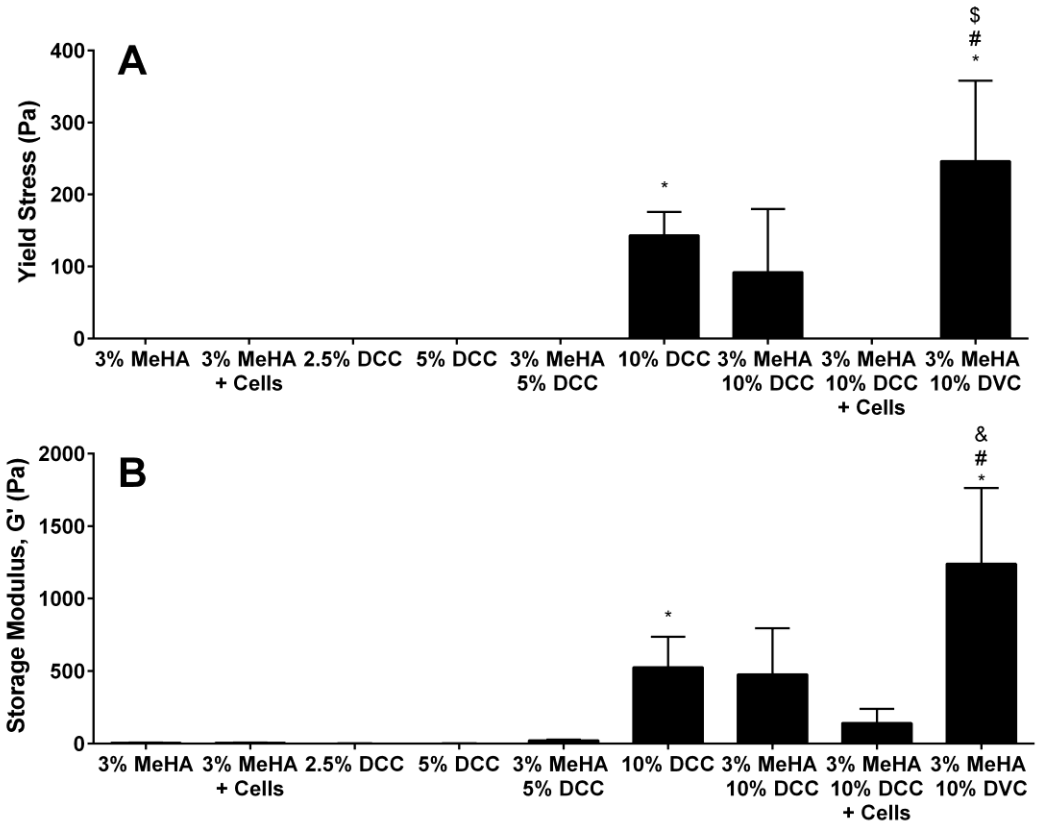

Figure 4.3: Yield Stress (A) and Storage Modulus (B) of Hydrogel Precursor Solutions

Only the 10% DCC, 3% MeHA + 10% DCC, and 3% MeHA + 10% DVC groups exhibited a measurable yield stress, while all groups had a measurable storage modulus. Data reported as mean + standard deviation (n=5); *significantly different from 3% MeHA acellular group ($p<0.05$), #significantly different from 3% MeHA + 10% DCC acellular group ($p<0.05$), $significantly different from 10% DCC group ($p<0.05$), &significantly different from all other groups ($p<0.05$).

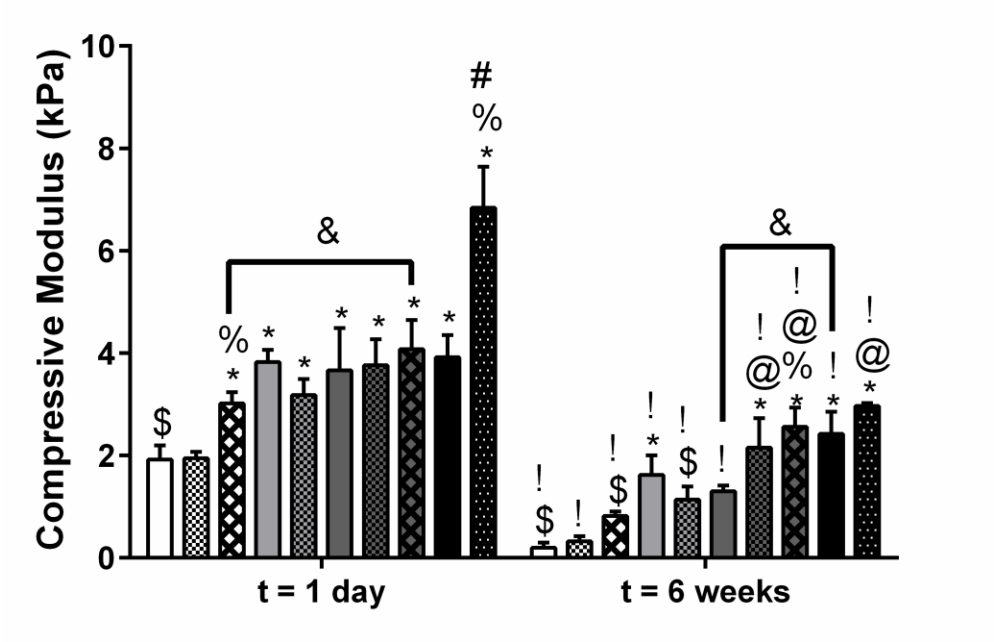

Figure 4.4: Compressive Moduli of Crosslinked Hydrogels After 1 Day and 6 Weeks of Culture

Gels containing at least 10% DCC or DVC microparticles had significantly larger moduli than 3% MeHA gels alone. Data reported as mean + standard deviation (n=5); *significantly different from 3% MeHA at same time point ($p<0.05$), %significantly different from acellular group of same formulation at same time point ($p<0.05$), #significantly different from all other groups at same time point ($p<0.05$), $significantly different from 3% MeHA + 10% DCC at same time point ($p<0.05$), @significantly different from 3% MeHA + TGF-β_3 and 3% MeHA + 5% DCC at same time point ($p<0.05$), &$p<0.05$ for specified comparison, !significantly different from same group at first time point ($p<0.05$).

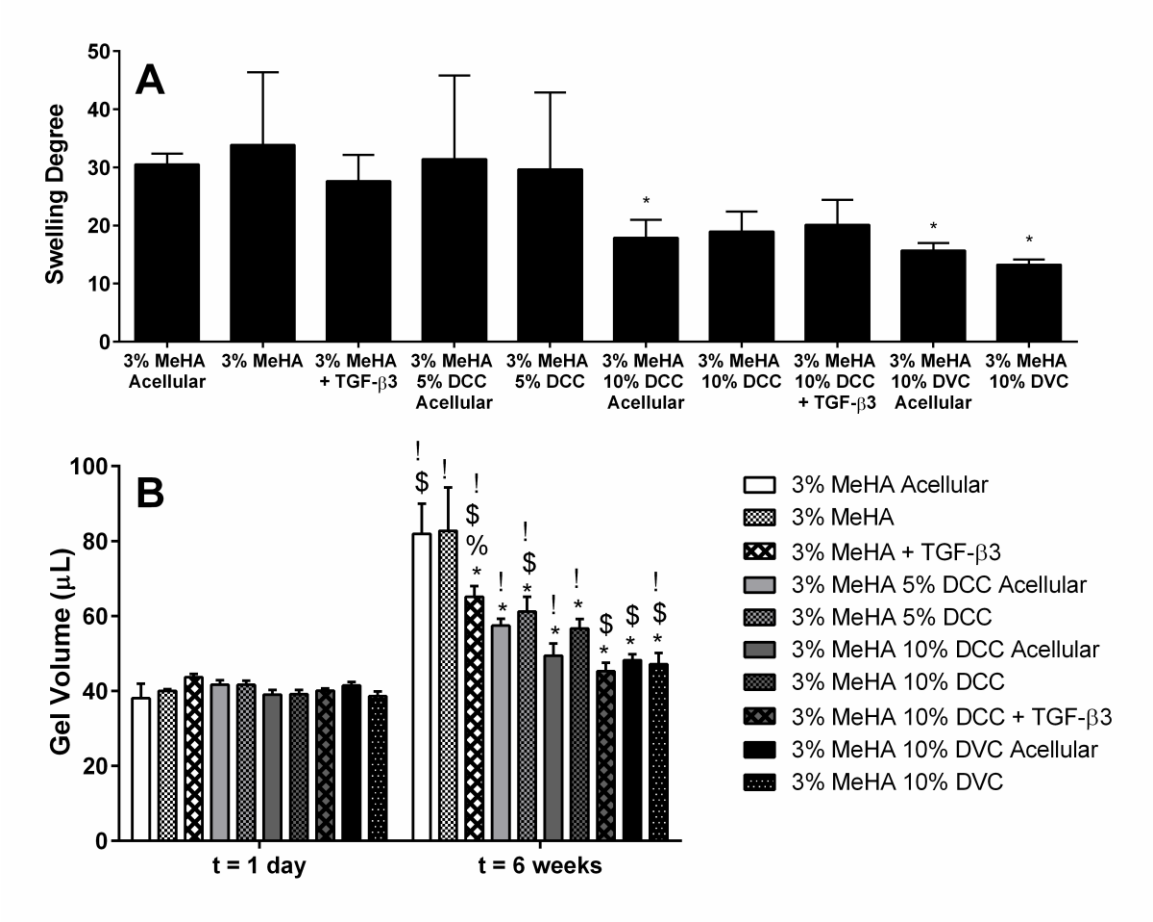

Figure 4.5: Swelling Degree (A) and Volume (B) of Crosslinked Hydrogels

The only gels with significantly smaller swelling degrees than the 3% MeHA gels were the 3% MeHA + 10% DCC acellular group and the 3% MeHA + 10% DVC acellular and cellular groups. At day 1, there were no significant differences between groups. However, the inclusion of DCC or DVC or exposure to TGF-β_3 significantly reduced the volume at 6 weeks. Data reported as mean + standard deviation (n=5); *significantly different from 3%MeHA at same time point ($p<0.05$), %significantly different from acellular group of same formulation at same time point ($p<0.05$), $significantly different from 3%MeHA + 10% DCC at same time point ($p<0.05$), !significantly different from same group at first time point ($p<0.05$).

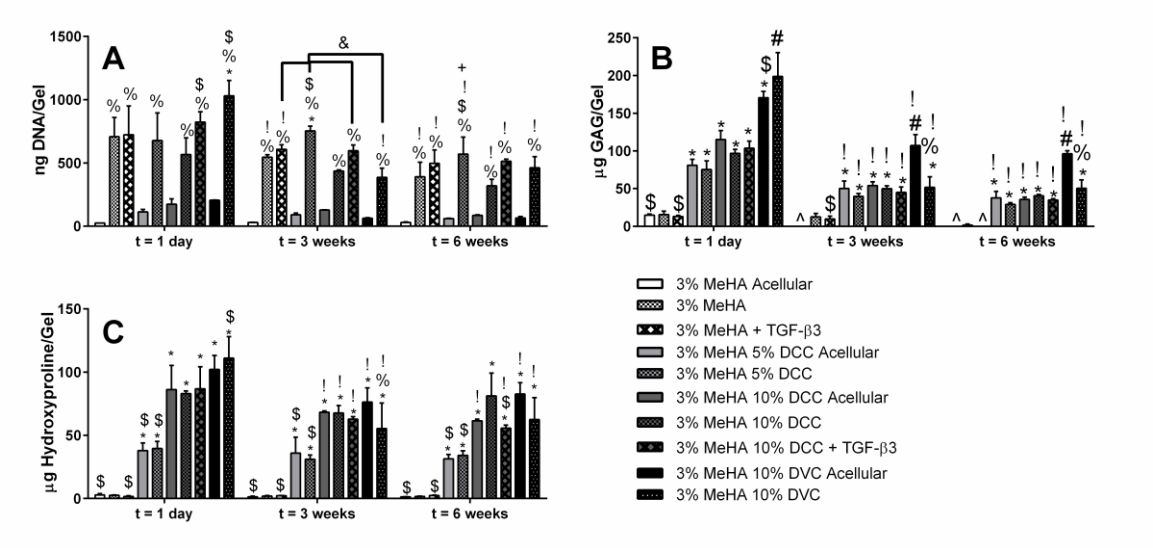

Figure 4.6: Biochemical Content of Gels over the 6 Week Culture Period

A) DNA content, B) GAG content, and C) Hydroxyproline content. All gels contained significantly higher DNA contents than their respective acellular groups at all time points and all gels containing DCC or DVC had significant reductions in GAG over the 6 week culture period. Data reported as mean + standard deviation (n=5); ^below detectable limit, *significantly different from 3%MeHA at same time point ($p<0.05$), %significantly different from acellular group of same formulation at same time point ($p<0.05$), #significantly different from all other groups at same time point ($p<0.05$), $significantly different from 3% MeHA + 10% DCC at same time point ($p<0.05$), !significantly different from same group at first time point ($p<0.05$), +significantly different from same group at previous time point ($p<0.05$).

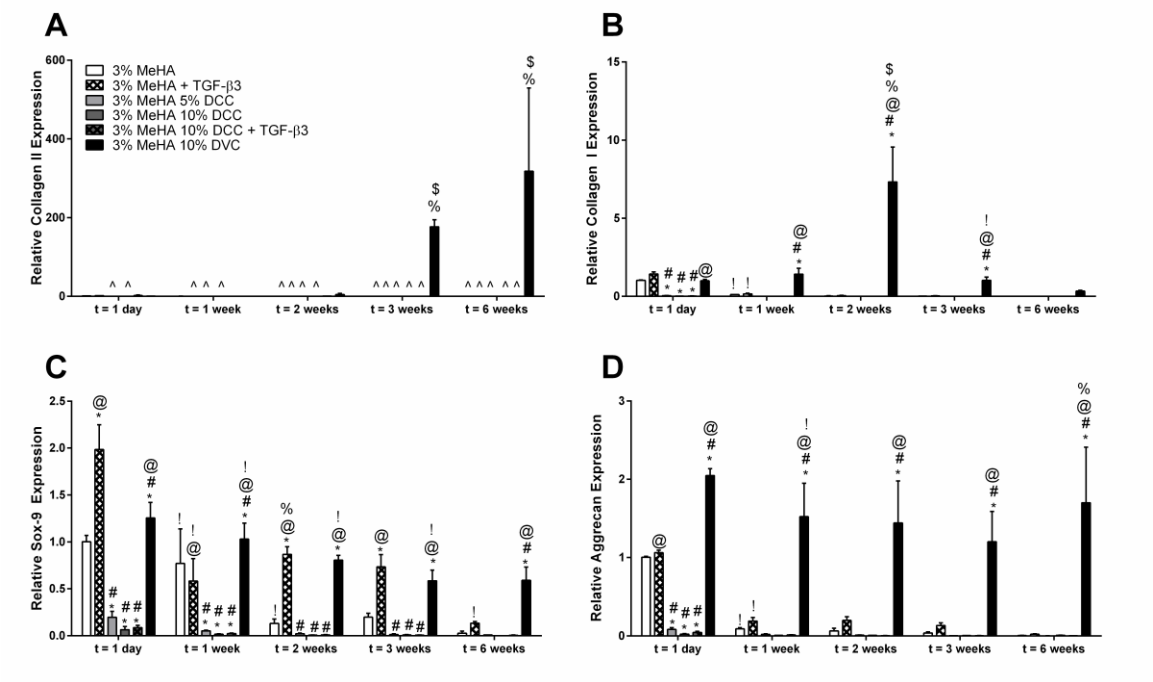

Figure 4.7: Relative Gene Expression of A) Collagen II, B) Collagen I, C) Sox-9, and D) Aggrecan

The DVC group consistently outperformed the other groups in collagen II, Sox-9, and aggrecan expression, even when compared to TGF-β_3 exposed groups. Data reported as mean + standard deviation (n=5); *significantly different from 3%MeHA at same time point ($p<0.05$), #significantly different from 3%MeHA +TGF-β_3 at same time point ($p<0.05$), @significantly different from all DCC containing groups at same time point ($p<0.05$), %significantly higher than same group at previous time point ($p<0.05$), $significantly higher than same group at first time point ($p<0.05$), !significantly lower than same group at previous time point ($p<0.05$), ^expression not detected.

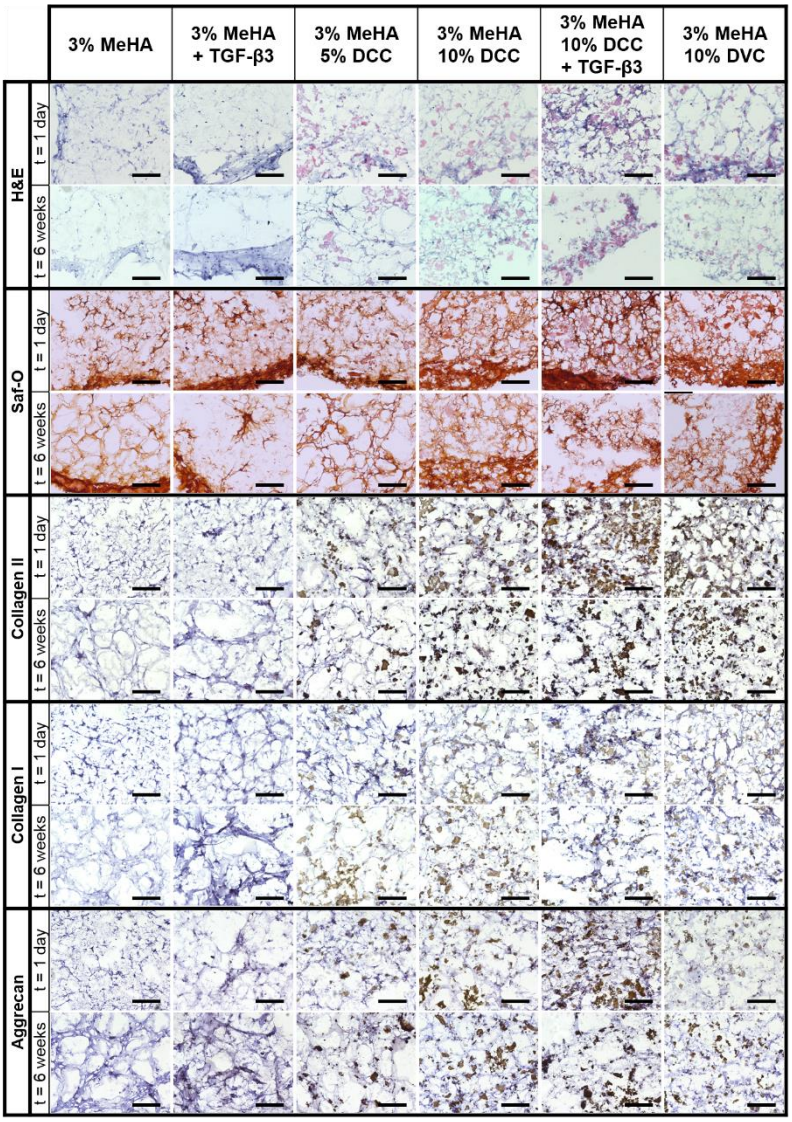

Figure 4.8: Histological Analysis of Gels

All gels stained red/orange for GAGs, although no increase in the amount of staining was noted over the culture period. However, nodular Saf-O staining was noted in the 3% MeHA + TGF-β_3 group. All DCC and DVC containing groups stained for Collagen II, however no changes were noted in the location and intensity of collagen II staining over the culture period. Collagen I staining was noted again in all DCC and DVC containing groups. However, the intensity of collagen I staining decreased over the culture period for the 3% MeHA + 5% DCC and 3% MeHA + 10% DCC groups and appeared to increase slightly for the 3% MeHA + 10% DVC group. Aggrecan staining was noted in all DCC and DVC containing groups, where the aggrecan staining became more intense near the DCC and DVC microparticles in the 3% MeHA + 10% DCC + TGF-β_3 and 3% MeHA + 10% DVC groups over the culture period. Scale bars are 200 µm.

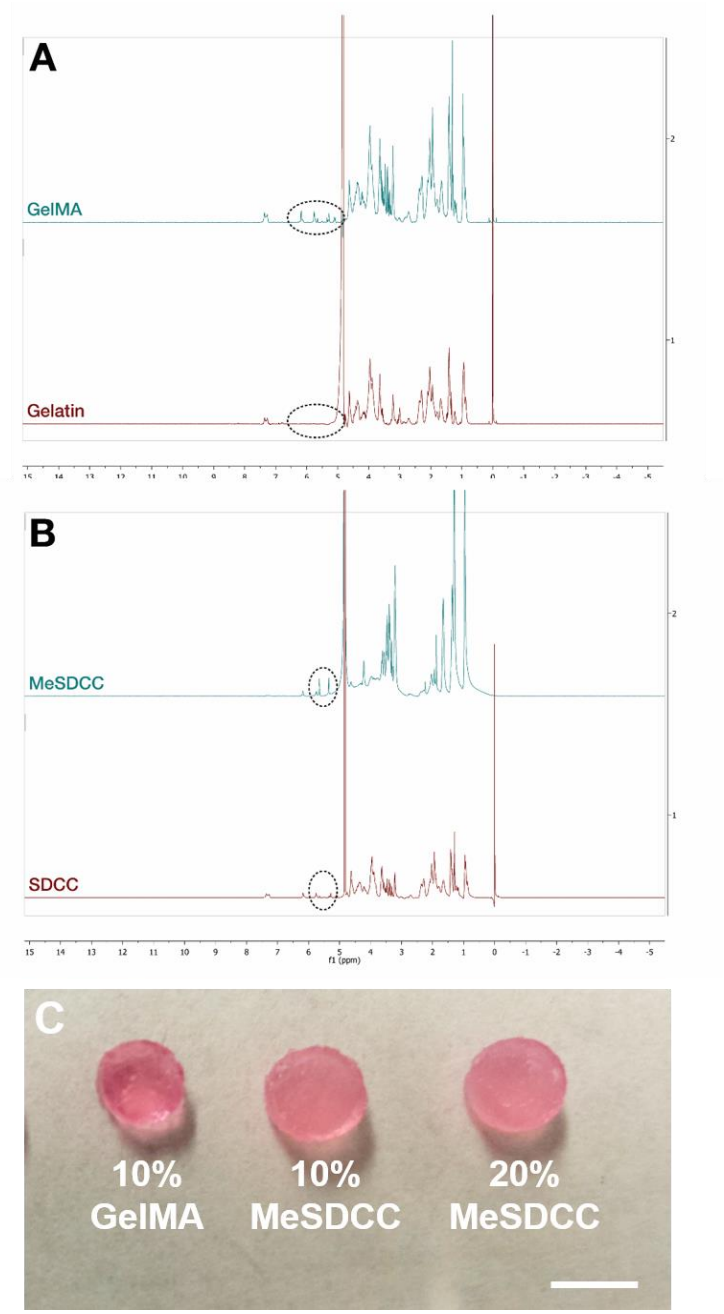

Figure 5.1: NMR of GelMA (A) and MeSDCC (B) Before and After Methacrylation and (C) Gross Morphology of Crosslinked Hydrogels

Methacrylation was confirmed on both materials by the emergence of methacrylate peaks between 5 and 6.5 ppm. The GelMA and MeSDCC were successfully crosslinked into hydrogels. The photograph is of the GelMA and MeSDCC gels 6 weeks after crosslinking and they are pink from soaking in cell media. The scale bar is 5 mm.

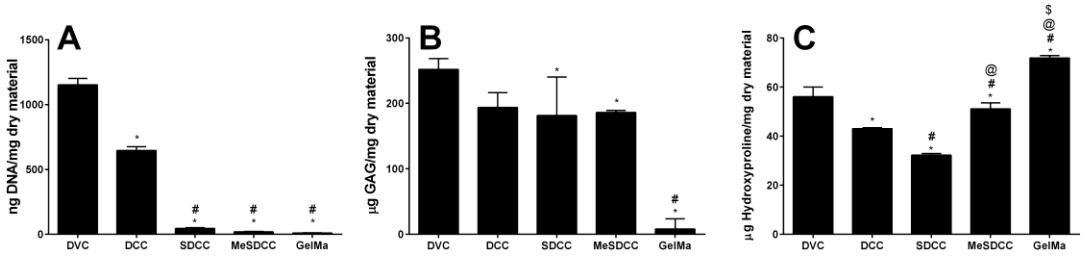

Figure 5.2: Biochemical Contents of DVC, DCC, SDCC, MeSDCC, and GelMA

A) PicoGreen content, B) GAG content, and C) Hydroxyproline content of each material. Decellularization removed 44% of the DNA, 23% of the GAGs, and 23% of the hydroxyproline ($p<0.05$). After solubilizing and after methacrylating, the DNA content further reduced to 4% and 1.7% of that of the original DVC DNA content, respectively ($p<0.05$). Data reported as mean + standard deviation (n=5); *significantly different from DVC ($p<0.05$), #significantly different from DCC ($p<0.05$), @significantly different from SDCC ($p<0.05$), $significantly different from MeSDCC ($p<0.05$).

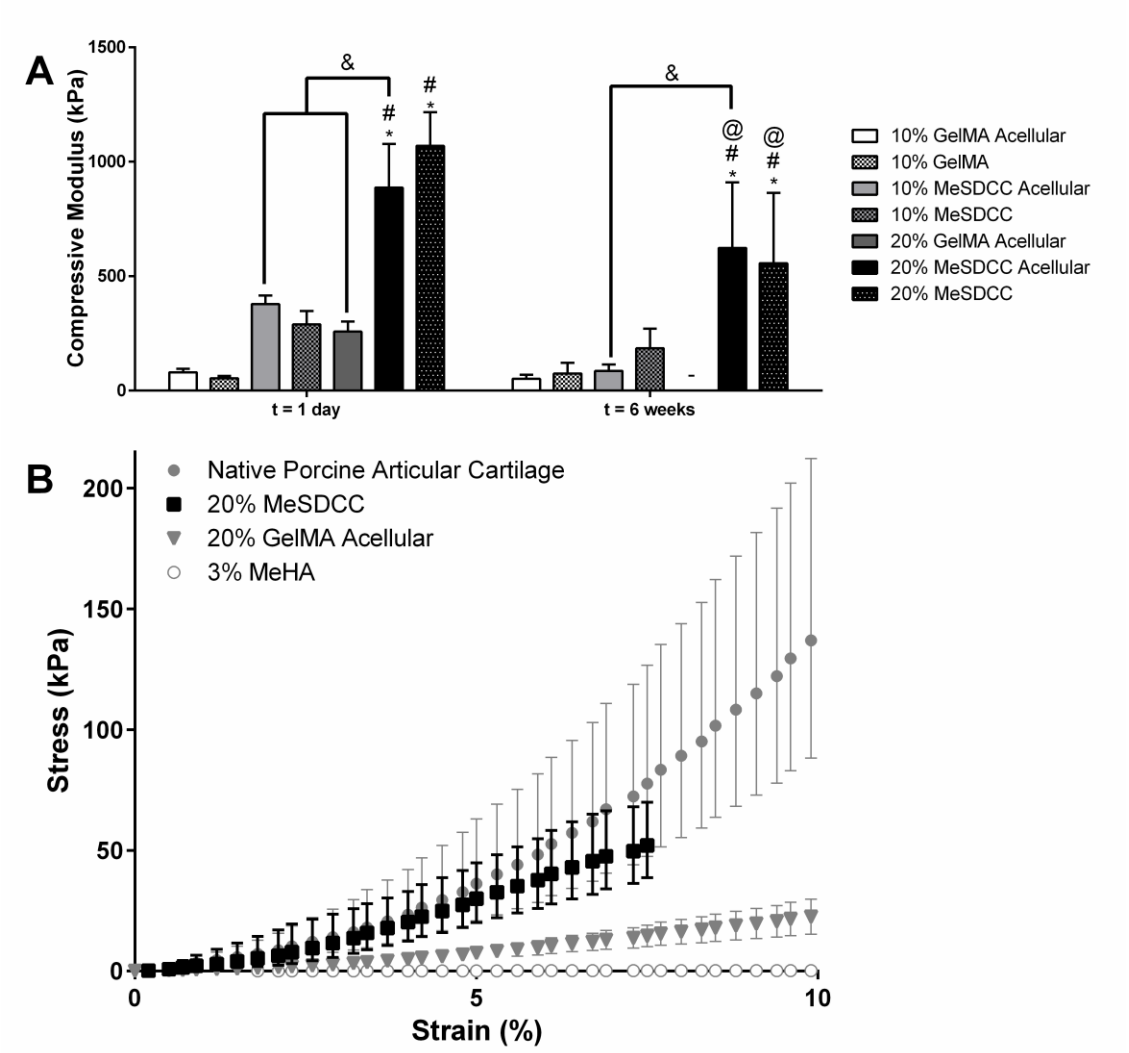

Figure 5.3: Mechanical Testing of Crosslinked Hydrogels

A) Compressive modulus of gels after 1 day and 6 weeks of culture. At day 1, the compressive modulus of the 10% MeSDCC and 20% MeSDCC cellular groups were 5.3 and 20 times larger than the 10% GelMA gels, respectively. Data reported as mean + standard deviation (n=5); * significantly different from 10% GelMA at same time point ($p<0.05$), #significantly different from 10% MeSDCC at same time point ($p<0.05$), &$p<0.05$ for specified comparison, @significantly different from same group at first time point ($p<0.05$), -not tested. B) Stress-Strain Curves of Native Porcine Cartilage Compared to Select Hydrogels. Data are reported as mean ± 95% confidence interval. The stress strain profile of native porcine cartilage were compared to that of 20% MeSDCC, 20% GelMA acellular, and 3% MeHA gels, where 20% MeSDCC was the only hydrogel that fell within the 95% confidence interval of native porcine cartilage until they began to fracture at 7.5% strain on average.

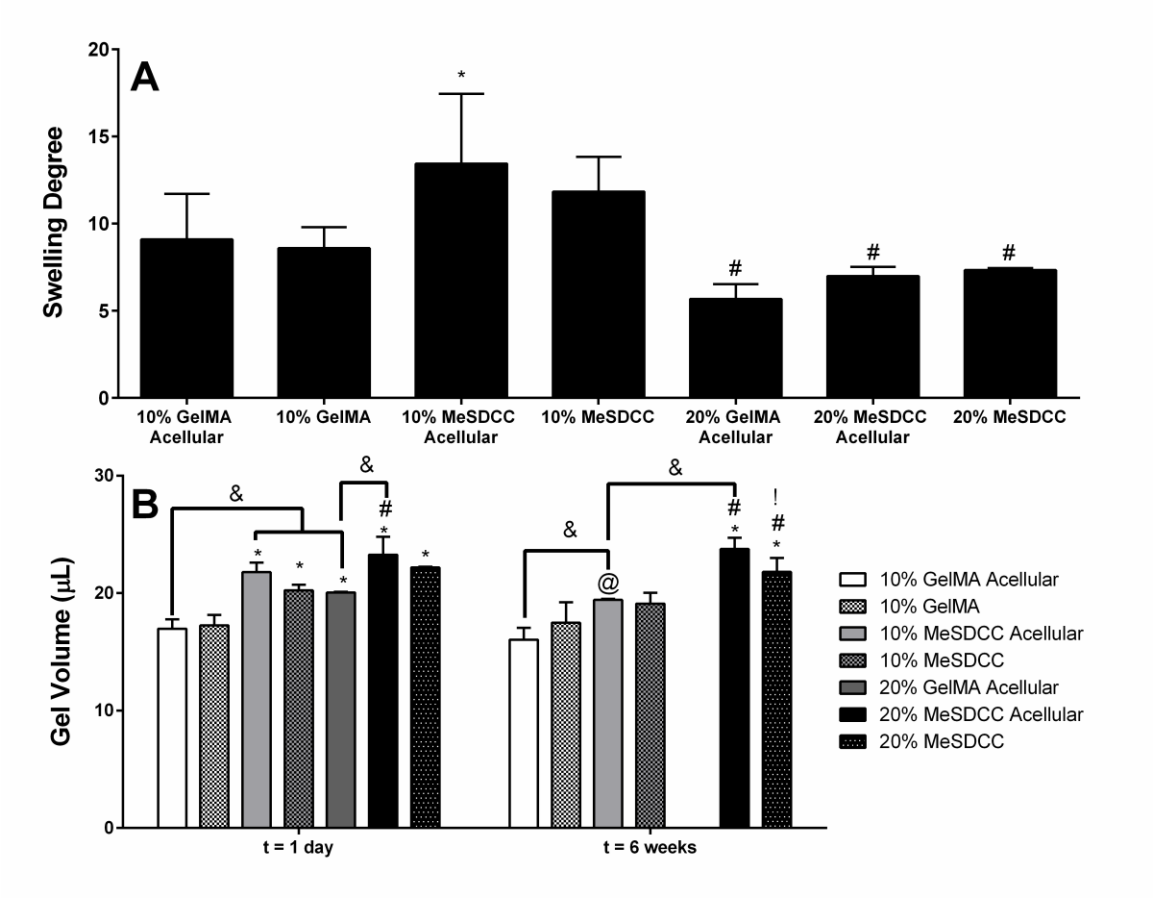

Figure 5.4: Swelling Degree (A) and Volume (B) of Crosslinked Hydrogels

A) The 10% MeSDCC gel had a significantly higher swelling degree compared to 10% GelMA, while the 20% GelMA and 20% MeSDCC groups had significantly lower swelling degrees compared to 10% MeSDCC. B) The only group that had a significant change in volume was the 10% MeSDCC acellular group, which experienced an 11% volume reduction ($p<0.05$). Data reported as mean + standard deviation (n=5); *significantly different from 10% GelMA at same time point ($p<0.05$), #significantly different from 10% MeSDCC at same time point ($p<0.05$), !significantly different from acellular group at same time point ($p<0.05$), &$p<0.05$ for specified comparison, @significantly different from same group at first time point ($p<0.05$), -not tested.

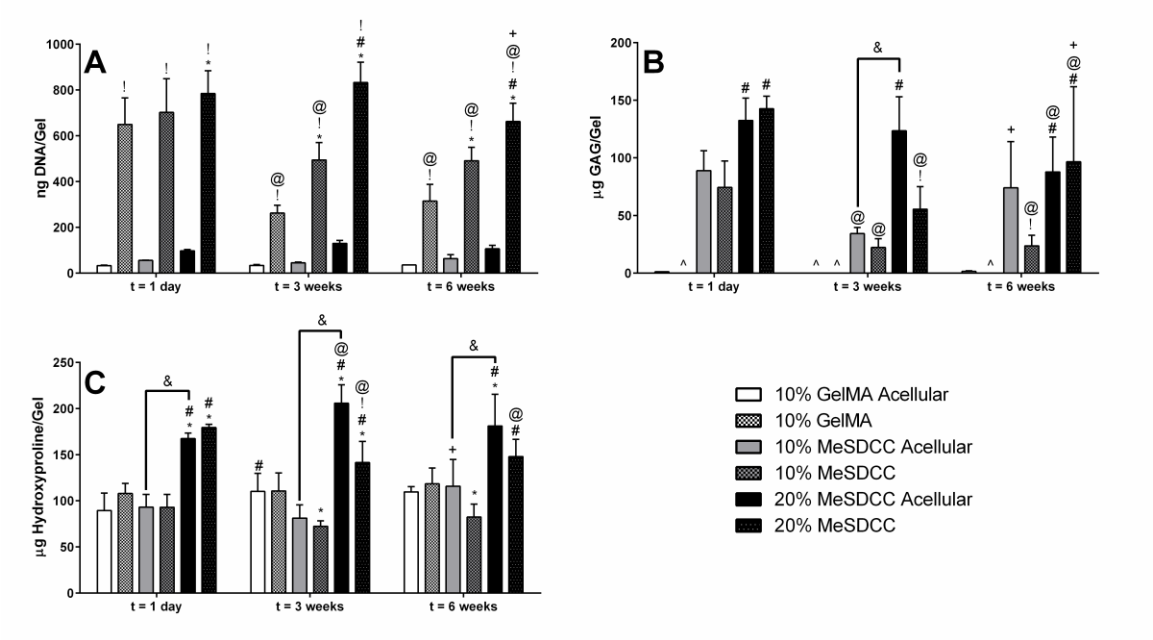

Figure 5.5: Biochemical Content of Gels over the 6 Week Culture Period

A) DNA content, B) GAG content, and C) Hydroxyproline content. All cellular groups had significantly higher DNA contents than their respective acellular groups at all time points ($p<0.05$). Over the course of the 6 week culture period, all cellular groups had a significant reduction in DNA content, both the 10% MeSDCC group and the 20% MeSDCC groups experienced a significant reduction in GAG content, and the only group that experienced a significant loss in hydroxyproline was the 20% MeSDCC group. Data reported as mean + standard deviation (n=5); ^below detectable limit, *significantly different from 10% GelMA at same time point ($p<0.05$), #significantly different from 10% MeSDCC at same time point ($p<0.05$), !significantly different from acellular group at same time point ($p<0.05$), &$p<0.05$ for specified comparison, @significantly different from same group at first time point ($p<0.05$), +significantly different from same group at previous time point ($p<0.05$).

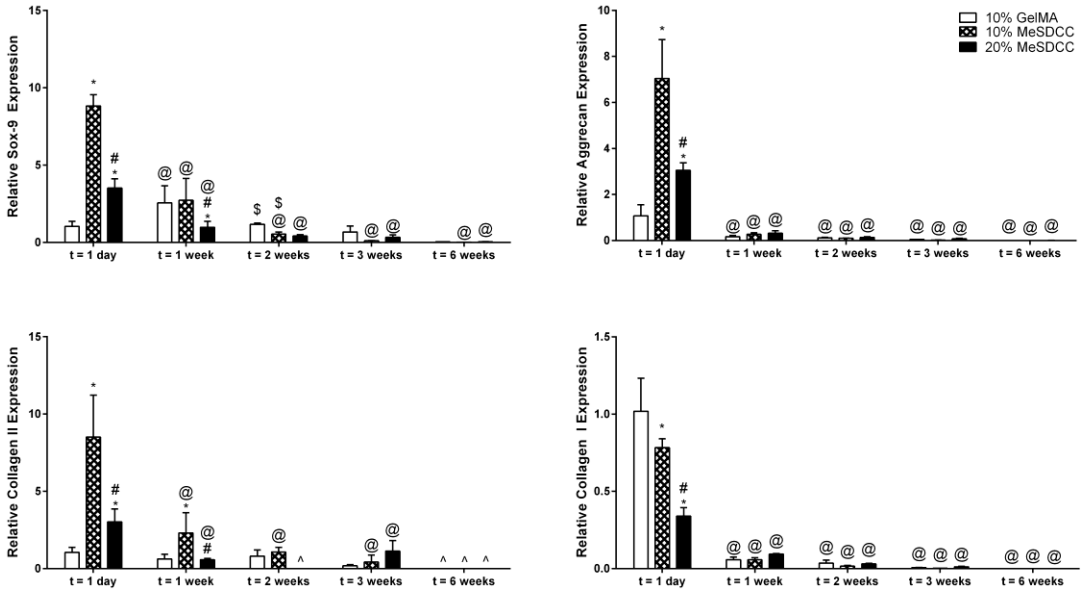

Figure 5.6: Relative Gene Expression of A) Sox-9, B) Aggrecan, C) Collagen II, and D) Collagen I

MeSDCC gels significantly upregulated chondrogenic genes compared to GelMA as early as day 1. Data reported as mean + standard deviation (n=5); *significantly different from 10% GelMA at same time point ($p<0.05$), #significantly different from 10% MeSDCC at same time point ($p<0.05$), @significantly different from same group at first time point ($p<0.05$), $significantly different from same group at previous time point ($p<0.05$), ^below detectable limit.

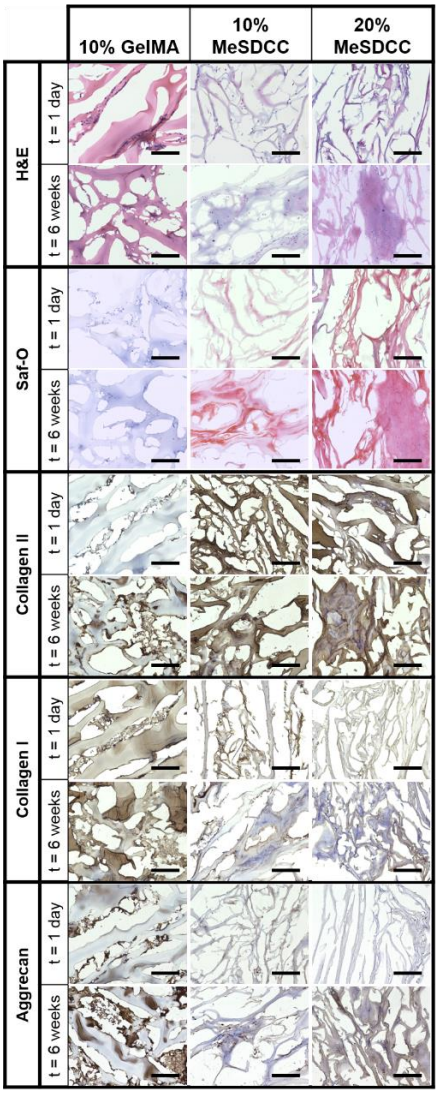

Figure 5.7: Histological Evaluation of Gels

H&E stained the nuclei dark purple and MeSDCC light purple. GelMA and new tissue formation in the 20% MeSDCC group at 6 weeks was stained pink. Regions of new tissue formation can be observed within the 20% and 20% MeSDCC groups at 6 weeks. All MeSDCC gels stained red/orange for GAGs, while no GAG staining was observed in the 10% GelMA group. Regions of new tissue formation surrounding rBMSCs were observed to stain for GAGs. All MeSDCC groups stained for collagen II, although no increase in collagen II staining was observed for those groups throughout culture. However, the 10% GelMA group had an increase in collagen II staining at 6 weeks. Minimal collagen I staining was observed in the MeSDCC groups. Collagen I staining was noted in the 10% GelMA group, although there were no significant changes in staining over the culture period. Last, a slight increase in aggrecan staining was observed in the 10% GelMA and 20% MeSDCC groups over the culture period. Scale bars are 200 µm.

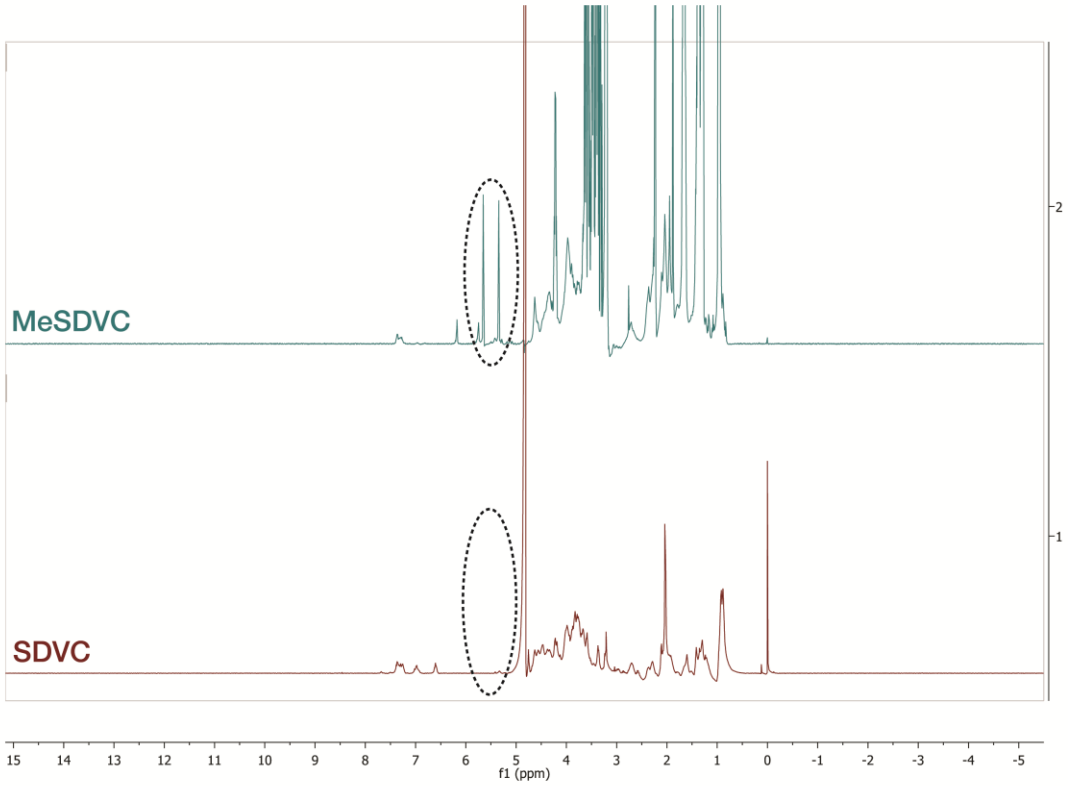

Figure 6.1: NMR of MeSDVC Before and After Methacrylation

Methacrylation was confirmed by the emergence of methacrylate peaks circled between 5 and 6.5 ppm.

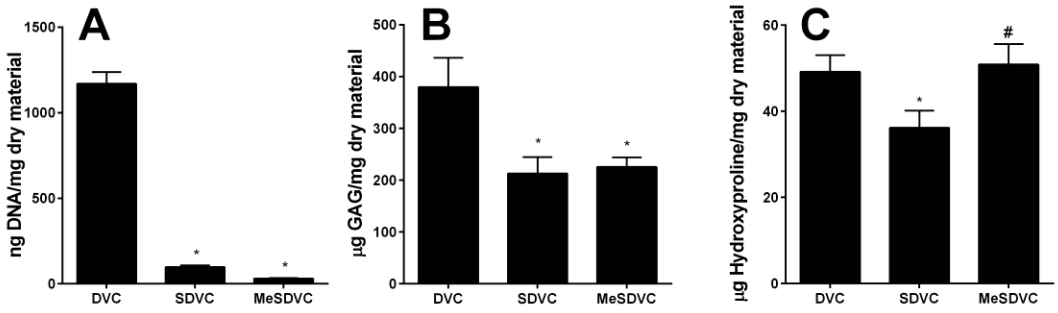

Figure 6.2: Biochemical Contents of DVC, SDVC, and MeSDVC

A) PicoGreen content, B) GAG content, and C) Hydroxyproline content of each material. The SDVC and MeSDVC had DNA contents that were 92% and 97% less than DVC, respectively, and had GAG contents that were 44% and 41% less than that of DVC, respectively ($p<0.05$). The hydroxyproline content of SDVC was 26% lower than that of DVC ($p<0.05$). While the hydroxyproline content of MeSDVC was not significant from DVC, it was 41% higher than that of SDVC ($p<0.05$). Data reported as mean + standard deviation (n=5); *statistically significant from DVC ($p<0.05$), #statistically significant from SDVC ($p<0.05$).

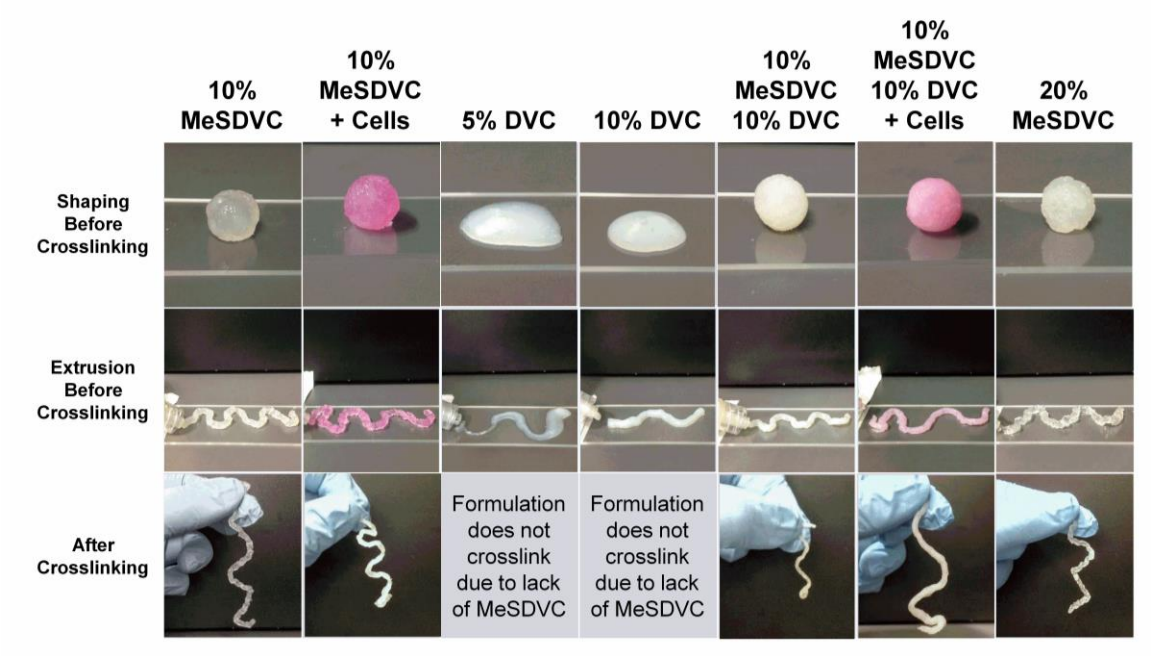

Figure 6.3: Macroscopic Rheological Evaluation of Hydrogel Precursors Before and After Crosslinking

All formulations were acellular unless noted and cellular formulations were pink in color due to presence of cell culture medium. Non-Newtonian behavior was observed in all solutions. However, the 5% DVC and 10% DVC formulations were the only solutions that could not be molded and shaped into a sphere. Shape retention (indicated by the solution retaining extrusion orifice diameter) was noted in all solutions except the 5% DVC solution. Finally, all formulations containing MeSDVC retained shaping after crosslinking.

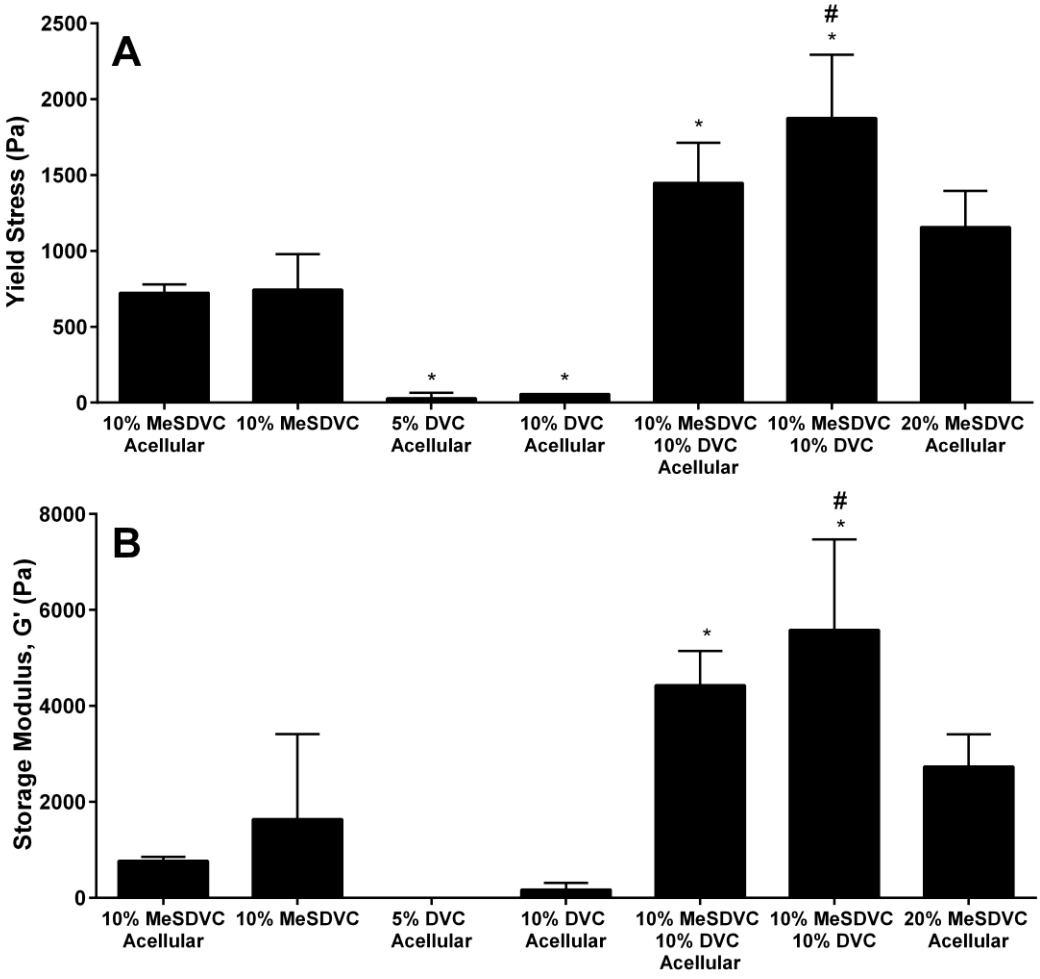

Figure 6.4: Yield Stress (A) and Storage Modulus (B) of Hydrogel Precursor Solutions

All solutions had a measurable yield stress and storage modulus, while the groups containing both MeSDVC and DVC had the highest reported values. No significant differences were observed with the incorporation of cells. Data reported as mean + standard deviation (n=5); *significantly different from 10% MeSDVC acellular, #significantly different from 20% MeSDVC acellular.

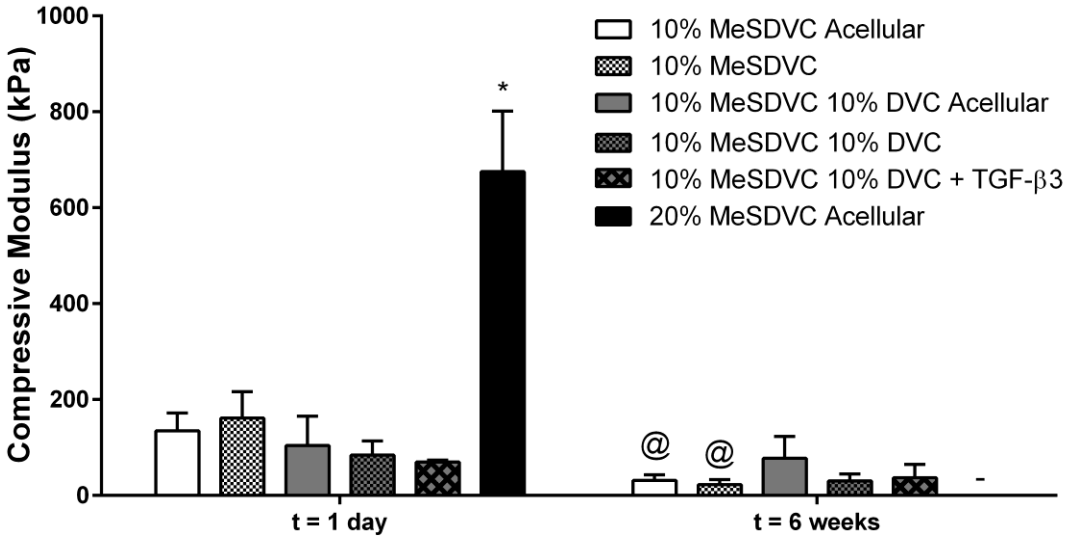

Figure 6.5: Compressive Modulus of Crosslinked Hydrogels After 1 Day and 6 Weeks of Culture

None of the groups were significantly different from the 10% MeSDVC acellular group except the 20% MeSDVC acellular group, which had a modulus of 675 ± 130 kPa ($p<0.05$). Additionally, the only groups that significantly deviated from their original compressive modulus over the 6 week period were the 10% MeSDVC acellular and cellular groups. Data reported as mean + standard deviation (n=5); *significantly different from all other groups at same time point ($p<0.05$), @significantly different from same group at first time point ($p<0.05$), -not tested.

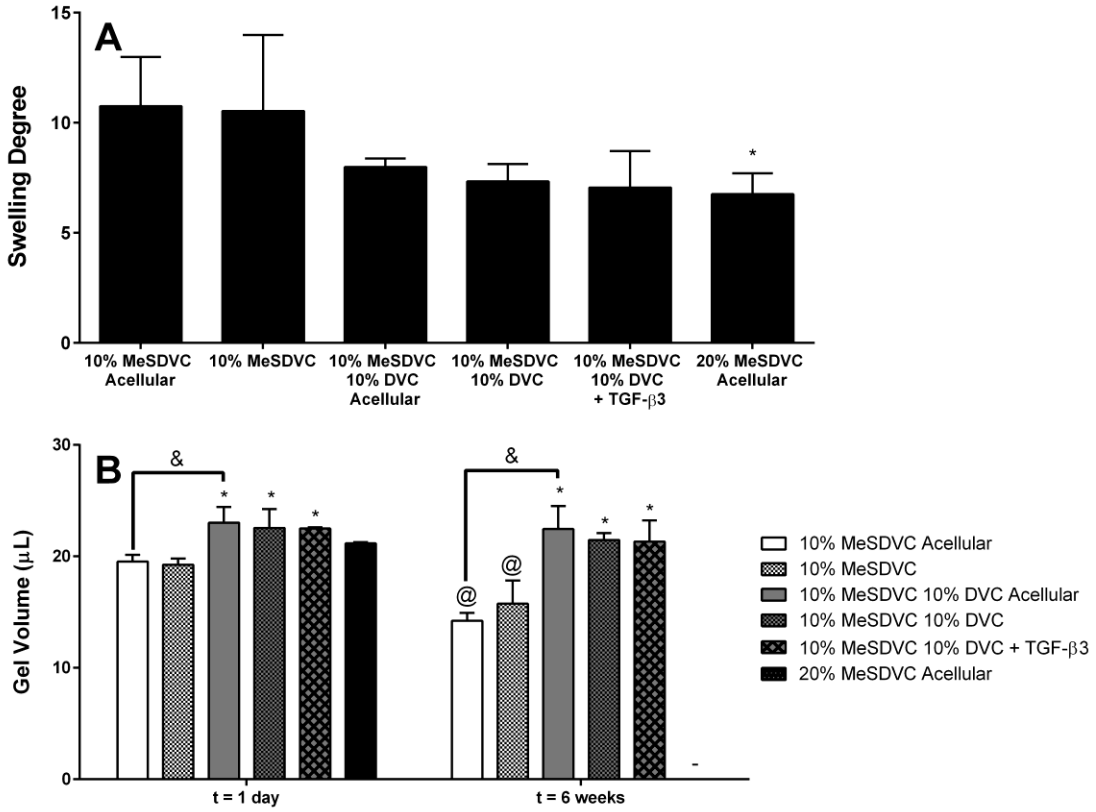

Figure 6.6: Swelling Degree (A) and Volume (B) of Crosslinked Hydrogel Pastes

A) The only group that had a significantly lower swelling degree than that of the 10% MeSDVC group was the 20% MeSDVC acellular group. B) Over the course of the 6 weeks, the only groups that had a significant reduction in volume were the 10% MeSDVC acellular and cellular groups. Data reported as mean + standard deviation (n=5); *statistically significant from 10% MeSDVC at same time point ($p<0.05$), !statistically significant from acellular group at same time point ($p<0.05$), &$p<0.05$ for specified comparison, @statistically significant from same group at first time point ($p<0.05$), -not tested.

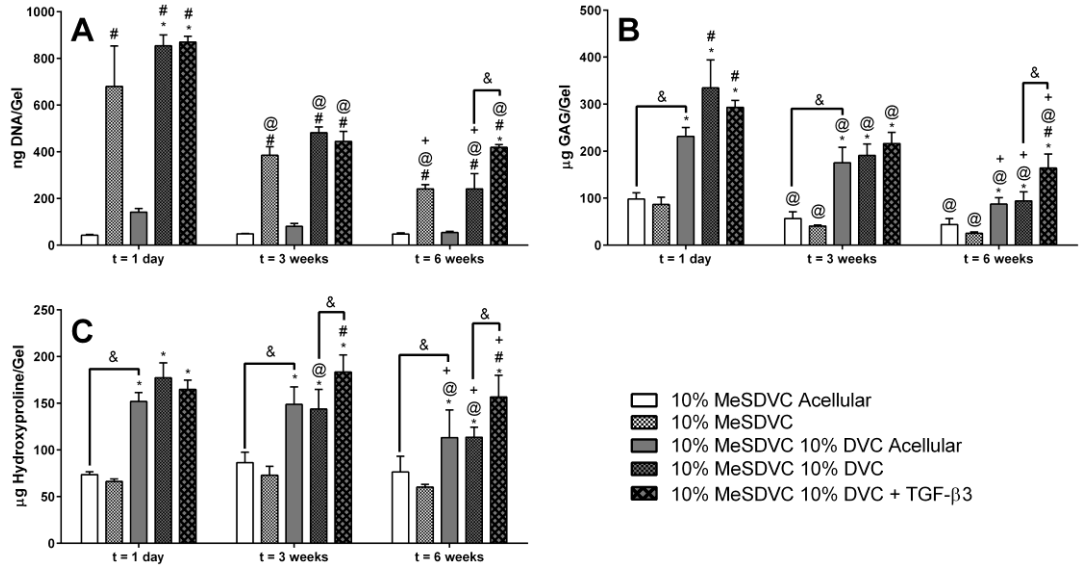

Figure 6.7: Biochemical Content of Gels over the 6 Week Culture Period

A) DNA content, B) GAG content, and C) Hydroxyproline Content. All cellular groups had significantly higher DNA contents than their respective acellular groups at all time points. Over the course of the 6 week culture period, all groups had significant reductions in biochemical content ($p<0.05$), except for the TGF-β_3 exposed group, which did not have a significant reduction in hydroxyproline. Data reported as mean + standard deviation (n=5); *significantly different from 10% MeSDVC at same time point ($p<0.05$), #significantly different from acellular group at same time point ($p<0.05$), &$p<0.05$ for specified comparison, @significantly different from same group at first time point ($p<0.05$), +significantly different from same group at previous time point ($p<0.05$).

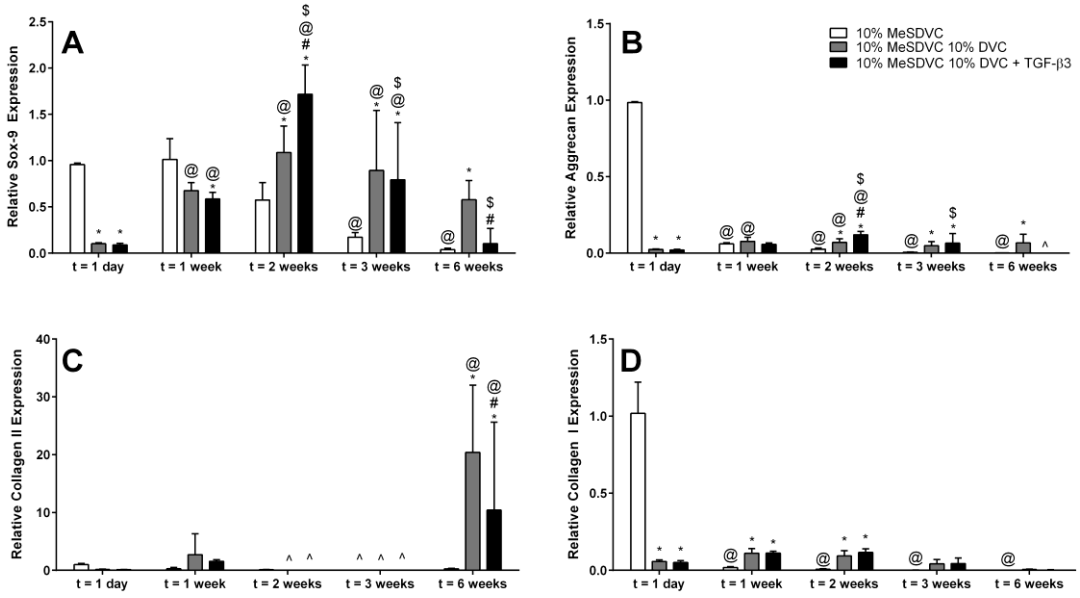

Figure 6.8: Relative Gene Expression of A) Sox-9, B) Aggrecan, C) Collagen II, and D) Collagen I

From 2 weeks onward, the DVC-incorporating groups repeatedly outperformed the MeSDVC group in chondrogenic gene expression, especially at 6 weeks with collagen II. Data reported as mean + standard deviation (n=5); *statistically significant from 10% MeSDVC at same time point ($p<0.05$), #statistically significant from 10% MeSDVC 10% DVC at same time point ($p<0.05$), @statistically significant from same group at first time point ($p<0.05$), $statistically significant from same group at previous time point ($p<0.05$), ^below detectable limit.

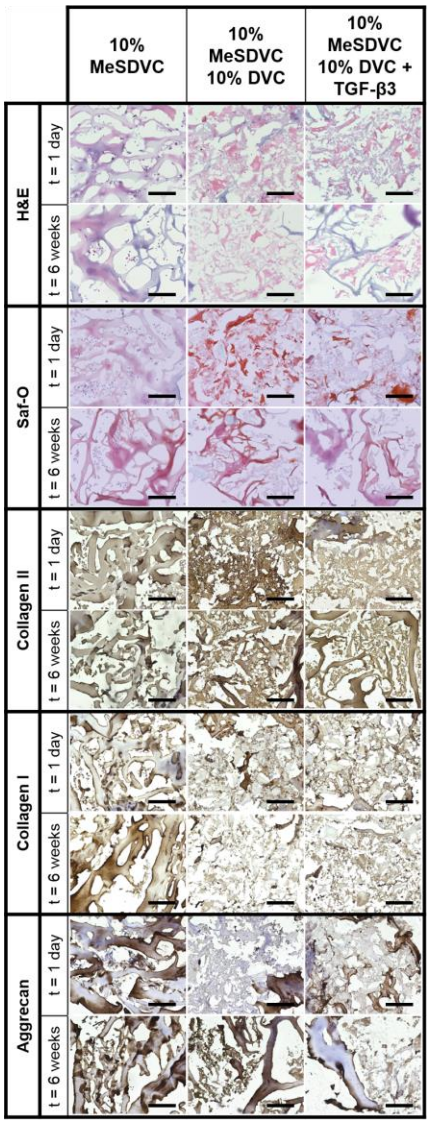

Figure 6.9: Histological Evaluation of Gels

H&E staining revealed the cells remained evenly distributed throughout culture. MeSDVC and DVC particles were stained a dark red/orange color with Saf-O staining and the color of the DVC particles appeared to fade over the 6 weeks. A slight increase in collagen II staining was noted in the DVC-incorporating groups at 6 weeks. A slight increase in collagen I staining was observed for the 10% MeSDVC group at 6 weeks, whereas the DVC-incorporated groups had a slight decrease in staining at 6 weeks. A slight increase in aggrecan staining at 6 weeks was observed next to the cells of the 10% MeSDVC group. Additionally, the 10% MeSDVC 10% DVC group had a slight increase in aggrecan staining near the location of the rBMSCs at 6 weeks. Last, the 10% MeSDVC + 10% DVC + TGF-β_3 group had no discernable changes in aggrecan staining over the 6 weeks. Scale bars are 200 μm.

Figure 7.1: Implantation of Hydrogel Pastes in a Human Cadaver Elbow

A hydrogel paste, consisting of methacrylated hyaluronic acid and decellularized cartilage microparticles, was implanted in an articular cartilage defect created in a human cadaver elbow joint. The paste was able to be implanted and shaped by the surgeon. The paste was retained within the defect site prior to UV crosslinking. After crosslinking, the joint was able to be articulated without dislodging the paste from the defect site.

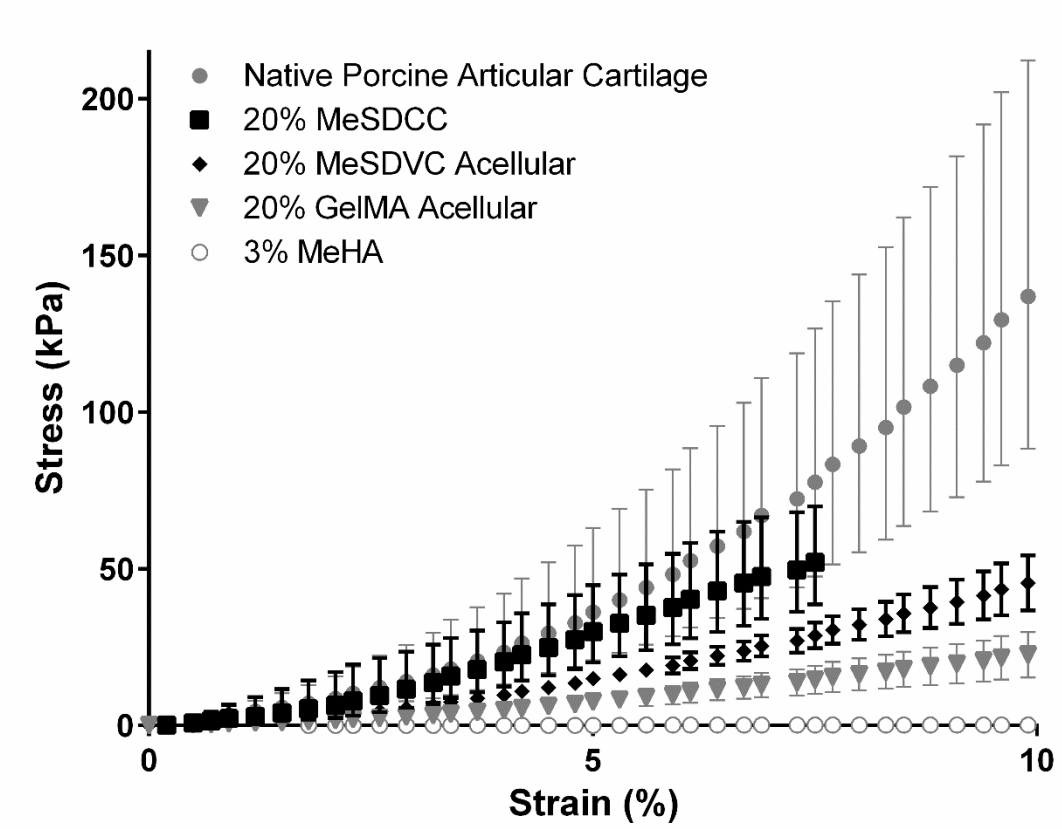

Figure 7.2: Stress-Strain Curves of Native Porcine Cartilage Compared to Select Hydrogels

The stress strain profiles of native porcine cartilage were compared to that of 20% MeSDCC, 20% MeSDVC acellular, 20% GelMA acellular, and 3% MeHA gels, where 20% MeSDCC was the only hydrogel that fell within the 95% confidence interval of native porcine cartilage until they began to fracture at 7.5% strain on average. The next closest hydrogel matching the stress-strain profile of native cartilage was 20% MeSDVC, which did not fracture early like the 20% MeSDCC gels. Data are reported as mean ± 95% confidence interval.

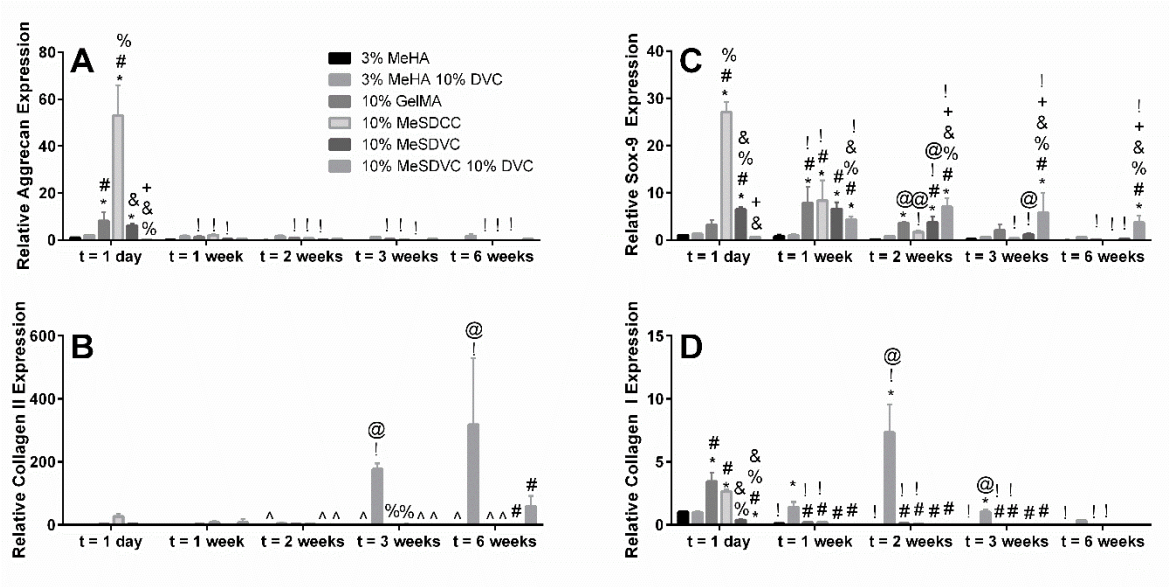

Figure 7.3 Relative Gene Expression of Select Gels from Aims 2-3.

Relative gene expression observed for A) aggrecan, B) collagen II, C) Sox-9, and D) collagen I. The 10% MeSDCC gels had significantly higher aggrecan and Sox-9 expression at day 1 compared to the other groups, but high levels of collagen II gene expression were only observed for the DVC-containing groups. Data reported as mean + standard deviation (n=5); *Significantly different from 3% MeHA at same time point ($p<0.05$), #significantly different from 3% MeHA 10% DVC at same time point ($p<0.05$), %significantly different from 10% GelMA at same time point ($p<0.05$), &significantly different from 10% MeSDCC at same time point ($p<0.05$), +significantly different from 10% MeSDVC at same time point ($p<0.05$), !significantly different from same group at first time point ($p<0.05$), @significantly different from same group at previous time point ($p<0.05$), ^below detectable limit.

APPENDIX B: Tables

CHAPTER 1: Tables 1.1-1.2

CHAPTER 2: No Tables

CHAPTER 3: No Tables

CHAPTER 4: No Tables

CHAPTER 5: No Tables

CHAPTER 6: No Tables

CHAPTER 7: No Tables

Table 2.1: Applications of Nanomaterials in Osteochondral Interfaces

Reference(s)	Nanomaterial	Additional Material(s)	Biological Model	Scaffold Formulation	Highlighted Finding
Bian *et al.* (2012)	β-TCP nanoparticle	Collagen I Acrylamide	*In vitro*: scaffold cultured with rabbit BMSCs for 7 days	Triphasic	Gel casting avoided delamination between phases
Cheng *et al.* (2011)	Collagen I nanofibers	NA	*In vitro*: scaffold cultured with rabbit BMSCs for 5 weeks	Triphasic	Calcified cartilage layer formed in triphasic constructs as compared to biphasic controls
Chung *et al.* (2011a, b)	HAp nanoparticles	POC	*In vivo*: New Zealand White Rabbits osteochondral defect for 26 weeks	Nanocomposite	Nanocomposites induced more trabecular bone formation and had superior mechanical properties compared to microcomposites
Erisken *et al.* (2008, 2010)	PCL nanofibers, HAp nanoparticles	NA	*In vitro*: cultured with MC3T3-E1 cells for 4 weeks	Continuous gradient	Tissue constructs formed a gradient in ECM deposition and construct mechanical properties approached native tissue as culture period increased
Erisken *et al.* (2011)	PCL nanofibers, β-GP nanoparticles	Insulin	*In vitro*: cultured with human adipose-derived stromal cells for 8 weeks	Opposing continuous gradients	Differentiation of seeded cells towards chondrogenic or osteogenic lineage depended upon position in the scaffold
Filardo *et al.* (2010), Kon *et al.* (2009, 2010b, 2011)	Collagen I nanofibers, HAp nanoparticles	NA	*In vivo*: Human osteochondral defect	Triphasic	The triphasic constructs demonstrate safety and potential in human clinical trials
Kon *et al.* (2010a, c)	Collagen I nanofibers, HAp nanoparticles	NA	*In vivo*: Sheep and horse osteochondral defect for 6 months	Triphasic	Comparable extent of regeneration observed with or without autologous chondrocytes suggesting the constructs recruit native cells
Grogan *et al.* (2012)	Iron oxide nanoparticles, maghemite nanoparticles, magnetite nanoparticles	Magnetite, alginate, agarose	*In vivo*: New Zealand White Rabbits osteochondral defect for 4 weeks	Biphasic	Manipulation of the magnetic field *in vitro* and *in situ* results in multi-directional cellular arrangements

Table 2.1 (Continued)

Harley *et al.*(2010a)	CaP nanoparticles	Collagen I, Collagen II, CS	Not directly evaluated	Biphasic with continuous interface	Liquid-phase cosynthesis successfully resulted in a continuous interface between phases
Hu *et al.* (2009)	PLLA nanofibers		*In vitro*: cultured with human BMSCs for 6 weeks	Nanocomposite	PLLA scaffold supports both chondrogenic and osteogenic differentiation when exposed to the respective growth signals
Khanarian *et al.* (2012)	HAp nanoparticles	Agarose, Micron-sized HAp	*In vitro*: cultured with bovine chondrocytes for 2 weeks	Nanocomposite	Superior ECM deposition with gels composed of micron-sized HAp in comparison to nanoHAp
Lee *et al.* (2012)	Fluorescent silica nanoparticles	Heparin-conjugated fibrin	*In vivo*: male nude rat osteochondral defect for 21 days	NA	IOMTS successfully monitored MSC migration and can be used the effect of growth factors on cartilage repair
Liu *et al.* (2009)	HAp nanoparticles	Collagen I	Not directly evaluated	Continuous gradient	Opposing gradients of Ca and P successfully formed with HAp nucleation in interior of scaffold
Liu *et al.* (2011)	Star-Shaped PLLA nanoparticles	NA	*In vivo*: New Zealand White Rabbit osteochondral defect for 8 weeks	Nanocomposite	Microspheres assembled from PLLA nanoparticles resulted in enhanced cartilage regeneration compared to control microspheres
Matsusaki *et al.* (2008)	HAp nanoparticles	Rabbit synovial MSCs	*In vivo*: Japanese White Rabbit osteochondral defect for 6 weeks	Nanocomposite	Scaffolds containing HAp exhibited accelerated osteoinduction as compared to scaffolds without HAp
Mohan *et al.* (2011)	HAp nanoparticles	PLGA microspheres containing chondrogenic or osteogenic factors	*In vivo*: New Zealand White Rabbit osteochondral defect for 12 weeks	Continuous gradient	Greatest extent of regeneration achieved when both material and signal gradients were present
Nirmala *et al.* (2010)	PCL nanofibers, HAp and Ag nanoparticles	NA	Not directly evaluated	Nanocomposite	Incorporating Ag resulted in superior mechanical properties and mineral depositon

Table 2.1 (Continued)

Qu *et al.* (2011)	HAp nanoparticles	PVA, PA6	*In vivo*: Implanted intramuscularly in rabbit for 12 weeks	Biphasic	Osteogenesis and chondrogenesis observed in respective layers after 12 week implantation
Rodriguez *et al.* (2012)	Carbon nanotubes or nanofibers	PVA	*In vivo*: Wistar Rat osteochondral defect for 12 weeks	Nanocomposite	Significantly more calcium and phosphorus deposition occurred in constructs with carbon nanofibers compared to constructs with carbon nanotubes and gels of PVA only
Tampieri *et al.* (2008)	Collagen I nanofibers, HAp nanoparticles	HA	*In vivo*: ID mice for 8 weeks subcutaneously	Triphasic	Scaffold layers selectively support cell differentiation towards osteogenic or chondrogenic lineages
Tampieri *et al.* (2011)	Collagen I nanofibers, HAp nanoparticles, magnetite nanoparticles	NA	Not directly evaluated	Triphasic	Scaffolds containing magnetite nanoparticles had superior mechanical properties compared to scaffolds without magnetite
Xue *et al.* (2010)	HAp nanoparticles	PLGA	*In vivo*: SD rats osteochondral defect for 12 weeks	Nanocomposite	Greatest extent of regeneration observed in PLGA scaffolds containing HAp compared to PLGA control
Yunos *et al.* (2011)	PDLLA nanofibers, HAp nanoparticles	Bioglass	*In vitro*: cultured with ATDC5 chondrocyte cells line for 10 days	Biphasic	Chondrocyte cells were able to attach, proliferate, and migrate into the scaffolds

β-GP: β-glycerophosphate; β-TCP: β-tricalcium phosphate; Ag: silver; BMSCs: bone marrow stem cells; Ca: calcium; CaP: calcium phosphate; CS: chondroitin sulfate; ECM: extracellular matrix; HA: hyaluronic acid; HAp: hydroxyapatite; ID: immunodeficient; IOMTS: in vivo osteochondral mesenchymal stem cells tracking system; MSCs: mesenchymal stem cells; NA: not applicable; P: phosphorous; PA6: polyamide6; PCL: polycaprolactone; PDLLA: poly(D,L-Lactide); PLGA: poly(lactic-co-glycolic acid); PLLA: poly(L-lactic acid); POC: poly(1,8-octanediol-co-citrate); PVA: polyvinyl alcohol; SD: Sprague-Dawley.

Table 2.2 Applications of Nanomaterials in Bone-Tendon and Bone-Ligament Interfaces

Reference(s)	Nanomaterial	Additional Material(s)	Biological Model	Scaffold Formulation	Highlighted Finding
Li *et al.* (2009)	PLGA nanofibers, CaP nanoparticles	NA	*In vitro*: cultured with MC3T3 cells for 3 days	Continuous gradient	Mineral gradient resulted in a gradient of stiffness and cell density
Ramalingham *et al.* (2012)	PCL nanofibers, amorphous CaP nanoparticles	NA	*In vitro*: cultured with MC3T3-E1 cells for 7 days	Continuous gradient	Adhesion and proliferation of seeded cells were enhanced as CaP concentration increased along length of scaffold
Samavedi *et al.* (2011)	PCL and PEU nanofibers, HAp nanoparticles	NA	*In vitro*: cultured with MC3T3-E1 cells for 7 days	Continuous gradient	Mechanical gradient with differences in tensile moduli observed along length of scaffold
Spalazzi *et al.* (2008)	PLGA nanofibers	PLGA/ Bioactive glass microspheres	*In vitro*: cultured with bovine tendons	Biphasic	Scaffold induced compression of tendons led to increased ECM deposition compared to tendon control
Xie *et al.* (2010)	PLGA nanofibers	NA	*In vitro*: cultured with rat tendon fibroblasts for 7 days	Biphasic	Tendon fibroblasts and deposited collagen I were aligned in aligned portion of scaffold and were randomly distributed in randomly oriented part of scaffold

CaP: calcium phosphate; HAp: hydroxyapatite; NA: not applicable; PCL: polycaprolactone; PEU:poly(ester urethane); PLGA: poly(lactic-co glycolic acid);